



THESIS - MN142532

# HEADING ANALYSIS OF WEATHERVANING TURRET MOORED UNITS

FAHMY ARDHIANSYAH, ST  
NRP. 4115 203 002

SUPERVISOR  
Aries Sulisetyono, Ph.D  
Wasis Dwi Aryawan, Ph.D

POST GRADUATE PROGRAME IN MARINE TECHNOLOGY  
CONCENTRATION IN SHIP HYDRODYNAMICS  
FACULTY OF MARINE TECHNOLOGY  
INSTITUT TEKNOLOGI SEPULUH NOPEMBER  
SURABAYA  
2017

## LEMBAR PENGESAHAN TESIS

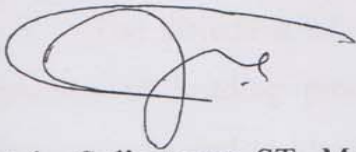
Tesis disusun untuk memenuhi salah satu syarat memperoleh gelar  
Magister Teknik (MT)  
di  
Institut Teknologi Sepuluh Nopember

Oleh:

**FAHMY ARDHIANSYAH**  
NRP. 4115 203 002

Telah direvisi sesuai dengan hasil Ujian Tesis  
Tanggal Ujian : 23 Januari 2017  
Periode Wisuda : Maret 2017

Disetujui oleh:



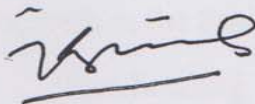
1. Aries Sulisetyono, ST., MA.Sc., Ph.D.  
NIP. 19710320 199512 1 002

(Pembimbing)



2. Ir. Wasis Dwi Aryawan, M.Sc., Ph.D.  
NIP. 19670406 199203 1 001

(Pembimbing)




3. Dr. Ir. I Ketut Suastika, M.Sc.  
NIP. 19691231 200604 1 178

(Penguji)



an. Direktur Pascasarjana  
Asisten Direktur Pascasarjana

  
Prof. Dr. Ir. Tri Widjaja, M.Eng.  
NIP. 19611021 198603 1 001

# HEADING ANALYSIS OF WEATHERVANING TURRET MOORED UNITS

Student Name : Fahmy Ardhiansyah, ST  
ID Number : 4115 203 002  
Supervisor : Aries Sulisetyono, Ph.D  
Wasis Dwi Aryawan, Ph.D

## ABSTRACT

This thesis report is present the heading study of weathervaning turret moored unit. With heading analysis over each of the sea states contained in time-series, mean heading of the floating structure can be obtained. Basically heading analysis will help the designer to perform analysis of structural strength, sloshing in tanks, green water prediction, loading/offloading operation, and fatigue life estimation. With heading analysis the designer will get a proper loading condition for their further analysis on weathervaning turret moored unit. Especially to optimized mooring system design based on heading analysis result which is will be performed in this thesis other than the heading analysis itself.

The result of heading analysis calculation indicated that the most affected external forces that causing vessel mean heading is dedicated by wind, it is seen the relative heading between wind and vessel heading is quite small ( $<10$ degree) with large occurrence probability (up to 45%). This probably due to the wind force coefficient is larger than current coefficient and also the wind age area is larger than hydrodynamic drag area.

Moreover the application of heading analysis considered in this study is for mooring system design. The result indicated that heading analysis is important to the designer to determine the pattern of anchor mooring. Nine (9) proposed mooring pattern has been investigated to check the mooring performance to withstand in rough water and fatigue life estimation as well in accordance to a well-known classification society.

**Keywords:** Heading Analysis, Weathervaning Units, Mooring System Design.



## PREFACE

*Assalamu'alaikum Wr. Wb.*

*Indeed this work is due to Allah and for Allah...  
and Salawat on Prophet Muhammad and his family...*

This thesis is submitted in order to complete the Master of Engineering (*Magister Teknik*) study in department of Naval Architecture and Shipbuilding Engineering at ITS Surabaya. This thesis have main concentration on Ship Hydrodynamic which is following by design of mooring system interest. This work was initiated from the author involvement during his job in ABADI MASELA FLNG project.

Hopefully this thesis will give encouragement to the reader which have intention in ship hydrodynamic and mooring system design. Moreover the MOSES software, which the academic license is given by Bentley Engineering to ITS, is one of the powerful hydrodynamic tools to solve quite complicated cases along the study. The syntax is also reported in this thesis report that will give another user to feel more enthusiast when he/she face a challenging hydrodynamic cases to solve.

### Acknowledgements

The author would like to say thank you to everyone to their support, great comments, sharing of experience and knowledge that can improve encouragement to finish this research. At the moment author would say a very big thank you to this following figures:

1. My family; my wife: Mainas Ziyah Aghnia, my kids: Nusaibah and Ibrahim. You all is my inspiration and my motivation, thanks for all full support and never ending encouragement to continue the study.
2. Ponorogo's family and Gresik's family; Yang Kung and Yang Ti also Aki and Uti. It's a pleasure to me to express my gratitude to all of you.
3. The supervisors: Bapak Aries Sulistyono, Ph.D and Bapak Wasis Dwi Aryawan, Ph.D who give a lot of comments, discussion, and also great motivation.
4. All lecturer in Marine Technology Post Graduate Program: Achmad Zubaydi, Prof; Djauhar Manfaat, Prof, IKAP Utama, Prof; Daniel M. Rosyid, Prof; Ketut Suastika, Dr; Herman Pratikno, Dr; Yeyes Mulyadi, Dr. Buana Ma'aruf, Prof.
5. Ocean Engineering Department peoples, especially: Rudi Waluyo, Dr; Murdjito, M.Eng; and also pak Murdjito and co., M. Kadafi, MT, Norman M. Sabana, ST.
6. Ship Design Laboratory in Department of Naval Architecture and Shipbuilding Engineering peoples, especially: Achmad Baidowi, MT, Danu Utama, MT
7. Class of *Boikot* 2015 who spent an enjoying and relaxing moment along the study. This class will always suggest *Boikot* from a wrong doings to do a goodness for sure.
8. PTTI and PTGM colleague, especially: Daniel Ampulembang and Rudy Heryanto.
9. And everybody who cannot mention one by one in this report.

Finally, for finishing the study in ITS author could only wish may Allah reward you with the best. ☺☺☺☺☺

*Wassalamu'alaikum Wr. Wb.*

Surabaya, January 2017

***Fahmy Ardhiansyah***



## TABLE OF CONTENTS

ABSTRACT .....	iii
PREFACE .....	v
LIST OF FIGURES .....	ix
LIST OF TABLES .....	xi
1. INTRODUCTION.....	1
1.1 Introduction.....	1
1.2 Problem Definitions .....	2
1.3 Research Objective .....	2
1.4 Research Question .....	2
1.5 Hypothesis.....	2
2. LITERATURE STUDY AND THEORETICAL BACKGROUND.....	3
2.1 Literature Study .....	3
2.2 Theoretical Background.....	4
2.2.1 Wave Prediction and Climatology.....	4
2.2.2 Wind Loads .....	7
2.2.3 Current Loads .....	11
2.2.4 Wave Drift Forces and Moments .....	14
2.2.5 Sea Loads.....	15
2.2.6 Floating Structure Dynamics .....	16
2.2.7 Fatigue Analysis .....	16
3. METHODOLOGY .....	19
3.1 Environment Data .....	20
3.2 Numerical Model .....	27
3.2.1 Analysis Coordinate System.....	27
3.2.2 Vessel Information .....	28
3.2.3 Wind and Current Load on Vessel .....	29
3.2.4 Wave Drift and Vessel Modelling.....	33
3.2.5 Environmental Modelling.....	34

3.2.6	Heading Analysis Algorithm .....	35
3.2.7	Heading Angles Calculation .....	36
3.3	Model Verification .....	41
3.4	Assessing the Outcome .....	42
3.5	Mooring System Design.....	43
3.5.1	Mooring System Characteristic.....	43
3.5.2	Mooring Leg Components .....	43
3.5.3	Marine Growth and Corrosion.....	46
3.5.4	Environmental Condition.....	48
3.5.5	Analysis Matrix and Load Cases .....	49
3.5.6	Design Criteria .....	52
4.	RESULT AND DISCUSSION .....	53
4.1	Model Verification Result .....	53
4.2	Wave Heading Analysis .....	59
4.2.1	Response in Wave.....	59
4.2.2	Free Decay Test .....	63
4.2.3	Hydrodynamic Coefficient.....	66
4.2.4	Weathervaning Analysis .....	70
4.2.5	Heading Analysis Outcome .....	71
4.3	Mooring System Design.....	77
4.3.1	Mooring Leg and Hull Clearance Analysis .....	80
4.3.2	Green Water and Chain Table Slamming Analysis .....	82
4.3.3	Mooring Line and Anchor Loads.....	83
4.3.4	Low Frequency Vessel Offset.....	99
4.3.5	Fatigue Life.....	100
5.	CONCLUSION.....	105
	REFERENCES .....	107
	APPENDIX	



## LIST OF FIGURES

Figure 2-1 Beaufort's Wind Force Scale .....	4
Figure 2-2 Definitions Used here for Forces and Moments.....	9
Figure 2-3 Example of Wind Load Coefficients.....	10
Figure 3-1 Analysis Methodology .....	19
Figure 3-2 Relation between Wind Direction and Wind Speed.....	21
Figure 3-3 Annual Probability of Wind Direction .....	21
Figure 3-4 Relation between Current Direction and Current Speed .....	22
Figure 3-5 Annual Probability of Current Direction.....	22
Figure 3-6 Relation between Wind Wave Direction and Significant Wave Height .....	23
Figure 3-7 Annual Probability of Wind Wave Direction.....	23
Figure 3-8 Relation between Westerly Swell and Significant Wave Height .....	24
Figure 3-9 Annual Probability of Westerly Swell Direction .....	24
Figure 3-10 Relation between Peak Period and Significant Wave Height of Easterly Sea.....	25
Figure 3-11 Relation between Peak Period and Significant Wave Height of Westerly Sea .....	25
Figure 3-12 Relation between Peak Period and Significant Wave Height of Westerly Swell .....	26
Figure 3-13 Sign Convention Coordinate System .....	27
Figure 3-14 Wind Load Coefficients .....	29
Figure 3-15 Current Load Coefficients .....	29
Figure 3-16 Vessel Side Area .....	31
Figure 3-17 Vessel Front Area.....	31
Figure 3-18 Vessel Panel Model (totally 977 panels).....	31
Figure 3-19 Heading Analysis Calculation Procedure.....	36
Figure 3-20 Equilibrium Calculation .....	38
Figure 3-21 Heading Analysis Algorithm.....	39
Figure 3-22 External Turret Mooring System Design .....	44
Figure 3-23 Chain Table Layout.....	46

Figure 3-24 Schematic View of Mooring System.....	47
Figure 4-1 Quarter-seas RAO Compare to AQWA.....	56
Figure 4-2 Added Mass Compare to WAMIT .....	57
Figure 4-3 Damping Compare to WAMIT.....	58
Figure 4-4 Vessel Motion Response Operator .....	61
Figure 4-5 Mean Drifting Forces.....	62
Figure 4-6 Heave Free Decay Test: Maximum for Each Cycles.....	65
Figure 4-7 Roll Free Decay Test: Maximum for Each Cycles .....	65
Figure 4-8 Pitch Free Decay Test: Maximum for Each Cycles.....	65
Figure 4-9 Weathervaning Analysis .....	70
Figure 4-10 Occurrence Probability of vessel's Heading Angles .....	71
Figure 4-11 Relation between Wind Speed and Incident Wind Direction .....	72
Figure 4-12 Occurrence Probability of Wind Direction.....	72
Figure 4-13 Relation between Current Speed and Incident Current Direction .....	73
Figure 4-14 Occurrence Probability of Incident Current Direction .....	73
Figure 4-15 Relation between Significant Wave Height and Incident Wave Direction.....	74
Figure 4-16 Occurrence Probability of Incident Wave Direction .....	74
Figure 4-17 Relation between Significant Wave Height and incident Swell Direction.....	75
Figure 4-18 Occurrence Probability of Incident Swell Direction.....	75
Figure 4-19 Wind and Current Area Comparison .....	76
Figure 4-20 Mooring Pattern Layout #1.....	78
Figure 4-21 Elevation View of Vessel Bow and Anchor Leg: Calm Water. ....	81
Figure 4-22 200-yr Maximum Upstream Offset and Maximum Bow-Up Pitch. ..	81
Figure 4-23 3-Hour Simulation Relative Wave Elevation .....	82
Figure 4-24 Maximum Mooring Tension Load in Intact and Damage Cases .....	96
Figure 4-25 Environment Loadcase .....	97
Figure 4-26 Mooring Line Loads Summary.....	97
Figure 4-27 Vessel Low Frequency Offset: All Cases.....	99
Figure 4-28 Mooring Fatigue Design Curves.....	100
Figure 4-29 Summary of Fatigue Analysis .....	103

## LIST OF TABLES

Table 2-1 Turret Moored Units Typical and Behaviour .....	3
Table 3-1 Vessel Principal Particulars .....	28
Table 3-2 Wind Load Coefficients.....	30
Table 3-3 Current Load Coefficients .....	30
Table 3-4 Lateral Wind Screen for Topside.....	32
Table 3-5 Longitudinal Wind Screen for Topside .....	32
Table 3-6 Sample of MOSES Syntax .....	33
Table 3-7 A Sample Logging File to Estimate Heading Angles.....	40
Table 3-8 Geometry and Description.....	41
Table 3-9 Mooring Leg Properties.....	45
Table 3-10 Mooring Leg Lengths .....	45
Table 3-11 10-yr Return Period Environment Omni-Directional .....	48
Table 3-12 200-yr Return Period Environment Omni-Directional .....	48
Table 3-13 Mooring System Design Criteria.....	52
Table 4-1 Natural Period and Critical Damping .....	63
Table 4-2 Layout of Mooring Pattern .....	77
Table 4-3 Mooring Loads Summary Result.....	84
Table 4-4 Pile Anchor and Drag Anchor Design Load.....	87
Table 4-5 Summary of Fatigue Analysis .....	102



# 1. INTRODUCTION

## 1.1 Introduction

Design wave heading is to be in accordance with the operational conditions for the sea states contributing the most to the long term value of the dominant load effect (BV, 2010). The availability of berthing, connection, offloading and disconnection can be estimated on the basis of multi-vessel heading / mooring analysis for a significant amount of sea-states represented usually by time series of wind, current and wave (wind, sea & swell) over a large period of time (5 to 15 years: the larger the database, the better) (Jun, 2007)

From the heading analysis over each of the sea states contained in the time-series, the mean heading of the floating structure can be obtained. Then from the vessel heading, the relative heading of the vessel to the wind-sea, swell, wind and current could be derived, showing the trend of the floating structure behavior correlation with respect to the various metocean components. (Francois, 2004)

In the early 1960s, a new type of mooring system was developed for drillships. A rotating turret was inserted into the hull of The Offshore Company's "Discoverer I" and mooring lines were extended out from the bottom of the turret and anchored to the seabed in a circular pattern. This SPM system allowed the drillship to continuously weathervane into the predominant seas without interrupting on-board drilling activities. At the same time SPM fluid-transfer systems (CALM buoy systems) were also being developed to allow easy offloading of liquids in shallow water offshore. The production "turret mooring system" evolved from these two concepts and was adapted to F(P)SO units that had to remain on location to provide a reliable means for storage and offloading for years without incurring significant downtime regardless of environmental conditions. Today, two types of turret systems are commonly used for F(P)SOs – the internal turret system where the turret is mounted within the F(P)SO hull, and an external turret system where the turret is mounted on an extended structure cantilevered off the vessel bow. (London, 2001)

Heading sensitivity study is necessary to find out the optimum mooring system layout in accordance to highest environment load and also cyclic environment load as well. Even the most probable cyclic load has no highest environment load it can be caused a fatigue damage to the mooring system. A number of mooring pattern will be varied to be found the best mooring pattern options.

From heading analysis algorithm as proposed by (T. Terashima, 2011) and (Morandini, 2007) the important point is an angle where the moment at the turret position is zero or near to zero, gives the balance heading angle of the vessel. Because the behavior of turret is free from moment that showing weathervaning effect. In this study the static approach by double check static equilibrium which is faster and easier way to get the heading angles result. A double check static equilibrium approach is believed can speed up computation without compromising the quality outcomes. It should be noted that dynamic equilibrium by time domain simulation in minimum 10,800s (3hrs) is still believed the most accurate, but time demanding consequences.

## **1.2 Problem Definitions**

The problems are defined as follows:

1. The long-term response of weathervaneing turret moored floating unit in long-term seastate by heading analysis calculation.
2. The optimum mooring system design respect to heading analysis result.

## **1.3 Research Objective**

The objective are defined as follows:

1. Assess heading analysis outcome as function of heading probability occurrences of weathervaning turret moored floating units.
2. Identify optimum mooring layout design respect to heading analysis result.

## **1.4 Research Question**

The question are defined as follows:

*'How the importance of heading analysis in term of mooring system design is?'*

## **1.5 Hypothesis**

The hypothesis are defined as follows:

1. Numerous heading of floating unit will occurred relative to wave, wind, and current.
2. Heading analysis outcome will generated better hydrodynamic response condition rather than a normal practice.
3. Relative heading angles will be critical for structural strength response and fatigue life estimation.

## 2. LITERATURE STUDY AND THEORETICAL BACKGROUND

### 2.1 Literature Study

Heading analysis shall be necessary to be carried out for turret moored vessel unit. It was believed that such analysis would be a parameter for structural strength integrity and fatigue life estimation as well. Various hydrodynamic force and moment to be governed as per generated thousand number of sea state data respect to the scatter diagram. A fishtailing motions phenomenon would be occurred for single point moored units such a turret moored vessel due to time varying sea state. Failure of motions prediction will lead to lack of confidence for mooring design loads. Table 2.1 shown the behavior and typical of turret moored unit, it will be a prospect and constraint for this system depend on field condition (Howell, 2006).

**Table 2-1 Turret Moored Units Typical and Behaviour**

	Turret-Moored
Vessel orientation	360 degree weathervaning
Environment	Mild to extreme, directional to spread
Field layout	Fairly adaptable, partial to distributed flow line arrangements
Riser number & arrangement	Requires commitment, moderate expansion capability
Riser systems	Location of turret (bow) requires robust riser design
Stationkeeping performance	Number of anchor legs, offset minimized
Vessel motions	Weathervaning capability reduce motions
Vessel arrangement	Turret provides “compact” load and fluid transfer system
Offloading performance	FPSO typically aligned with mean environment

Basically heading analysis help the designers with regards to structural design, offloading operation, sloshing, green water and vessel kinematics assessment, as relative heading between waves and vessel is believed to be a critical parameter when assessing the extreme and fatigue performance of floating structure. (Morandini, 2007)

Problems relating to weathervaning have been reported due to yaw instability in various Floating, Production, Storage and Offloading (FPSO) systems operating around the world thus disrupting the production/deck operations. Hydrodynamic analyses are economical means of analyzing the dynamics of a turret based system when subjected to different sea states. (Yadav, 2007)

As part of experiments a series of model tests in regular waves were conducted. Numerical computations for linear motion response of the FPSO were conducted using well established boundary element packages. It is found that the model deviated significantly from linear behavior in cases where there were involuntary heading changes. (Munipalli, 2007)

## 2.2 Theoretical Background

Theoretical background is refer to ref (Journée, 2001) as stated is Section 2.2.1 through Section 2.2.3 in this report. The theory are cover wave prediction and climatology, wind loads, current loads, and wave drift forces and moments.

### 2.2.1 Wave Prediction and Climatology

In 1805, the British Admiral Sir Francis Beaufort devised an observation scale for measuring winds at sea. His scale measures winds by observing their effects on sailing ships and waves. Beaufort's scale was later adapted for use on land and is still used today by many weather stations. A definition of this Beaufort wind force scale is given in figure 2.1







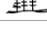

WIND SPEEDS					BEAUFORT WIND FORCE SCALE					
Beaufort Number	Knots	miles per hr. (U.S. Statute)	meters per sec.	km per hr.	Wind Press. $\frac{1}{2}$ N/m <sup>2</sup>	Beaufort description for square rigged ships 1806	Racing Sailor's description (C.A. Marchay, 1964)	U.S. Weather Service description	Dutch KNMI description	Beaufort Number
0	0	1	0	0	0			Calm	Windstil	0
1	1	3	0.5	2	0.14	Just Steerage Way	Boredom	Light air	zwakke	1
2	4	6	2.1	7	2.4	1-3 knots close hauled	Mild pleasure	Light breeze		2
3	7	10	3.6	13	7.7	4-5 knots close hauled	Pleasure	Gentle breeze	matige	3
4	11	16	5.7	20	19	6-7 knots close hauled	Great Pleasure	Moderate breeze		4
5	17	21	9	32	46	Hull Swept Full Sail	 Delight	Fresh breeze	vrij krachtige	5
6	22	27	11	41	77	115	 Delight tinged with anxiety	Strong breeze	krachtige	6
7	28	33	14	52	125	172	 Anxiety tinged with fear	Moderate Gale	harde	7
8	34	40	18	63	182	250	 Fear tinged with terror	Gale	stormachtige	8
9	41	47	21	76	270	350	 Great terror	Strong Gale	storm	9
10	48	55	25	89	360	480	 Panic	Whole Gale	zware storm	10
11	56	63	29	104	500	630	 I want my mummy!!	Storm	zeer zware storm	11
12	above 63	above 75	above 33	above 120	above 630	bare poles	 Yes, Mr. Jones	Hurricane	orkaan	12

Figure 2-1 Beaufort's Wind Force Scale



## Long Term Wave Prediction

Longer term wave climatology is used to predict the statistical chance that a given wave sensitive offshore operation - such as lifting a major top-side element into place - will be delayed by sea conditions which are too rough. The current section treats the necessary input data on wave climate.

In general, wave climatology often centers on answering one question: What is the chance that some chosen threshold wave condition will be exceeded during some interval – usually days, weeks or even a year? To determine this, one must collect - or obtain in some other way such as outlined in the previous section - and analyze the pairs of data ( $H_{1/3}$  and  $T$ ) and possibly even including the wave direction,  $\mu$ , as well) representing each 'storm' period.

## Wave Scatter Diagram

Sets of characteristic wave data values can be grouped and arranged in a table such as that given below based upon data from the northern North Sea. A 'storm' here is an arbitrary time period - often of 3 or 6 hours - for which a single pair of values has been collected.

The number in each cell of this table indicates the chance (on the basis of 1000 observations in this case) that a significant wave height (in meters) is between the values in the left column and in the range of wave periods listed at the top and bottom of the table. Figure below shows a graph of this table.

$H_{sig}$ (m)	4-5	5-6	6-7	7-8	8-9	9-10	10-11	11-12	12-13	13-14	$\Sigma_{row}$
>12											
11.5-12.0						0+		0+			1
11.0-11.5											
10.5-11.0											
10.0-10.5											
9.5-10.0					0+		1		0+		2
9.0-9.5							0+		0+		1
8.5-9.0						1	1	1	1		4
8.0-8.5						1	1	0+			2
7.5-8.0					0+	1	2	1	1		6
7.0-7.5					1	2	3		1		7
6.5-7.0					1	5	3	1	0+		10
6.0-6.5					4	7	4	1	1	0+	17
5.5-6.0				2	5	7	3	2			19
5.0-5.5				4	10	8	3	1	1	0+	26
4.5-5.0			1	11	18	9	1	1	0+	0+	36
4.0-4.5			3	14	16	12	3	2	1		50
3.5-4.0			5	19	20	9	4	1	1		72
3.0-3.5		1	21	28	21	12	6	1			93
2.5-3.0		3	37	37	23	7	3	1	1		104
2.0-2.5		14	52	52	21	8	4	1			154
1.5-2.0	1	28	49	26	21	18	6	1	1		156
1.0-1.5	6	34	42	29	19	13	5	1	0+		138
0.5-1.0	1	8	15	16	11	4	1	1	0+		35
0.0-0.5		1	0+			0+					3
Periods--	4-5	5-6	6-7	7-8	8-9	9-10	10-11	11-12	12-13	$\Sigma_{col}$	1
										Total	1000

Wave Climate Scatter Diagram for Northern North Sea

Note: 0+ in this table indicates that less than 0.5 observation in 1000 was recorded for the given cell.

This scatter diagram includes a good distinction between sea and swell. As has already been explained early in this chapter, swell tends to be low and to have a relatively long period. The cluster of values for wave heights below 2 meters with periods greater than 10 seconds is typically swell in this case.

Winter Data of Areas 8, 9, 15 and 16 of the North Atlantic (Global Wave Statistics)												
	$T_2$ (s)											
$H_{1/3}$ (m)	3.5	4.5	5.5	6.5	7.5	8.5	9.5	10.5	11.5	12.5	13.5	Total
14.5	0	0	0	0	2	30	154	362	466	370	202	1556
13.5	0	0	0	0	3	33	145	293	322	219	101	1116
12.5	0	0	0	0	7	72	289	539	548	345	149	1949
11.5	0	0	0	0	17	160	585	996	931	543	217	3449
10.5	0	0	0	1	41	263	1200	1852	1579	843	310	6159
9.5	0	0	0	4	109	845	2485	3443	2648	1283	432	11249
8.5	0	0	0	12	295	1996	5157	6223	4323	1882	572	20570
7.5	0	0	0	41	818	4723	10637	11242	6755	2594	703	37413
6.5	0	0	1	138	2273	10967	20620	18718	9665	3222	767	66371
5.5	0	0	7	471	6187	24075	36940	27702	11969	3387	694	111432
4.5	0	0	31	1388	15757	47072	56347	33539	11710	2731	471	169244
3.5	0	0	145	5017	34720	74007	64809	28964	7504	1444	202	217115
2.5	0	4	681	13441	56847	77259	45013	13962	2725	381	41	216384
1.5	0	40	2699	23254	47539	34532	11534	2208	282	27	2	122467
0.5	5	350	3314	8131	5538	1393	316	18	1	0	0	13491
Total	5	364	6581	52126	170773	277732	256031	150161	61738	19271	4863	999996

A second example of a wave scatter diagram is the table below for all wave directions in the winter season in areas 8, 9, 15 and 16 of the North Atlantic Ocean, as obtained from Global Wave Statistics.

These wave scatter diagrams can be used to determine the long term probability for storms exceeding certain sea states. Each cell in this table presents the probability of occurrence of its significant wave height and zero-crossing wave period range. This probability is equal to the number in this cell divided by the sum of the numbers of all cells in the table, for instance:

$$\Pr\{4 < H_{1/3} < 5 \text{ and } 8 < T_2 < 9\} = \frac{47072}{999996} = 0.047 = 4.7\%$$

For instance, the probability on a storm with a significant wave height between 4 and 6 meters with a zero-crossing period between 8 and 10 seconds is:

$$\Pr\{3 < H_{1/3} < 5 \text{ and } 8 < T_2 < 10\} = \frac{47072 + 5643 + 74007 + 64809}{999996} = 0.242 = 24.2\%$$

The probability for storms exceeding a certain significant wave height is found by adding the numbers of all cells with a significant wave height larger than this certain significant wave height and dividing this number by the sum of the numbers in all cells, for instance:

$$\Pr\{H_{1/3} > 10\} = \frac{6189 + 3449 + 1949 + 1116 + 1586}{999996} = 0.014 = 1.4\%$$

Note that the above scatter diagram is based exclusively on winter data. Such diagrams are often available on a monthly, seasonal or year basis. The data in these can be

quite different; think of an area in which there is a very pronounced hurricane season, for example. Statistically, the North Sea is roughest in the winter and smoothest in summer.

### 2.2.2 Wind Loads

Like all environmental phenomena, wind has a stochastic nature which greatly depends on time and location. It is usually characterized by fairly large fluctuations in velocity and direction. It is common meteorological practice to give the wind velocity in terms of the average over a certain interval of time, varying from 1 to 60 minutes or more.

Local winds are generally defined in terms of the average velocity and average direction at a standard height of 10 meters above the still water level. A number of empirical and theoretical formulas are available in the literature to determine the wind velocity at other elevations. An adequate vertical distribution of the true wind speed  $z$  meters above sea level is represented by:

$$\frac{V_{tw}(Z)}{V_{tw}(10)} = \left(\frac{Z}{10}\right)^{0.11} \quad (\text{at sea}) \quad (2.1)$$

In which:

$V_{tw}(z)$  = true wind speed at  $z$  meters height above the water surface

$V_{tw}(10)$  = true wind speed at 10 meters height above the water surface

Equation 2.1 is for sea conditions and results from the fact that the sea is surprisingly smooth from an aerodynamic point of view - about like a well mowed soccer field.

On land, equation 4.48 has a different exponent:

$$\frac{V_{tw}(Z)}{V_{tw}(10)} = \left(\frac{Z}{10}\right)^{0.16} \quad (\text{on land}) \quad (2.2)$$

At sea, the variation in the mean wind velocity is small compared to the wave period. The fluctuations around the mean wind speed will impose dynamic forces on an offshore structure, but in general these aerodynamic forces may be neglected in comparison with the hydrodynamic forces, when considering the structures dynamic behavior. The wind will be considered as steady, both in magnitude and direction, resulting in constant forces and a constant moment on a fixed floating or a sailing body.

The wind plays two roles in the behavior of a floating body:

- Its first is a direct role, where the wind exerts a force on the part of the structure exposed to the air. Wind forces are exerted due to the flow of air around the various parts. Only local winds are needed for the determination of these forces.
- The second is an indirect role. Winds generate waves and currents and through these influence a ship indirectly too. To determine these wind effects, one needs

information about the wind and storm conditions in a much larger area. Wave and current generation is a topic for oceanographers; the effects of waves and currents on floating bodies will be dealt with separately in later chapters.

Only the direct influence of the winds will be discussed here.

Forces and moments will be caused by the speed of the wind relative to the (moving) body. The forces and moments which the wind exerts on a structure can therefore be computed by:

$$\begin{aligned}
 X_w &= \frac{1}{2} \rho_{air} V_{rw}^2 \cdot C_{Xw}(\alpha_{rw}) \cdot A_T \\
 Y_w &= \frac{1}{2} \rho_{air} V_{rw}^2 \cdot C_{Yw}(\alpha_{rw}) \cdot A_L \\
 N_w &= \frac{1}{2} \rho_{air} V_{rw}^2 \cdot C_{Nw}(\alpha_{rw}) \cdot A_L \cdot L
 \end{aligned} \tag{2.3}$$

In which:

$X_w$	= steady longitudinal wind force (N)
$Y_w$	= steady lateral wind force (N)
$N_w$	= steady horizontal wind moment (Nm)
$\rho_{air} \approx \rho_{water}/800$	= density of air (kg/m <sup>3</sup> )
$V_{rw}$	= relative wind velocity (m/s)
$\alpha_w$	= relative wind direction (-), from astern is zero
$A_T$	= transverse projected wind area (m <sup>2</sup> )
$A_L$	= lateral projected wind area (m <sup>2</sup> )
$L$	= length of the ship (m)
$C^*_w(\alpha_{rw})$	= $\alpha_{rw}$ - dependent wind load coefficient (-)

Note that it is a "normal" convention to refer to the true wind direction as the direction from which the wind comes, while waves and currents are usually referred to in terms of where they are going. A North-West wind will cause South-East waves, therefore!

### Wind Loads on Moored Ships

For moored ships, only the true wind speed and direction determine the longitudinal and lateral forces and the yaw moment on the ship, as given in figure 2.2. Because of the absence of a steady velocity of the structure, the relative wind is similar to the true wind:

$$V_{rw} = V_{tw} \text{ and } \alpha_{rw} = \alpha_{tw} \tag{2.4}$$

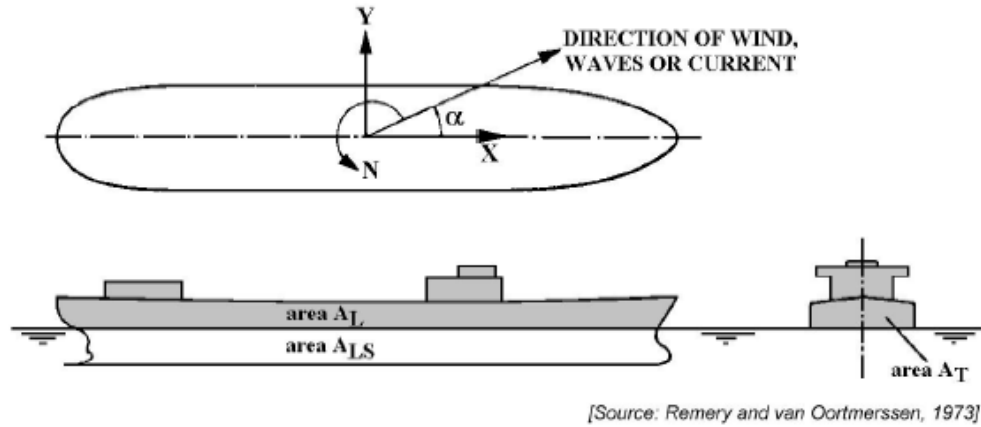


**Figure 2-2 Definitions Used here for Forces and Moments**

The total force and moment experienced by an object exposed to the wind is partly of viscous origin (pressure drag) and partly due to potential effects (lift force). For blunt bodies, the wind force is regarded as independent of the Reynolds number and proportional to the square of the wind velocity.

(Remery and van Oortmerssen, 1973) collected the wind data on 11 various tanker hulls. Their wind force and moment coefficients were expanded in Fourier series as a function of the angle of incidence. From the harmonic analysis, it was found that a fifth order representation of the wind data is sufficiently accurate, at least for preliminary design purposes:

$$\begin{aligned}
 C_{Xw} &= a_0 + \sum_{n=1}^5 a_n \sin(n. \alpha_{rw}) \\
 C_{Yw} &= \sum_{n=1}^5 b_n \sin(n. \alpha_{rw}) \\
 C_{Nw} &= \sum_{n=1}^5 c_n \sin(n. \alpha_{rw})
 \end{aligned}
 \tag{2.5}$$

with wind coefficients as listed below.

Tanker No. Length $L_{pp}$ Condition Bridge Location	1 loaded at $\frac{1}{2}L$	2 ballast at $\frac{1}{2}L$	3 loaded aft	4 ballast aft	5 225 m loaded at $\frac{1}{2}L$	6 225 m ballast at $\frac{1}{2}L$	7 225 m loaded aft	8 225 m ballast aft	9 172 m loaded aft	10 150 m loaded aft	11 150 m ballast aft
$a_0$	-0.121	-0.079	-0.022	0.014	-0.074	-0.055	-0.038	-0.039	-0.042	-0.075	-0.051
$a_1$	0.722	0.615	0.799	0.732	1.050	0.742	0.830	0.646	0.427	0.711	0.577
$a_2$	-0.052	-0.104	-0.077	-0.055	0.017	0.018	0.031	0.034	-0.072	-0.052	-0.052
$a_3$	0.059	0.025	-0.054	-0.017	-0.062	-0.012	0.012	0.024	0.109	0.043	0.051
$a_4$	0.102	0.076	0.012	-0.012	0.020	0.015	0.021	-0.031	0.075	0.064	0.062
$a_5$	-0.001	0.025	-0.012	-0.052	-0.110	-0.151	-0.072	-0.090	-0.047	-0.022	0.006
$b_1$	0.726	0.820	0.697	0.725	0.707	0.731	0.712	0.735	0.764	0.219	0.279
$b_2$	0.039	0.004	0.026	0.014	-0.012	-0.014	0.022	0.003	0.037	0.051	0.025
$b_3$	0.007	0.002	0.012	0.014	0.022	0.016	0.010	0.004	0.052	0.023	0.014
$b_4$	0.024	-0.004	0.022	0.015	0.007	0.001	-0.001	-0.005	0.012	0.022	0.021
$b_5$	-0.019	-0.003	-0.022	-0.020	-0.044	-0.025	-0.040	-0.017	-0.003	-0.022	-0.029
$10 \cdot c_1$	-0.451	-0.322	-0.765	-0.524	-0.216	-0.059	-0.526	-0.325	-1.025	-0.221	-0.244
$10 \cdot c_2$	-0.617	-0.200	-0.571	-0.722	-0.531	-0.720	-0.596	-0.722	-0.721	-0.621	-0.722
$10 \cdot c_3$	-0.110	-0.020	-0.102	-0.175	-0.062	-0.025	-0.111	-0.090	-0.245	-0.202	-0.244
$10 \cdot c_4$	-0.110	-0.096	-0.146	-0.029	-0.072	-0.017	-0.112	-0.047	-0.127	-0.145	-0.076
$10 \cdot c_5$	-0.010	-0.012	0.021	-0.021	0.024	-0.012	0.009	0.067	-0.022	0.020	0.024

Figure 2.3 shows, as an example, the measured wind forces and moment together with their Fourier approximation, for one of the tankers.

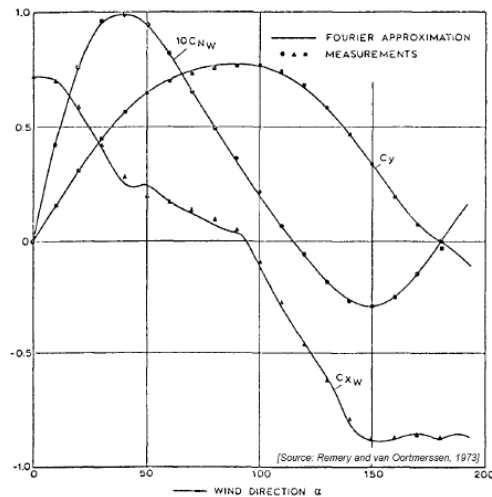


Figure 2-3 Example of Wind Load Coefficients

### Wind Loads on Other Moored Structures

The wind forces on other types of structures, as for instance semi-submersible platforms, can be approximated by dividing the structure into a number of components, all with a more or less elementary geometry, and estimating the wind force on each element. Drag coefficients are given in the literature for a lot of simple geometrical forms, such as spheres, Flat plates and cylinders of various cross sectional shapes. (Hoerner, 1965) and (Delany and Sorensen, 1970) are good sources of this information. The total wind load on the structure is found by adding the contributions of all the individual component parts. The fact that one element may influence the wind field of another element is neglected in this analysis.

### 2.2.3 Current Loads

There are several independent phenomena responsible for the occurrence of current: the ocean circulation system resulting in a steady current, the cyclical change in lunar and solar gravity causing tidal currents, wind and differences in sea water density. The steady wind velocity at the water surface is about 3 per cent of the wind velocity at 10 meters height. Tidal currents are of primary importance in areas of restricted water depth and can attain values up to 10 knots. However, such extreme velocities are rare; a 2-3 knots tidal current speed is common in restricted seas. The prediction of tidal currents is left for the oceanographers.

Although surface currents will be the governing ones for floating structures; the current distribution as a function of depth below the surface may also be of importance. For the design of a mooring system of a floating structure, the designer is especially interested in the probability that a particular extreme current velocity will be exceeded during a certain period of time. Observations obtained from current speed measurements are indispensable for this purpose. It may be useful to split up the total measured current in two or more components, for instance in a tidal and a non-tidal component, since the direction of the various components will be different, in general. The variation in velocity and direction of the current is very slow, and current may therefore be considered as a steady phenomenon.

The forces and moment exerted by a current on a floating object is composed of the following parts:

- A viscous part, due to friction between the structure and the fluid, and due to pressure drag. For blunt bodies the frictional force may be neglected, since it is small compared to the viscous pressure drag.
- A potential part, with a component due to a circulation around the object, and one from the free water surface wave resistance. In most cases, the latter component is small in comparison with the first and will be ignored.

The forces and moments, as given in figure 2.2, exerted by the current on a floating structure can be calculated from:

$$\begin{aligned}X_c &= \frac{1}{2} \rho \cdot V_c^2 \cdot C_{Xc}(\alpha_c) \cdot A_{TS} \\Y_c &= \frac{1}{2} \rho V_c^2 \cdot C_{Yc}(\alpha_c) \cdot A_{LS} \\N_c &= \frac{1}{2} \rho \cdot V_c^2 \cdot C_{Nc}(\alpha_c) \cdot A_{LS} \cdot L\end{aligned}\tag{2.6}$$

In which:

$X_c$	= steady longitudinal current force (N)
$Y_c$	= steady lateral current force (N)
$N_c$	= steady horizontal current moment (Nm)
$\rho$	= density of water (kg/m <sup>3</sup> )
$V_c$	= relative current velocity (m/s)
$\alpha_c$	= relative current direction (-), from astern is

zero

$A_{TS} \approx B.T$	= transverse projected current area (m <sup>2</sup> )
$A_{LS} \approx L.T$	= lateral projected current area (m <sup>2</sup> )
$L$	= length of the ship (m)
$B$	= breadth of the ship (m)
$T$	= draft of the ship (m)
$C_c(\alpha_c)$	= $\alpha_c$ - dependent current load coefficient (-)

### Current Loads on Moored Tankers

(Remery and van Oortmerssen, 1973) published current loads on several tanker models of different sizes, tested at MARIN. The coefficients  $C_{Xc}$ ,  $C_{Yc}$  and  $C_{Nc}$  were calculated from these results. A tanker hull is a rather slender body for a flow in the longitudinal direction and consequently the longitudinal force is mainly frictional. The total longitudinal force was very small for relatively low current speeds and could not be measured accurately. Moreover, extrapolation to full scale dimensions is difficult, since the longitudinal force is affected by scale effects.

For mooring problems the longitudinal force will hardly be of importance. An estimate of its magnitude can be made by calculating the flat plate frictional resistance, according to the ITTC skin friction line as given in equation:

$$ITTC - 1957: C_f = \frac{0.075}{(\log_{10}(Rn) - 2)^2} \quad (2.7)$$

$$X_c = \frac{0.075}{(\log_{10}(Rn) - 2)^2} \cdot \frac{1}{2} \rho V_c^2 \cdot \cos \alpha_c \cdot |\cos \alpha_c| \cdot S \quad (2.8)$$

While:

$$Rn = \frac{V_c \cdot |\cos \alpha_c| \cdot L}{\nu} \quad (2.9)$$

With:

$$S \approx L \cdot (B + 2T) = \text{wetted surface of the ship (m}^2\text{)}$$



$L$	= length of the ship (m)
$B$	= breadth of the ship (m)
$T$	= draft of the ship (m)
$V_c$	= current velocity (m/s)
$\alpha_c$	= current direction (-), from astern is zero
$\rho$	= density of water (ton/m <sup>3</sup> )
$Rn$	= Reynolds number (-)
$\nu$	= kinematic viscosity of water (m <sup>2</sup> /s)

Extrapolation of the transverse force and yaw moment to prototype values is no problem. For flow in the transverse direction a tanker is a blunt body and, since the bilge radius is small, flow separation occurs in the model in the same way as in the prototype. Therefore, the transverse force coefficient and the yaw moment coefficient are independent of the Reynolds number.

The coefficients for the transverse force and the yaw moment were expanded by MARIN in a Fourier series, as was done for the wind load coefficients as described in a previous section:

$$C_{Yc} = \sum_{n=1}^5 b_n \sin(n \cdot \alpha_c)$$

$$C_{Nc} = \sum_{n=1}^5 c_n \sin(n \cdot \alpha_c) \quad (2.10)$$

The average values of the coefficients  $b_n$  and  $c_n$  for the fifth order Fourier series, as published by (Remery and van Oortmerssen, 1973), are given in the table below.

$n$	$b_n$	$10 \cdot c_n$
1	0.908	-0.252
2	0.000	-0.904
3	-0.116	0.032
4	0.000	0.109
5	-0.033	0.011

These results are valid for deep water. For shallow water, the transverse current force and moment coefficients have to be multiplied by a coefficient, which is given in figure 4.15. The influence of the free surface is included in the data given on the coefficients  $b_n$  and  $c_n$  in the previous table. This influence, however, depends on the water depth and on the Froude number, and consequently changes if the current velocity or the tanker

dimensions change. For the condition to which these data apply, deep water and a prototype current speed in the order of 3 knots, the effect of the free surface is very small. For the case of a small clearance under the keel and a current direction of 90 degrees, damming up of the water at the weather side and a lowering of the water at the lee side of the ship occurs.

### **Current Loads on Other Moored Structures**

Current loads on other types of floating structures are usually estimated in the same way as is used for wind loads.

#### **2.2.4 Wave Drift Forces and Moments**

The theory relating to second order wave drift forces has been treated in this chapter. Some results of computations have been compared with results derived analytically and by means of model tests. These results apply to the mean drift forces in regular waves, which can be used to estimate the mean and low frequency drift forces in irregular waves. The low frequency part of the wave drift forces should theoretically, be determined by considering the drift forces in regular wave groups. In such cases the second order potential also contributes to the force, see (Pinkster, 1980). (Faltinsen and Loken, 1979) have indicated that, for vessels floating in beam seas, the sway drift forces calculated using only information on the mean drift forces in regular waves gives results which are sufficiently accurate for engineering purposes. Results given by (Pinkster and Hooft, 1978) and (Pinkster, 1979) on the low frequency drift forces on a barge and a semi-submersible in head waves generally confirms the conclusion provided the frequency of interest is low. Frequencies of interest for moored vessels are the natural frequencies of the horizontal motions induced by the presence of the mooring system. In some cases the natural frequencies of vertical motions can also be of interest from the point of view of vertical motions induced by the low frequency wave drift forces. It can be shown that, in at least one case, the mean wave drift forces in regular waves cannot be used to estimate the low frequency drift forces in irregular waves. This case concerns the low frequency sway drift force on a free floating, submerged cylinder in beam seas. According to (Ogilvie, 1963), the mean wave drift force in regular waves is zero for all wave frequencies. This means that the low frequency wave drift force in irregular waves estimated using only the mean wave drift force will be zero as well. Computations carried out using the method given by (Pinkster, 1979) which determines the low frequency force in regular wave groups show that this will not be true.

Wave drifting forces in the horizontal directions, which are non-dimensionalized can be calculated from:

$$\begin{aligned}
 F_{dx} &= 1/2 \rho_w g \zeta_a^2 \cdot C_{dx} \cdot B \\
 F_{dy} &= 1/2 \rho_w g \zeta_a^2 \cdot C_{dy} \cdot L \\
 M_{dz} &= 1/2 \rho_w g \zeta_a^2 \cdot C_{dm} \cdot LB
 \end{aligned}
 \tag{2.11}$$

With

- $\rho_w$  = water density
- $g$  = gravity acceleration
- $\zeta_a$  = incident wave amplitude

### 2.2.5 Sea Loads

When the size of the structure is comparable to the length of wave, the pressure on the structure may alter the wave field in the vicinity of the structure. In the calculation of wave forces, it is then necessary to account for the diffraction of the waves from the surface of the structure and the radiation of the wave from the structure if it moves (Chakrabarti, 1987).

**First Order Potential Forces:** Panel methods (also called boundary element methods, integral equation methods or sink-source methods) are the most common techniques used to analyze the linear steady state response of large-volume structures in regular waves (Faltinsen, 1990). They are based on potential theory. It is assumed that the oscillation amplitudes of the fluid and the body are small relative to cross-sectional dimension of the body. The methods can only predict damping due to radiation of surface waves and added mass. But they do not cover viscous effects. In linear analysis of response amplitude operator (RAO), forces and response are proportional to wave amplitude and response frequency are primarily at the wave frequency.

**Second Order Potential Forces:** The second order analysis determines additional forces and responses that are proportional to wave amplitude squared. The second order forces include steady force, a wide range of low frequency forces (which will excite surge, sway and yaw of a moored floating system) and high frequency forces (which will excite roll, pitch and heave springing of a TLP). The most common way to solve non-linear wave-structure problems is to use perturbation analysis with the wave amplitude as a small parameter. The non-linear problem is solved in second-order (Faltinsen, 1990).

### 2.2.6 Floating Structure Dynamics

Dynamic response of an offshore structure includes the sea-keeping motion of the vessel in waves, the vibration of the structure, and the response of the moored systems. The response of an offshore structure may be categorized by frequency-content as below:

- Wave-frequency response: response with period in the range of 5 - 15 seconds. This is the ordinary sea-keeping motion of a vessel. It may be calculated using the first-order motion theory.
- Slowly-varying response: response with period in the range of 100 - 200 seconds. This is the slow drift motion of a vessel with its moorings. The slowly-varying response is of equal importance as the linear first-order motions in design of mooring and riser systems. Wind can also result in slowly-varying oscillations of marine structures with high natural periods. This is caused by wind gusts with significant energy at periods of the order of magnitude of a minute.
- High-frequency response: response with period substantially below the wave period. For ocean-going ships, high frequency springing forces arise producing a high-frequency structural vibration that is termed whipping (Bhattacharyya, 1978). Owing to the high axial stiffness of the tethers, TLPs have natural periods of 2 to 4 seconds in heave, roll and pitch. Springing is a kind of resonance response to a harmonic oscillation (CMPT, 1998).
- Impulsive response: Slamming occurs on the ship/platform bottoms when impulse loads with high-pressure peaks are applied as a result of impact between a body and water. Ringing of TLP tethers is a kind of transient response to an impulsive load. The high frequency response and impulsive response cannot be considered independently of the structural response. Hydroelasticity is an important subject.

### 2.2.7 Fatigue Analysis

Fundamentally, the fatigue analysis approaches in engineering applications can be subdivided into the following categories:

- S-N based fatigue analysis approach
- The local stress or strain approach where the calculation includes the local notch effects in addition to the general stress concentration
- The fracture mechanics approach which gives allowance for the effects of cracks in the structure

These approaches have been well implemented in the fatigue design and assessment. However, fatigue limit state design is still one of the most difficult topics in structural design, assessment or reassessment. For marine structures, additional complications arise because of the corrosive environment. The fundamental difficulties associated with fatigue problems are related to:

- Lack of understanding of some of the underlying phenomena at both the microscopic and macroscopic levels
- Lack of accurate information on the parameters affecting the fatigue life of a structure

The general explicit fatigue design by analysis of marine structures involves a complex procedure. The dominant cause of the cyclic stresses within a marine structure is due to the sea environment that it experiences. Therefore, a fatigue assessment requires a description of the sea environment, or sequence of seastates, in which the structure is likely to meet over its planned operational life. Vessel motions, wave pressures, stress transfer functions, and the resulting fatigue stresses (generally expressed in terms of the number of cycles of various stress ranges) at locations of potential crack sites (hotspot) are then calculated. In order to describe the fatigue durability of joints of marine structures, experimental data based S-N curves are selected or fracture mechanics models are applied. This demand and capability information is then used to calculate fatigue lives via a damage summation process (typically via the Palmgren-Miner hypothesis) or critical crack size. This procedure is summarized as:

- Characterization of the Sea Environment
- Hydrodynamic Response Analysis
- Structural Analysis
- Stress Transfer Function
- Stress Concentration Factor
- Hotspot Stress Transfer Function
- Long-term Stress Range
- Selection of S-N Curves
- Fatigue Analysis and Design
- Fatigue Reliability Analysis
- Inspection, Maintenance, and Repair Plan



### 3. METHODOLOGY

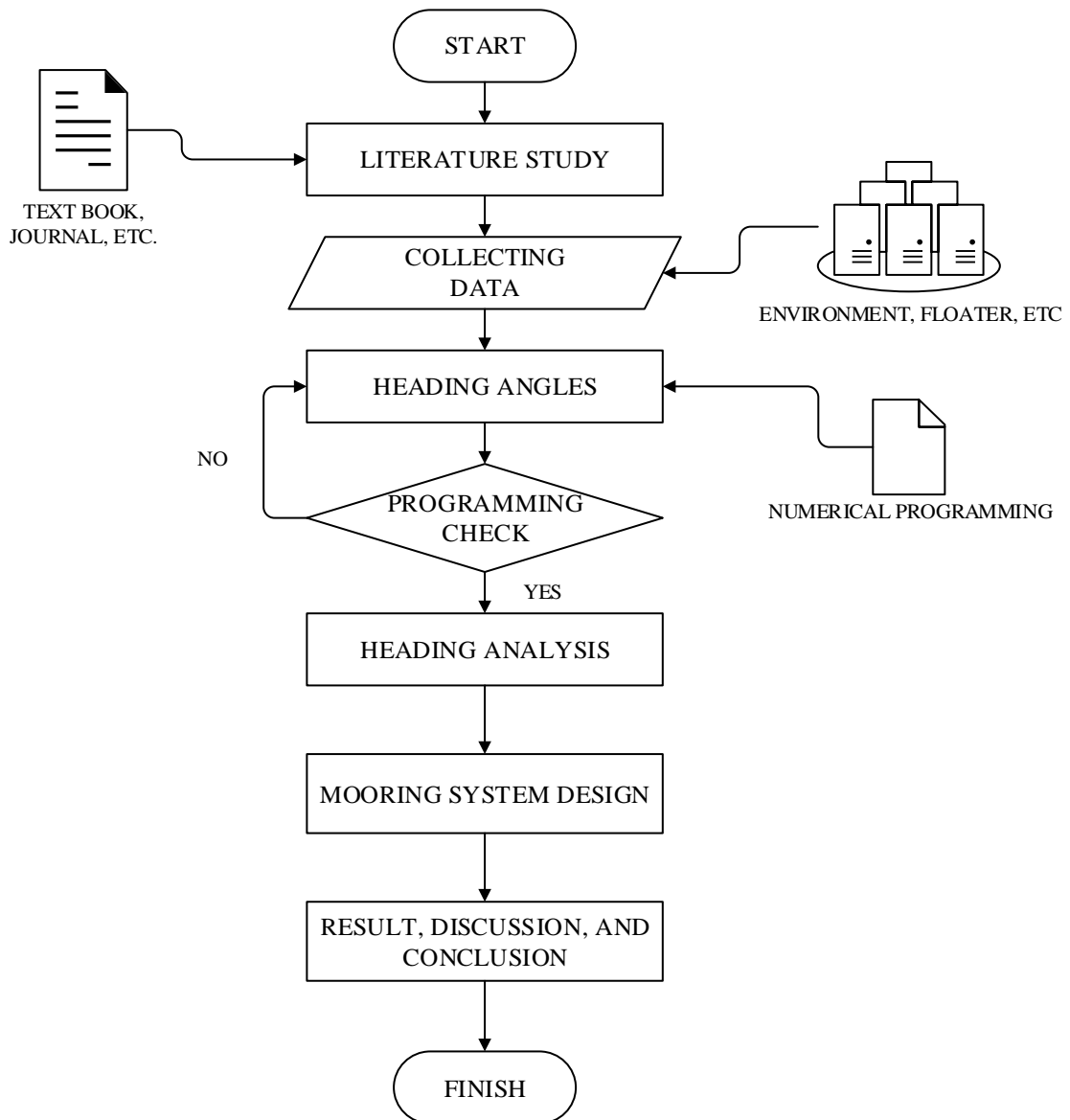


**Figure 3-1 Analysis Methodology**

There are three main step to perform heading analysis:

1. Collect and gather necessary data to enable proper heading analysis, ie environment data, vessel data, and another supporting data.
2. Build and generate numerical model of vessel by describing the capability to weathervane with respect to wind, current, and wave.
3. Assess the mean heading of the unit under the environment of each element of the environmental database.

### 3.1 Environment Data

Metoccean data are generally given in design data reports, in a statistical form that eliminates information of simultaneous occurrence of wave, wind, and current. Such information can be found on databases from hindcast or site measurements that normally form the source of design data. Such information is essential for any heading analysis and shall be provided for certain number of years, 2 years is believed being the absolute minimum.

Environment data that will be used for this research are presented in Figure 3-2 through Figure 3-11, totally 28,209 cases. Direction of wind, current, wave/swell is defined zero when towards North and to increase Counter-Clockwise. The longterm analysis will be conducted to obtain several heading angles of the units and to optimize mooring system design purpose.

As can be seen in Figure 3-2 and Figure 3-3 the relation between wind direction and wind speed is presented. A lump easterly winds are prevailing in winter and westerly winds are prevailing in summer. A strong wind more than 15 m/s (29 knots) are occurred mainly for westerly winds.

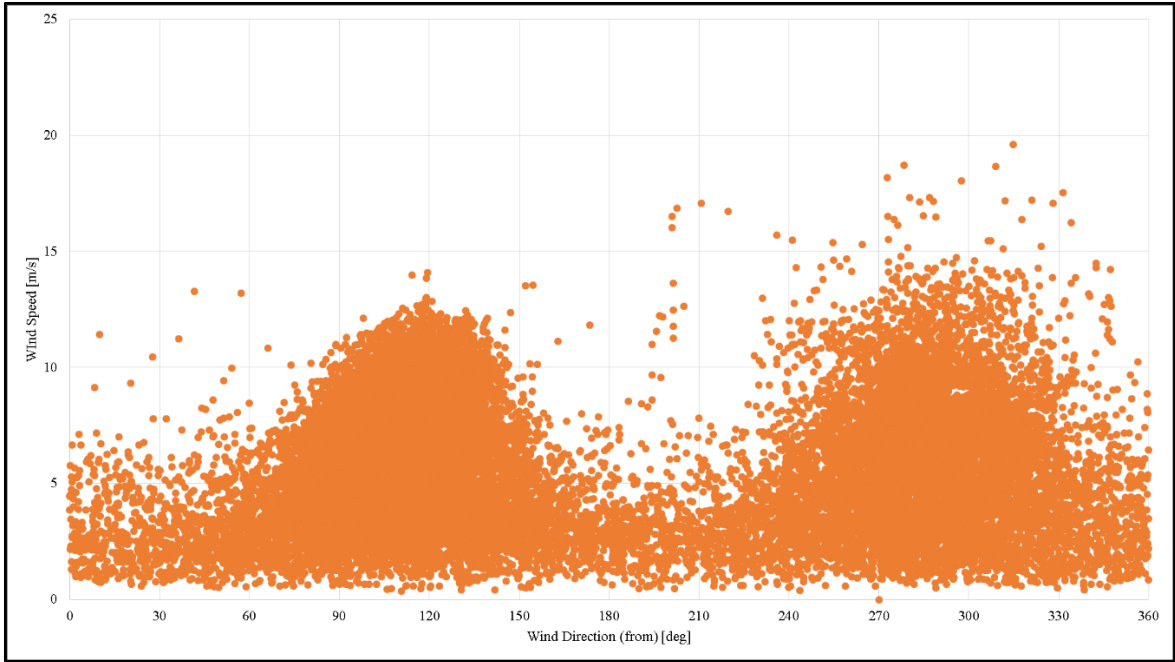
Current data are available in Figure 3-4 and Figure 3-5 show the relation between wind direction and wind speed, also the annual probability of them. Where easterly current and northerly current mainly to prevail.

Wind wave data are shown in Figure 3-6 and Figure 3-7, the relation between wave direction and significant wave height. Wave data are divided onto easterly waves and westerly wave. In the referring Figure, total annual probability of easterly waves is 100% and respectively for westerly waves. The figure showing two waves system are coexisting. Maximum value of significant wave height of westerly waves is larger than easterly waves because of stronger westerly waves winds.

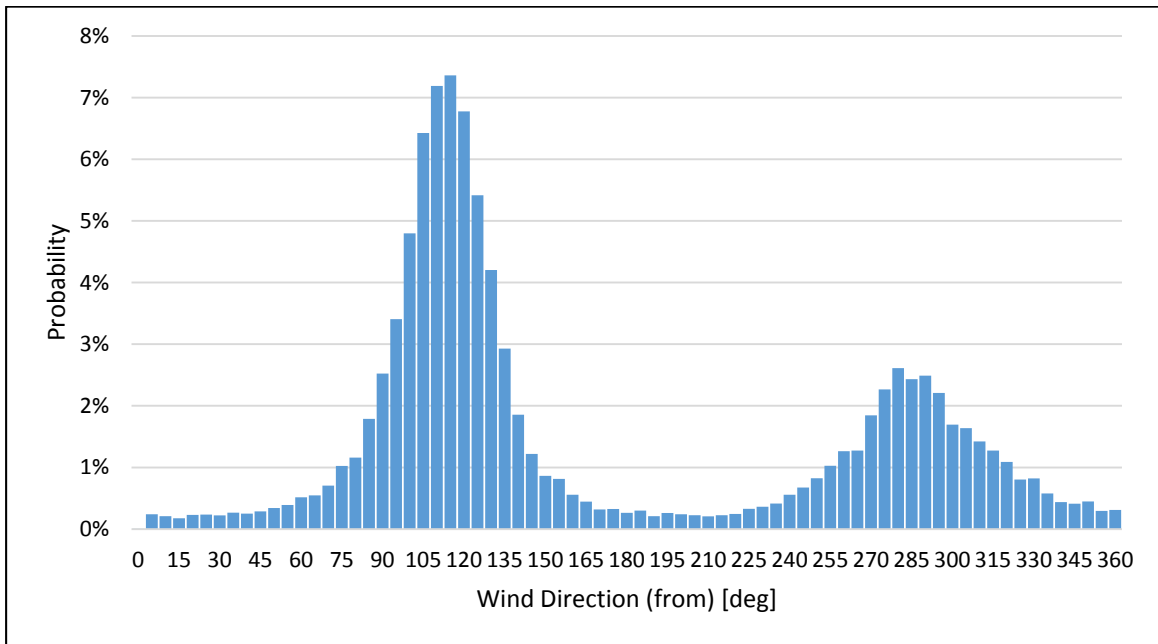
Swell occurrence as shown in Figure 3-8 and Figure 3-9 is almost limited to 240deg South West. Swell height is predicted up to 3.18 meter, which implies that large roll motions will be attributed to large swell.

Figure 3-10 and Figure 3-11 indicated the relation between wave peak period and significant wave height. As seen swell could be occurred at high wave peak period during low significant wave height.





**Figure 3-2 Relation between Wind Direction and Wind Speed**



**Figure 3-3 Annual Probability of Wind Direction**

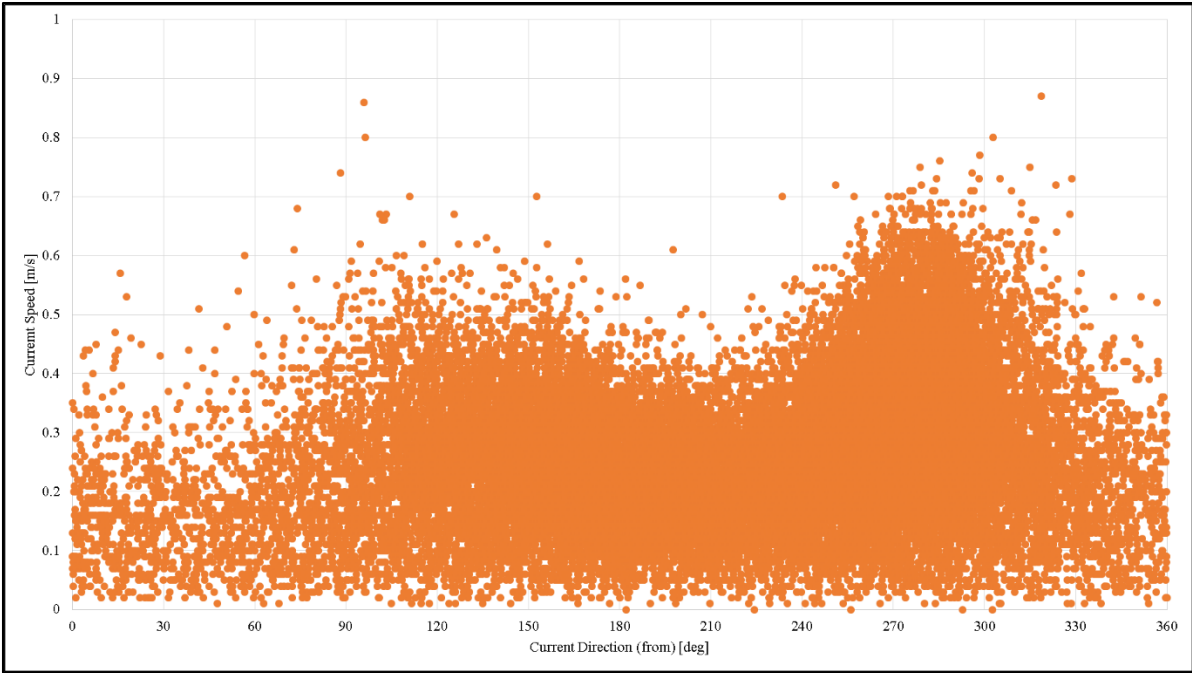


**Figure 3-4 Relation between Current Direction and Current Speed**

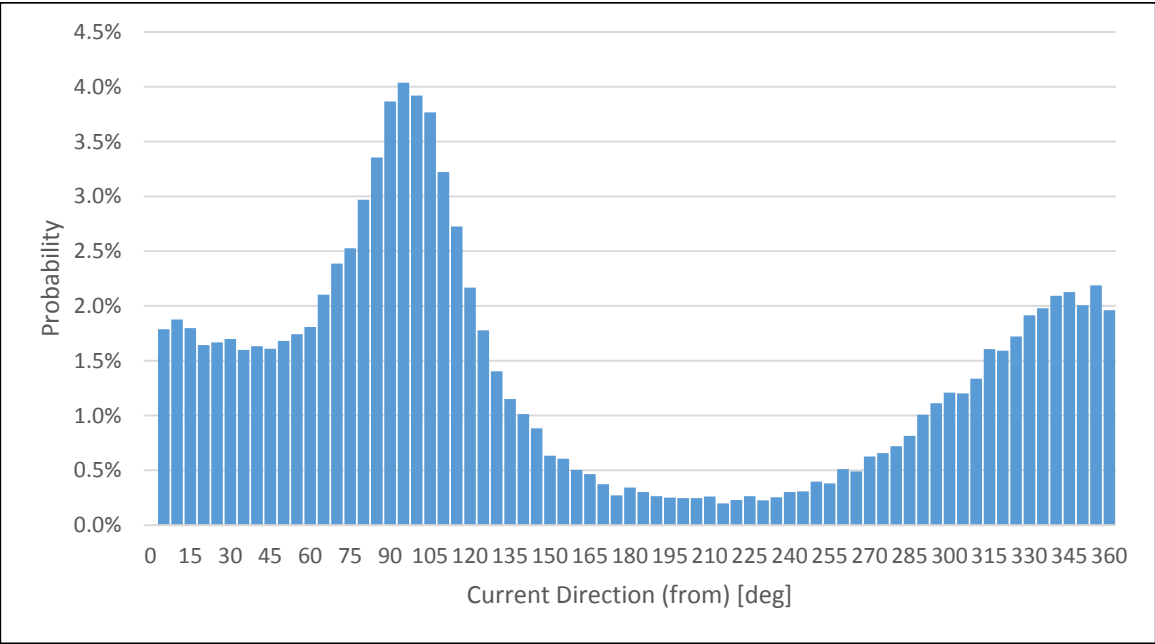


**Figure 3-5 Annual Probability of Current Direction**

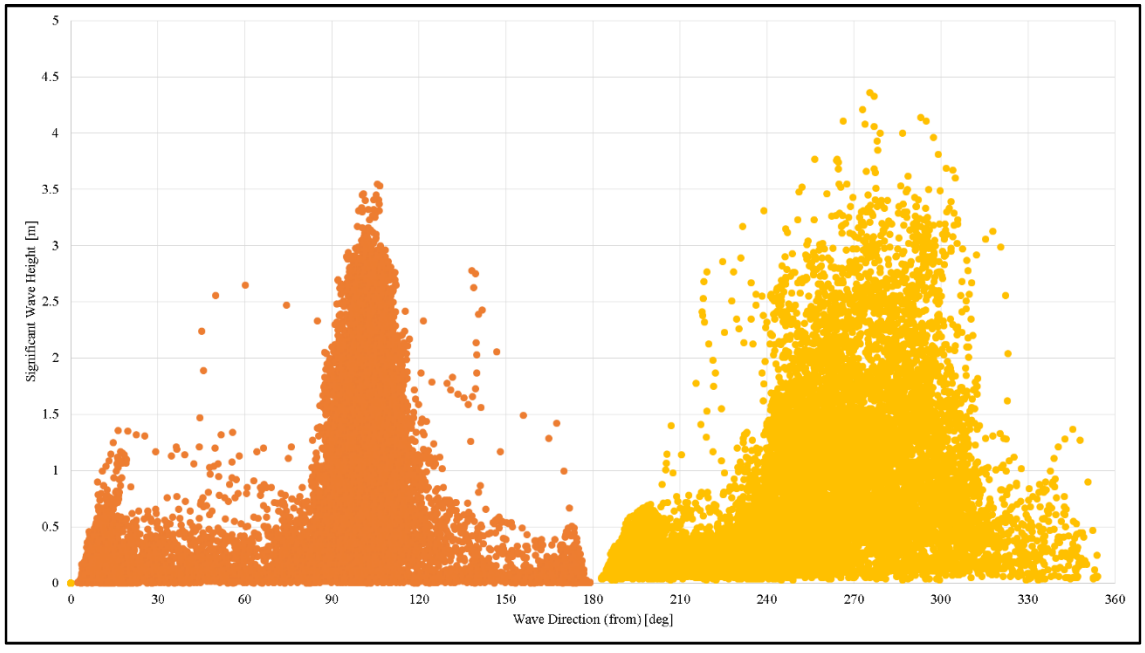


**Figure 3-6 Relation between Wind Wave Direction and Significant Wave Height**

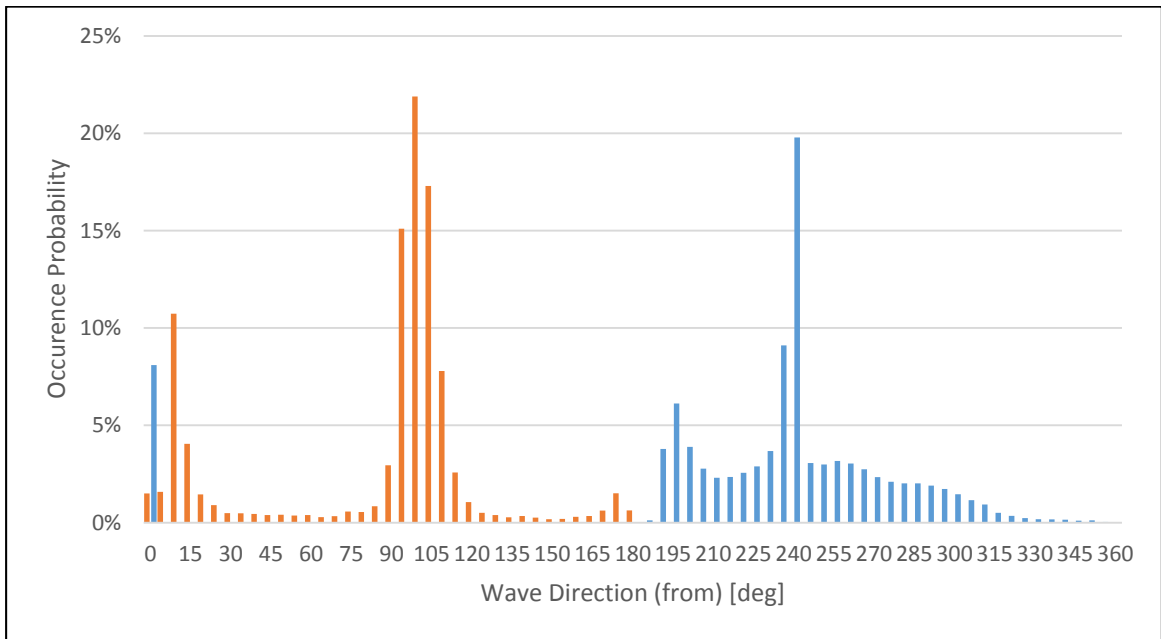


**Figure 3-7 Annual Probability of Wind Wave Direction**

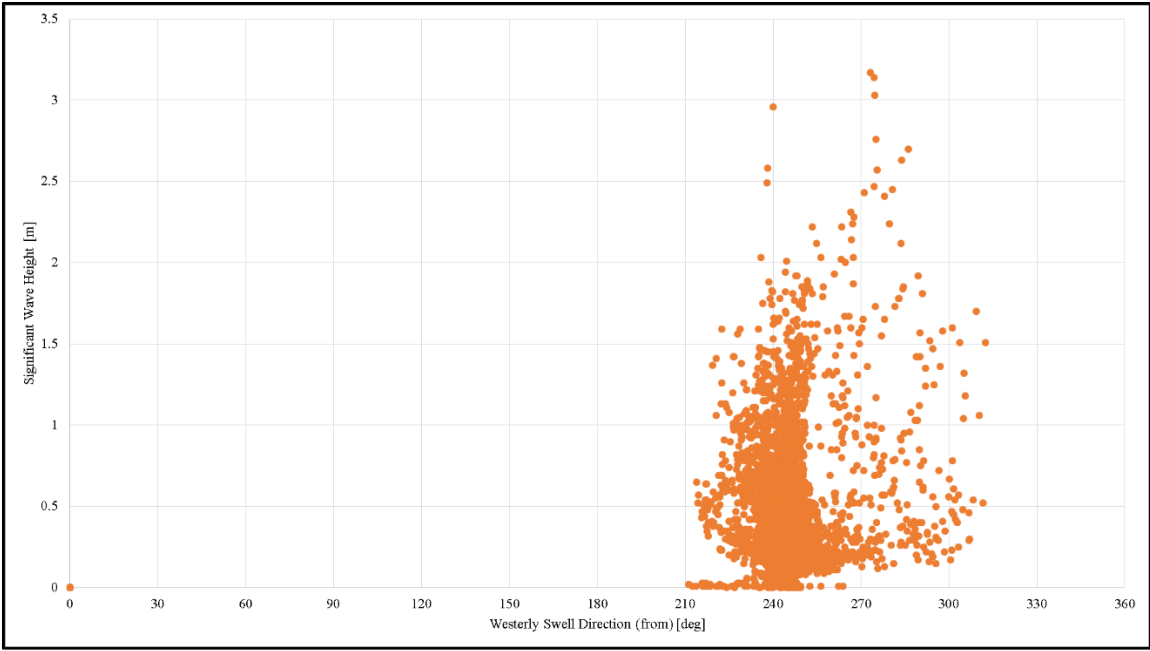


**Figure 3-8 Relation between Westerly Swell and Significant Wave Height**

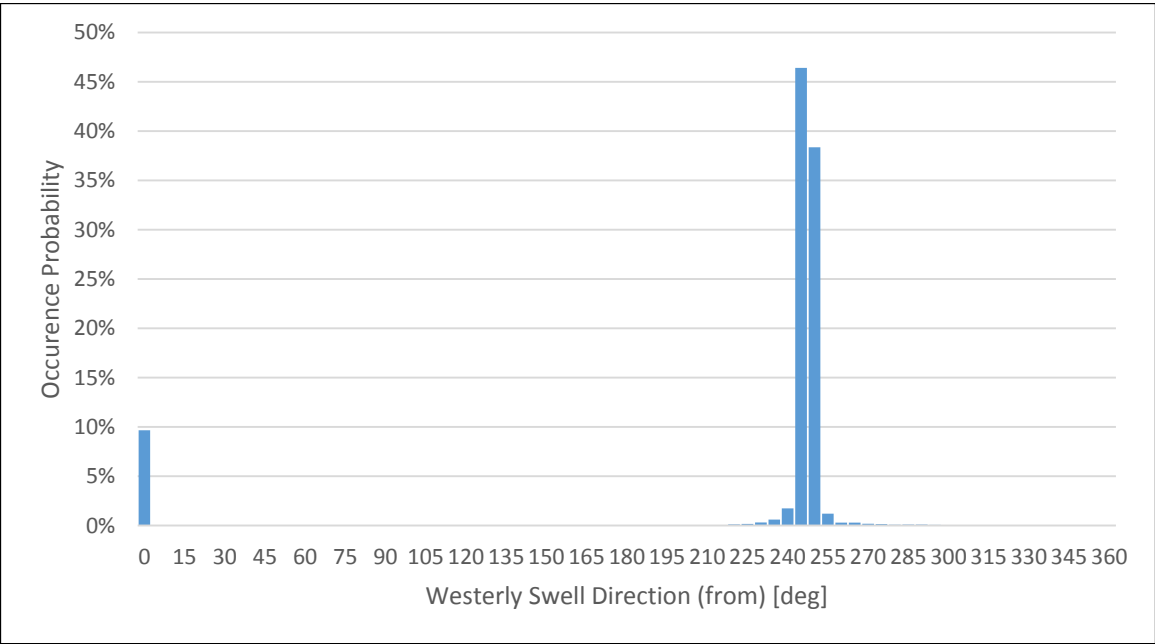


**Figure 3-9 Annual Probability of Westerly Swell Direction**

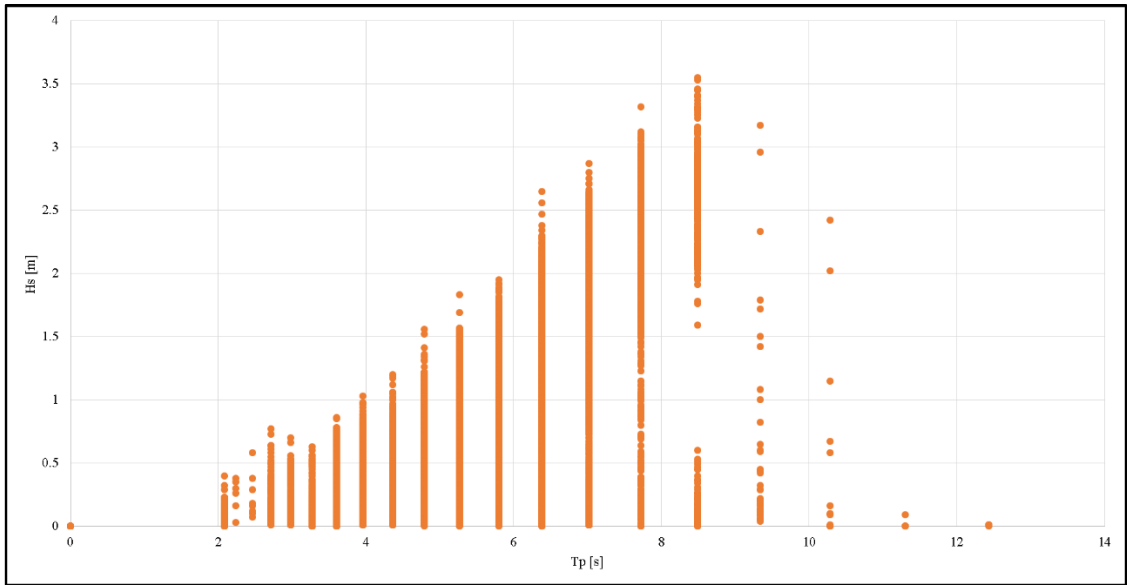


**Figure 3-10 Relation between Peak Period and Significant Wave Height of Easterly Sea**

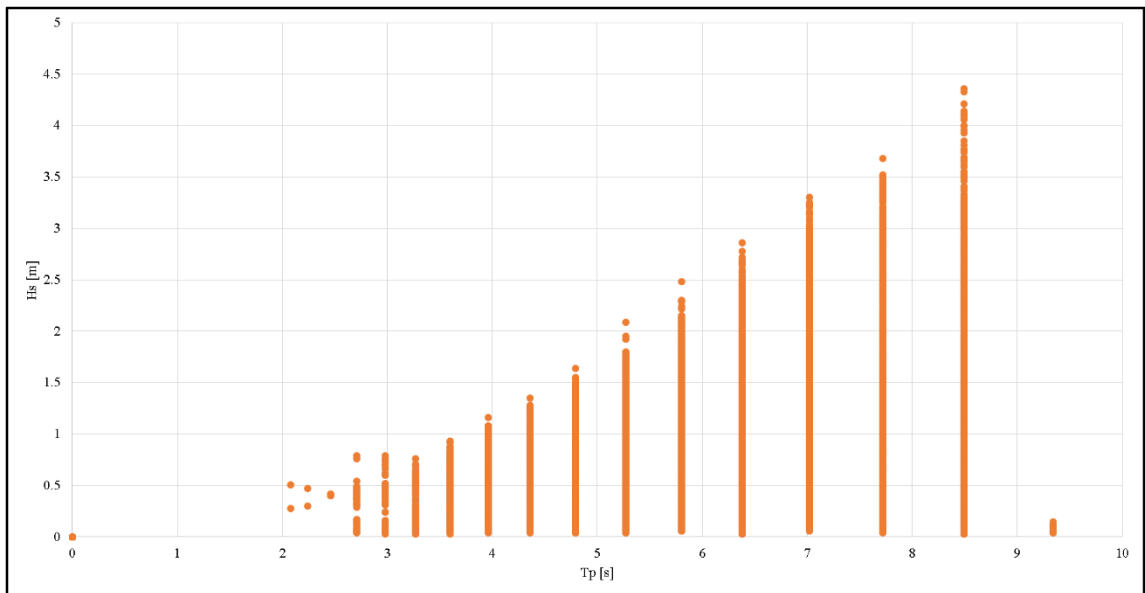


**Figure 3-11 Relation between Peak Period and Significant Wave Height of Westerly Sea**

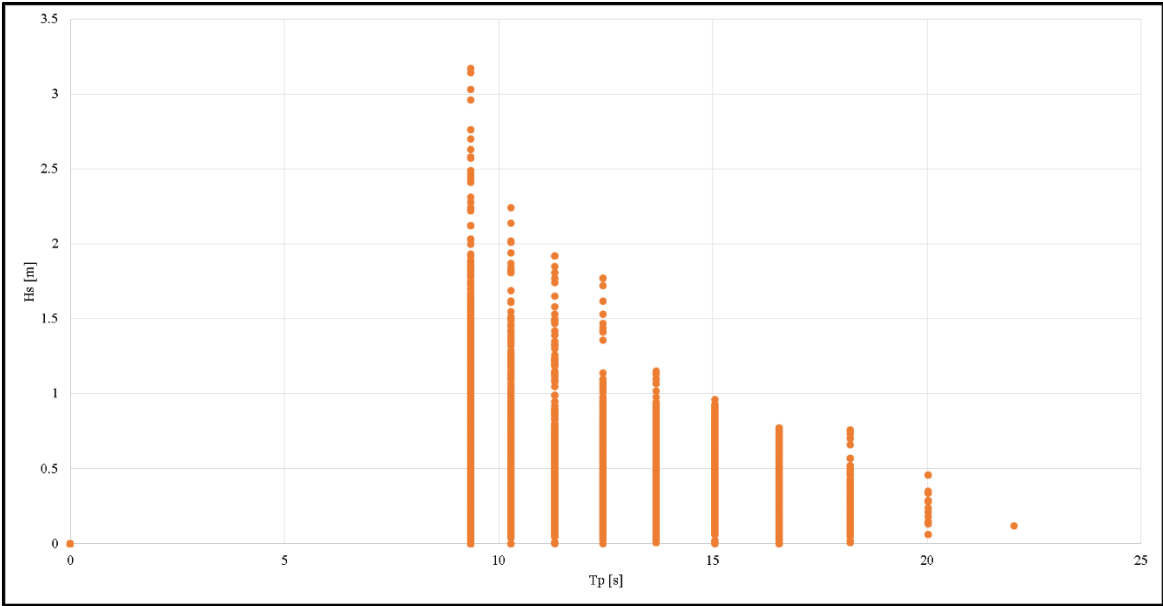


**Figure 3-12 Relation between Peak Period and Significant Wave Height of Westerly Swell**

## 3.2 Numerical Model

In order to perform heading analysis, the numerical model of the floating unit were generated which basically is the mooring analysis model. A 3D-diffraction software MOSES is used in this analysis. Details of MOSES software capabilities and analysis methodology are given in MOSES Manual (Ultramarine, 2012). The numerical model will be determine the characteristic of the unit with respect to wind, wave, and current that to be described as accurately possible with special care regarding the definition of reference points for numerous events.

### 3.2.1 Analysis Coordinate System

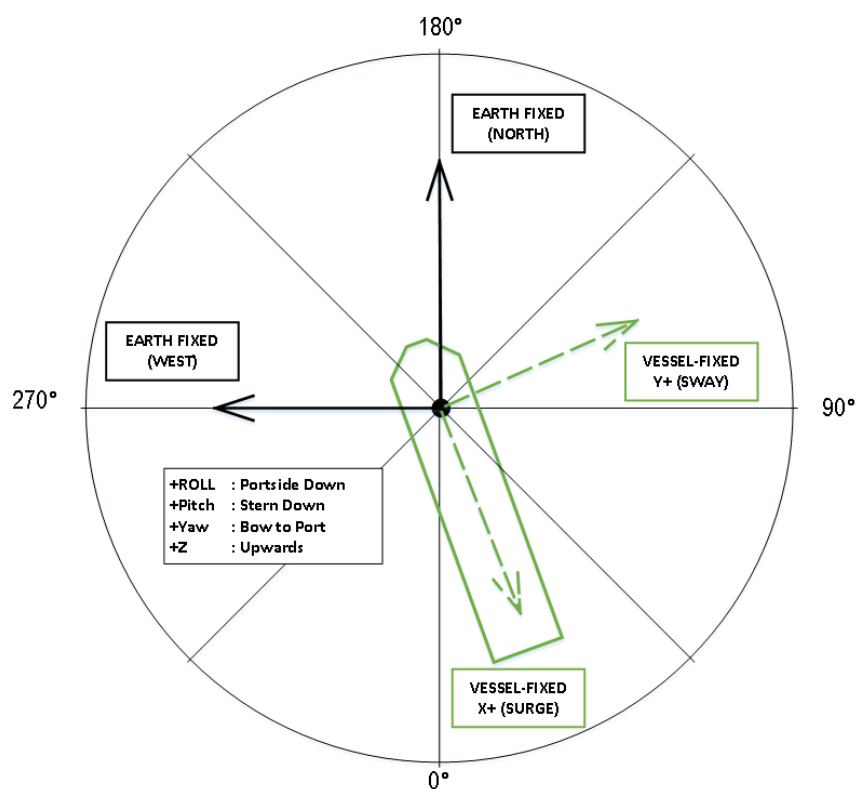


**Figure 3-13 Sign Convention Coordinate System**

First of all, prior to generate the numerical computation it should be determined the coordinate system. The sign conventions utilized for the analysis of motions and loads in earth-fixed and vessel-fixed local coordinate systems are defined below and are also shown in Figure 3-13.

- Earth-fixed coordinate system (EFCS):
  - The global X axis is coincident with the geographical North.
  - The global Y axis is coincident with the geographical West.
  - The global Z axis is vertically upwards, with  $Z=0$  at mean water level.

- Vessel-fixed coordinate system (VFCS):
  - The x-axis is along the vessel centerline, with  $x=0$  at vessel origin and positive to stern.
  - The y-axis is positive towards the starboard side of the vessel, with  $y=0$  at the vessel center line.
  - The z-axis is vertically upwards, with  $z=0$  at the vessel keel.

Note that plan view angles increase in a counter-clockwise (CCW) fashion. Unless otherwise noted, both in the analysis and presentation of results, wind, wave and current angles refer to the directions towards which these environments propagate (i.e. heading) in the present EFCS system. Additionally, a relative wave heading of 0deg. corresponds to waves approaching the vessel stern-on, while a relative wave heading of 90deg. corresponds to waves approaching the vessel on the starboard beam.

### 3.2.2 Vessel Information

A box-shaped vessel with principal particular of turret moored unit in ballast draft operating condition are presented in Table 3-1.

**Table 3-1 Vessel Principal Particulars**

<b>Vessel Particular</b>		
LOA	[m]	: 500.0
B	[m]	: 82.0
D	[m]	: 37.2
Draft (even keel)	[m]	: 16.2
Freeboard	[m]	: 21.0
Displ.	[ton]	: 646,000
VCG	[m]	: 25.0
Kxx	[m]	: 28.1
Kyy	[m]	: 127.0
Kzz	[m]	: 127.8
GMT	[m]	: 18.83
Wind Area – Head on (Ax)	[m <sup>2</sup> ]	: 2,802
Wind Area – Beam on (Ay)	[m <sup>2</sup> ]	: 26,640
Current Area – Head on (Ax)	[m <sup>2</sup> ]	: 1,328
Current Area – Beam on (Ay)	[m <sup>2</sup> ]	: 7,800



### 3.2.3 Wind and Current Load on Vessel

Wind and current load basic theory are already stated in Section 2.2.2 and Section 2.2.3 in previous chapter. The wind and current coefficient that will be implemented in this analysis shall be better from wind tunnel test experiment. Currently author can't do such experiment and also can't get sufficient data regarding this issue, so in this research wind and current forces coefficient are assumed based on OCIMF recommendation. Further reading as more information can be seen in Prediction of Wind and Current Loads on VLCCs (OCIMF, 1994).

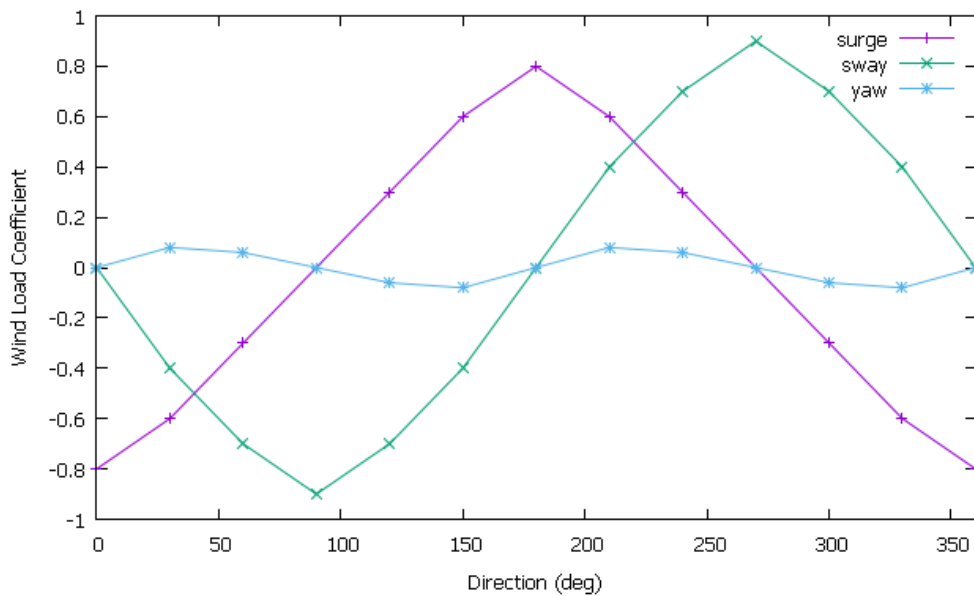


**Figure 3-14 Wind Load Coefficients**

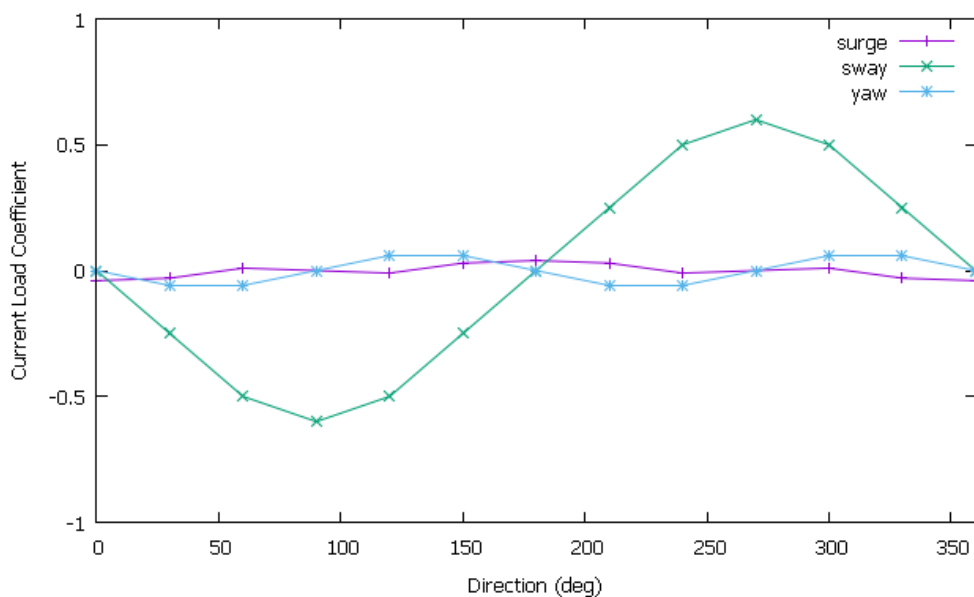


**Figure 3-15 Current Load Coefficients**

Current and wind coefficients will be used for this analysis can be seen in Figure 3-14 and Figure 3-15. The angels are relative heading between vessel and wind/current heading defined in VFCS, i.e 0deg is stern-on and 90deg is beam-on from starboard. Corresponding value can be found in Table 3-2 and Table 3-3.

**Table 3-2 Wind Load Coefficients**

Direction	Surge	Sway	Yaw
0	-0.8	0	0
30	-0.6	-0.4	0.08
60	-0.3	-0.7	0.06
90	0	-0.9	0
120	0.3	-0.7	-0.06
150	0.6	-0.4	-0.08
180	0.8	0	0
210	0.6	0.4	0.08
240	0.3	0.7	0.06
270	0	0.9	0
300	-0.3	0.7	-0.06
330	-0.6	0.4	-0.08
360	-0.8	0	0

**Table 3-3 Current Load Coefficients**

Direction	Surge	Sway	Yaw
0	-0.04	0	0
30	-0.025	-0.25	-0.06
60	0.01	-0.5	-0.06
90	0	-0.6	0
120	-0.01	-0.5	0.06
150	0.025	-0.25	0.06
180	0.04	0	0
210	0.025	0.25	-0.06
240	-0.01	0.5	-0.06
270	0	0.6	0
300	0.01	0.5	0.06
330	-0.025	0.25	0.06
360	-0.04	0	0

Area used in numerical calculation are illustrated in Figure 3-16 and Figure 3-17. It can be seen blue continuous line represent water level in ballast draft condition. Vessel hull

body present by green line. Respectively red line represent living quarter, topside module, flare tower, and turret structure.

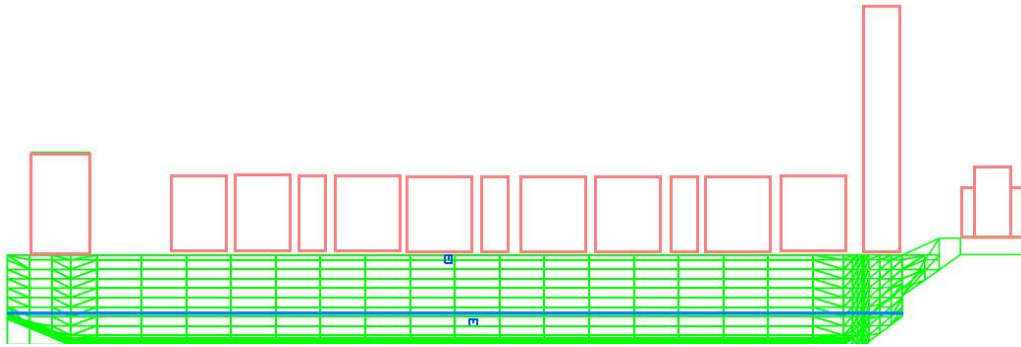


**Figure 3-16 Vessel Side Area**

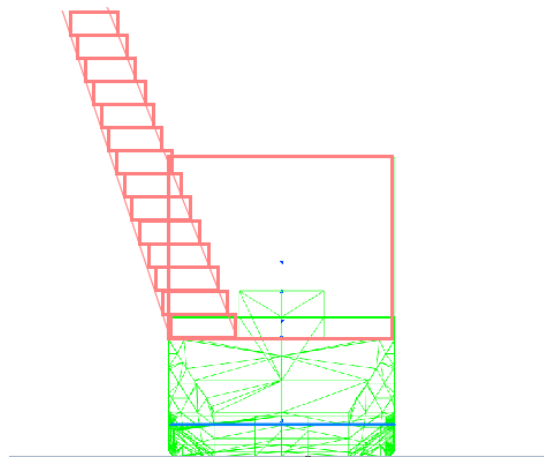


**Figure 3-17 Vessel Front Area**

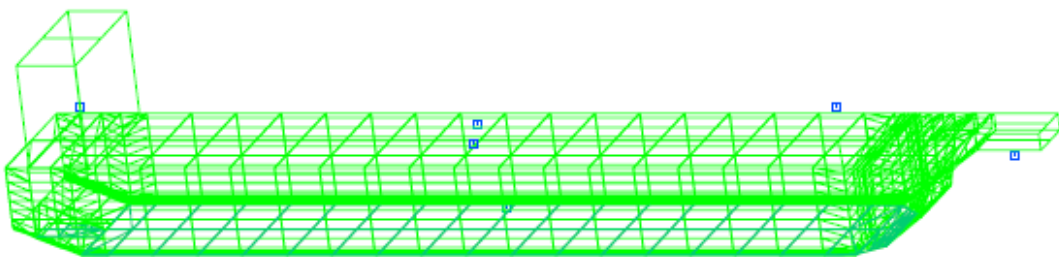


**Figure 3-18 Vessel Panel Model (totally 977 panels)**

**Table 3-4 Lateral Wind Screen for Topside**

Item	X start frm bow (mm)	X end frm bow (mm)	Y start frm CL (mm)	Y end frm CL (mm)	Z start frm keel (mm)	Z end frm keel (mm)	Length (m)	Height (m)	Area (m <sup>2</sup> )	Ch	Cs	Area x Ch x Cs (m <sup>2</sup> )	Centroid (m)		
													X frm bow (+) to stern	Y frm CL (+) to stbd	Z frm WL (+) upward
Turret [1/6]	-50765	-10964			45061	53941	39.80	8.88	353.43	1.00	1.00	353.43	-30.86		49.50
Turret [2/6]	-50765	-15229			53941	60706	35.54	6.77	240.40	1.00	1.00	240.40	-33.00		57.32
Turret [3/6]	-50765	-18701			60706	69328	32.06	8.62	276.46	1.00	1.00	276.46	-34.73		65.02
Turret [4/6]	-50765	-22490			69328	74946	28.28	5.62	158.85	1.00	1.00	158.85	-36.63		72.14
Turret [5/6]	-49409	-24335			74946	81694	25.07	6.75	169.20	1.00	1.00	169.20	-36.87		78.32
Turret [6/6]	-48464	-26558			81694	88007	21.91	6.31	138.29	1.00	1.00	138.29	-37.51		84.85
Flare Tower	3380	21285			38500	131951	17.91	93.45	1673.24	1.30	1.50	3262.82	12.33		85.23
Block A [1]	31885	57787			38500	83401	25.90	44.90	1163.03	1.00	1.00	1163.03	44.84		60.95
Block A [2]	62355	90866			38500	73184	28.51	34.68	988.88	1.00	1.00	988.88	76.61		55.84
Block A [3]	71269	84225			73184	95634	12.96	22.45	290.86	1.00	1.00	290.86	77.75		84.41
Block A [4]	90866	108635			38500	69674	17.77	31.17	553.93	1.00	1.00	553.93	99.75		54.09
Block A [5]	108635	138209			38500	71930	30.57	33.43	1022.09	1.00	1.00	1022.09	123.92		55.22
Block A [6]	119816	122208			71930	88511	2.39	16.58	39.66	1.00	1.00	39.66	121.01		80.22
Block B [1]	143130	175210			38500	71862	32.08	33.36	1070.25	1.00	1.00	1070.25	159.17		55.18
Block B [2]	157196	161096			71916	89518	3.90	17.60	68.65	1.00	1.00	68.65	159.15		80.72
Block B [3]	175210	191019			38500	69200	15.81	30.52	482.49	1.00	1.00	482.49	183.11		53.76
Block B [4]	191410	221526			38500	74105	30.12	35.61	1072.28	1.00	1.00	1072.28	206.47		56.30
Padestal Crane A [1]	220161	222490			50065	84217	2.33	34.15	79.54	1.30	1.00	103.40	221.33		67.14
Padestal Crane A [2]	217689	225664			84217	97846	7.88	13.63	107.33	1.30	1.00	139.53	221.63		91.03
Padestal Crane A [3]	177917	217682			84616	87597	39.77	2.98	118.54	1.30	1.00	154.10	197.80		86.11
Block C [1]	225540	253855			38500	75902	28.32	37.40	1059.04	1.00	1.00	1059.04	239.70		57.20
Block C [2]	236906	242324			75954	89966	5.42	14.01	75.92	1.00	1.00	75.92	239.62		82.96
Block C [3]	253855	269588			38500	68966	15.73	30.47	479.32	1.00	1.00	479.32	261.72		53.73
Block C [4]	269855	291609			38500	68975	21.75	30.48	662.95	1.00	1.00	662.95	280.73		53.74
Block C [5]	272009	276892			68969	76735	4.88	7.77	37.92	1.00	1.00	37.92	274.45		72.85
Block C [6]	291609	320447			38500	57988	28.84	19.49	561.99	1.00	1.00	561.99	306.03		48.24
Block C [7]	294847	317746			57988	77237	22.90	19.25	440.78	1.00	1.00	440.78	306.30		67.61
Block C [8]	302547	310238			77237	97470	7.69	20.23	155.61	1.00	1.00	155.61	306.39		87.35
Padestal Crane B [1]	322025	325387			38500	84408	3.36	45.91	154.34	1.30	1.00	200.65	323.71		61.45
Padestal Crane B [2]	321271	328149			84395	98437	6.88	14.04	96.58	1.30	1.00	125.56	324.71		91.42
Padestal Crane B [3]	279739	321271			85011	87891	41.53	2.88	119.61	1.30	1.00	155.50	300.51		86.45
Living Quarter [1]	346282	370982			38500	84200	24.70	45.70	1128.79	1.00	1.00	1128.79	358.63		61.35
Living Quarter [2]	347857	355385			84200	103543	7.53	19.34	145.61	1.00	1.00	145.61	351.62		93.87
Living Quarter [3]	370982	378982			38500	80204	8.00	41.70	333.63	1.00	1.00	333.63	374.98		59.35
Living Quarter [4]	378932	398462			38500	62504	19.53	24.00	468.80	1.00	1.00	468.80	388.70		50.50
Helideck	355875	398418			83000	87500	42.54	4.50	191.44	1.20	1.30	298.65	377.15		85.25
									16179.75			19879.32	159.53	0.00	65.18

**Table 3-5 Longitudinal Wind Screen for Topside**

Item	X start frm bow (mm)	X end frm bow (mm)	Y start frm CL (mm)	Y end frm CL (mm)	Z start frm keel (mm)	Z end frm keel (mm)	Length (m)	Height (m)	Area (m <sup>2</sup> )	Ch	Cs	Area x Ch x Cs (m <sup>2</sup> )	Centroid (m)		
													X frm bow (+) to stern	Y frm CL (+) to stbd	Z frm WL (+) upward
LQ [1]			-31925	31925	38500	83700	63.85	45.20	2886.02	1.00	1.00	2886.02		0.00	61.10
LQ [2]			-14395	-18347	82500	101217	3.95	18.72	73.97	1.00	1.00	73.97		-12.42	91.86
LQ [3]			-12672	-14380	95200	101242	1.71	6.04	10.32	1.00	1.00	10.32		-11.82	98.22
Helideck			3656	46107	82512	87012	42.45	4.50	191.03	1.20	1.30	298.01		24.88	84.76
Flare Tower			14019	31925	87012	131951	17.91	44.94	804.68	1.30	1.50	1569.12		22.97	109.48
									1080.00			4837.44	0.00	8.77	78.80

A total topside windage area in lateral and frontal is presented in Table 3-4 and Table 3-5. As can be seen the windage area is about 16,000 m<sup>2</sup> and 1,000 m<sup>2</sup> for lateral and longitudinal respectively. Furthermore the freeboard hull lateral and longitudinal windage area is about 9,900 m<sup>2</sup> and 1,700 m<sup>2</sup> respectively. Summing the lateral and longitudinal windage area is 26,640 m<sup>2</sup> and 2,802 m<sup>2</sup>.

### 3.2.4 Wave Drift and Vessel Modelling

Author will perform heading analysis to estimate the optimum mooring system design for vessel loading condition as stated in Table 3-1 above. Instead of wind and current load, wave drift forces and moments is another important thing to do heading analysis. To generate wave drift force, a software package MOSES will performing the hydrodynamic calculation to generate it and also do the vessel modelling.

A schematic view of vessel modelling by panel model (meshed hull) to be used for 3D diffraction analysis is presented in Figure 3-18. Total panels generated is 977 panels, its see less number of panels due to the vessel shape is quite simple barge shape just like a box. The vessel have long parallel middle body and a simple stern shape plus skeg in stern. Bow part is a complex one to be modelled, therefore need a refine mesh or a lot of panels number in this area. Several degree of accuracy has been tried to obtain the accurate hydrodynamic result. In MOSES, author utilize a refine function to generate better mesh quality and can do easier work without a lot of time consuming require. A simple syntax of MOSES command input file is presented below in Table 3-6.

**Table 3-6 Sample of MOSES Syntax**

<pre> \$ set dimension &amp;dimen -dimen meter m-ton  \$ read model Inmo  \$ plot model as interested view &amp;pict iso &amp;pict bow &amp;pict side  \$ set draft &amp;instate %vessel -condition 16.2  \$ hydrodynamic computation hydro     g_press     V_MATRICES     END     e_total end freq_r     rao     fp_std &amp;body(cg %vessel)     EQU_SUM     matrices -file     end     exforce -file     end end &amp;finish </pre>	<p>Define dimension</p> <p>MOSES to the model</p> <p>Plot model in isometric, bow, and side view</p> <p>Set draft 16.2 m</p> <p>Hydrodynamic calculation by generating pressure along the body</p> <p>Generate frequency response of the vessel</p> <p>Finish of Syntax</p>
--	---

### 3.2.5 Environmental Modelling

The environmental modelling will be performed in accordance with Section 3.1. First is wind load. Wind loads will be modelled utilizing the NPD wind spectrum, specifically in below detail.

$$S_{NPD}(f) = \frac{320 \left(\frac{U_0}{10}\right)^2 \left(\frac{z}{10}\right)^{0.45}}{(1 + f^{0.468})^{3.561}} \quad (3.1)$$

$S_{NPD}(f)$  : Spectral density at frequency  $f$  [(m/s<sup>2</sup>)/Hz]

$f$  : frequency (Hz)

$$f^{0\%} = \frac{172f \left(\frac{z}{10}\right)^{2/3}}{\left(\frac{U_0}{10}\right)^{3/4}}$$

$U_0$  : 1-hour averaged wind speed at reference elevation (10m above MSL) [m/s]

$z$  : Elevation above MSL (m)

The second one is current. The current force on the vessel will be modelled as a static force. Only surface current will be utilized to define the current speed in below the water line. The effect of current on the wave drift forces and damping will also be taken into account.

The third is wave/swell. Both wave wind-driven sea and swell will be modelled using the following generalized, five-parameter JONSWAP wave spectrum:

$$S(f) = \alpha H_s^2 T_p^{-4} f^{-5} \exp[-1.25(T_p f)^{-4}] \gamma \exp[-(T_p f - 1)^2 / 2\sigma^2] \quad (3.2)$$

$S(f)$  : Spectral wave energy distribution (m<sup>2</sup>/Hz)

$H_s$  : Significant wave height (m)

$f$  : wave frequency (Hz)

$fp$  : peak wave frequency (Hz) = 1/ $T_p$

$T_p$  : peak wave period (s)

$\gamma$  : spectral peakedness

$\sigma$   $\sigma_a$  for  $f > fp$

$\sigma_b$  for  $f \geq fp$

$$a = 0.064 / [0.230 + 0.0336g - 0.185 (1.9 + g)^{-1}]$$

Waves will be assumed to be long-crested and no directional spreading will be considered.

### 3.2.6 Heading Analysis Algorithm

As stated by (T. Terashima, 2011), the set in heading angle is subject to external forces as show in equation below. Which is described as steady component of azimuth moment induced by wind, current, and wave (two wind waves and swell components) at turret position.

$$\begin{aligned}
 M_t(\chi) &= -L_m \left( F_{wy}(\chi_w) + F_{cy}(\chi_c) + \sum_{j=1}^3 F_{dy}^S(\chi_{w,s}(j)) \right) + M_{wz}(\chi_w) + M_{cz}(\chi_c) + \sum_{j=1}^3 M_{dz}^S(\chi_{w,s}(j)) \\
 F_{dy}^S(\chi_{w,s}(j)) &= \int_{-\frac{\pi}{2}}^{\frac{\pi}{2}} \int_{-\frac{\pi}{2}}^{\frac{\pi}{2}} \frac{F_{dy}(\omega, \chi_{w,s}(j) + \theta)}{\zeta_a^2} 2S(\omega, j) G(\theta, j) d\omega d\theta \\
 M_{dz}^S(\chi_{w,s}(j)) &= \int_{-\frac{\pi}{2}}^{\frac{\pi}{2}} \int_{-\frac{\pi}{2}}^{\frac{\pi}{2}} \frac{M_{dz}(\omega, \chi_{w,s}(j) + \theta)}{\zeta_a^2} 2S(\omega, j) G(\theta, j) d\omega d\theta
 \end{aligned} \tag{3.3}$$

$j$  : number wave and swell, where  $j=1$ :easterly wave,  $=2$ :westernly wave,  $=3$ :swell

$\chi_w, \chi_c, \chi_{ws}(j)$  : incident angle of wind, current, and wave/swell where head is defined zero

$L_m$  : distance from turret position to the midship

$S(\omega, j)$  : frequency spectrum of incident wave/swell

$G(\theta, j)$  : directional distribution of incident wave/swell

Another author in (Morandini, 2007) also stated the algorithm regarding heading analysis. The slow drift loads are divided from the diagonal terms of the Quadratic Transfer Functions (QTFs) of the unit. The slow drift loads are computed based on Newman's approximation. The formula used, however, involve four summations instead of two in the original formulation.

$$\begin{aligned}
 FD(t) &= \left[ \sum_{k=1}^{100} a_k \sqrt{|QTF(\alpha_H, \omega_k, \omega_k)|} \cos(\omega_k t + \varphi_k) \right] \bullet \\
 & \left[ \sum_{k=1}^{100} a_k \sqrt{|QTF(\alpha_H, \omega_k, \omega_k)|} \cos(\omega_k t + \varphi_k) \text{sign}\{QTF(\alpha_H, \omega_k, \omega_k)\} \right] + \\
 & \left[ \sum_{k=1}^{100} a_k \sqrt{|QTF(\alpha_H, \omega_k, \omega_k)|} \sin(\omega_k t + \varphi_k) \right] \bullet \\
 & \left[ \sum_{k=1}^{100} a_k \sqrt{|QTF(\alpha_H, \omega_k, \omega_k)|} \sin(\omega_k t + \varphi_k) \text{sign}\{QTF(\alpha_H, \omega_k, \omega_k)\} \right]
 \end{aligned} \tag{3.4}$$

$FD(t)$  is the one of three components in vessel axis system of slow drift loads at instant t, i.e.  $F_{Dx}$ ,  $F_{Dy}$ , or  $M_{D\psi}$

$\alpha_H$  is the wave incident relative to the vessel heading at instant t, i.e.  $\alpha_H = \beta_H - \psi$

$QTF(\alpha_H, \omega_K, \omega_K)$  is the relevant diagonal function interpolated for the instantaneous wave incident  $\alpha_H$ .

$sign(u)$  is equal to: 1 if  $u > 0$ , -1 if  $u < 0$ , 0 if  $u = 0$

The average value of  $FD(t)$  on the whole duration of simulation can be obtained by following equation.

$$FD_{mean} = 2 \int_{\omega_m}^{\omega_M} QTF(\alpha_H, \omega, \omega) S(\omega) d\omega$$

### 3.2.7 Heading Angles Calculation

The metocean reports provide the input environmental data for heading analysis. The mean vessel heading is determined for each sea-state. The long-term heading probability is used to determine extreme loads.

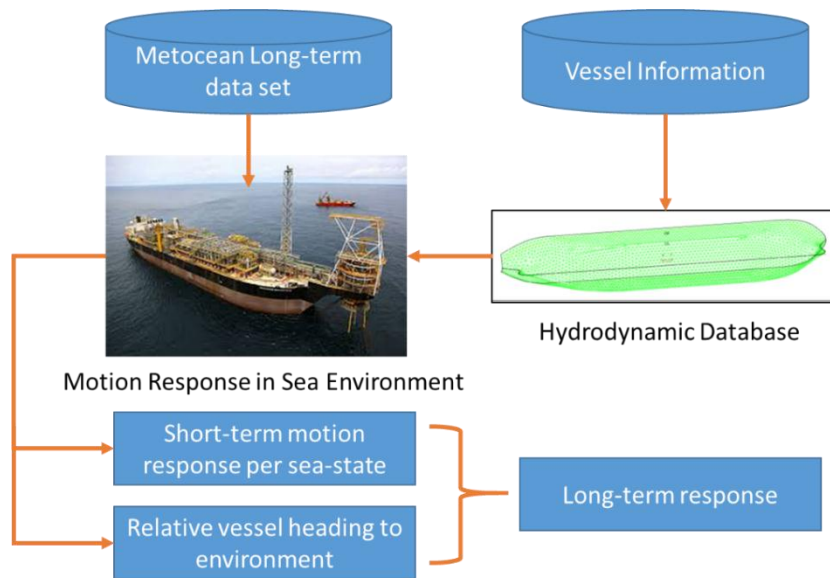


**Figure 3-19 Heading Analysis Calculation Procedure**

The environmental data includes a total of approximately 29,208 continuous three hourly hindcast sea states which represents 10 years of data. The environmental data includes:

- Wind wave JONSWAP spectrum parameters (i.e.  $H_s$ ,  $T_p$ ,  $\gamma$ ,  $\sigma_a$  and  $\sigma_b$ ) and direction. (Two wave components for our cases i.e. westerly and easterly wave)
- Swell wave JONSWAP spectrum parameters (i.e.  $H_s$ ,  $T_p$ ,  $\gamma$ ,  $\sigma_a$  and  $\sigma_b$ ) and direction. (Westerly swell for our cases)
- Wind mean speed and direction.
- Current mean speed and direction.

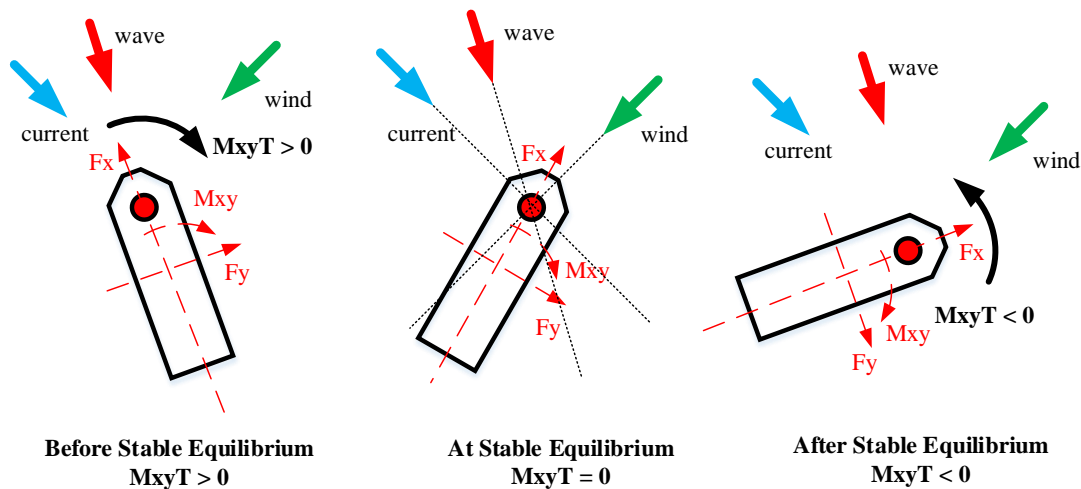


Figure 3-19 is presented simple procedure of heading analysis calculation. It was good to breaking down the methodology, as presented in Figure 3-21, to determine heading calculation in detail for a better understanding which starting from gather the vessel information and finish in obtaining a vessel long-term response in long-term metocean data set. The hydrodynamic database and the motion response in specific sea environment is presented in section 4.2.1 through 4.2.4. Furthermore the long-term response is presented in section 4.2.5. The procedure, which is adopted to (Sarala Resmi, 2011), is as follow:

1. A 3-D diffraction model of the vessel's hull was generated in MOSES based on the characteristics defined.
2. The calculated linearized roll damping is verified against field measurements and included in the hydrodynamic model.
3. A hydrodynamic database containing amplitude and phase of the RAOs for design parameters was prepared for frequency range of 0.1 rad/s to 1.5 rad/s with 0.05 rad/s increments and heading range of 0° to 360° with 22.5° increments.
4. The mooring arrangements were added to the MOSES model to perform static frequency domain simulation.
5. Wind and current coefficients from wind tunnel tests were added to the MOSES to include the wind drag and the current drag forces for the specified loading condition of the vessel and the headings relative to wind and current directions.
6. The three hourly environmental data, which contained sets of wind-sea, swell, wind and current data with their associated directions were included in the hydrodynamic model.
7. Using the MOSES software, the stable equilibrium positions for each three hourly sea state was calculated individually.
8. The vessel headings were post-processed to find the relative vessel heading to wind seas and swell seas at each three hourly sea state.

As can be seen in Figure 3-20 external forces acting on turret moored unit in three main condition of equilibrium. Before equilibrium, at equilibrium, and after equilibrium position respectively. At first stage of equilibrium, before stable equilibrium, the moment value at turret is more than zero. This will make the vessel heading change to new position to find moment is zero at second stage of equilibrium. The turret moored unit is also experience an after equilibrium stage, this due to the reserve of external force is still act to the vessel so its cause the moment is less than zero. But the vessel will back again to find

the moment is zero until and find a stable equilibrium position. Those condition is represent transient stage an steady stage in dynamic time domain simulation.



**Figure 3-20 Equilibrium Calculation**

From above two algorithms that stated by previous author in Section 3.2.5 the important point is an angle where the moment at the turret position is zero or near to zero, gives the balance heading angle of the vessel. Because the behavior of turret is free from moment that showing weathervaning effect. Balance heading will calculate for each environment condition as stated in Section 3.1, totally 29,208 cases.

In this thesis author will perform heading angles analysis by combination of software package MOSES and additional algorithm inside the syntax. The additional algorithm was generated to obtain estimation of heading angles position due to external load from environment to find zero moment at turret position. After the estimation value is obtained, an equilibrium command that already available in MOSES command is apply inside the syntax. A guess yaw angles algorithm are composed by following step:

1. Initialize stage. In this initial position, vessel force and moment due to external load is generated. Moment at the turret for this initial position shall be not have zero value.
2. Make a change position. To guess final yaw angle position, a delta angle is specified inside the algorithm. A determined increment angles shall set to estimated excursion each step and also get the force and moment at the changed position.
3. New state position. After delta angle was determined a new state position is obtained. In this new position the program will generate force and moment of the vessel and also new excursion position and the yaw angle.

4. Compute change until moment at turret  $\approx 0$ . If moment at turret already captured the zero or near to zero value, heading angles is already obtained. But if those condition didn't achieve step at point 2 and point 3 shall be redo until desired condition is achieved.

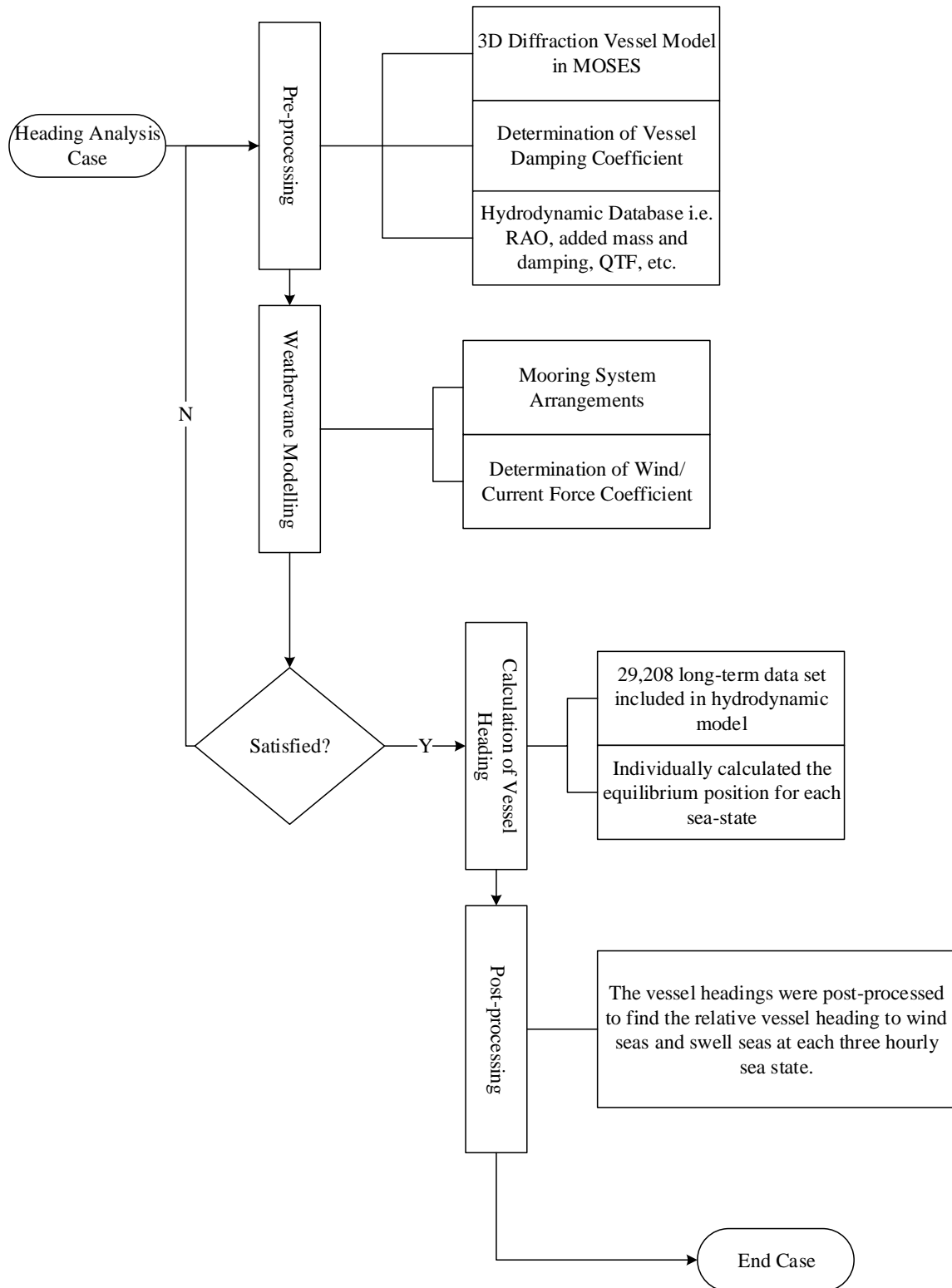


**Figure 3-21 Heading Analysis Algorithm**

A sample of logging process of heading angles calculation is presented in Table 3-7.

**Table 3-7 A Sample Logging File to Estimate Heading Angles**

<pre> START in initial position   loc initial = 0 0 -14.5 0 0 124.34  initialize stage   body is tanker   momloc = -40.00 0.00 33.00   tloc = 0.00 0.00 -14.50 0.00 0.00 124.34   oangle = 124.34 deg.   for = 44.16 42.28 -2197.3   mom = 96.65 -1769.4 3197.32   nmom = -1395.1-8.643E4 -1691.1   mom = 96.65 -1769.4 3197.32   yawm = 3197.32   delang = 10.00 deg.  start looping   old location   xo = 39.97   mul = 0.00   xo = 39.97   yo = 1.50   mul = 0.00   yo = 1.50   new force   xn = 39.97   mul = 0.00   xn = 39.97   yn = 1.61   mul = 0.00   yn = 1.61   make change and new state   tloc = -17.40 -34.64 -14.50 0.00 0.00 182.31   angle = 182.31 deg.   for = 57.48 -19.66 -2198.7   mom = -65.88 -1616.6 0.01   nmom = 648.89-8.605E4 786.53   mom = -65.88 -1616.6 0.01   yawm = 0.01   compute change   delang = 0.16   oangle = 182.31 deg.   yawm = 0.01 end looping        Time to Estimate Equilibrium : CP= loc guess = -28.78875 -31.25061 -14.5 0 0 -177.6913  find equilibrium loc after = -23.5669 -32.66275 -14.92084 -1.280055E-3 - 9.948925E-2 -178.0448 </pre>	<p>Start in initial position</p> <p>Initialize stage determination</p> <p>Looping process to find estimation of equilibrium angles</p> <p>Estimation of heading angles captured</p> <p>Applying equilibrium MOSES command</p>
--	---

### 3.3 Model Verification

It should be note that this thesis will carried on by utilizing MOSES software package. Prior to do analyzing for all loadcases, a simple model will be verified between MOSES and another codes that have a similar capabilities for computing wave loads and motions of offshore structure in waves. The MOSES model will be verified against AQWA to compare the hydrodynamic result for a same simple model in a difference tools. AQWA is one of a well proven computer program that widely used for scientific and engineering practice purpose.

In this study a simple box geometry is chosen with the proper number of panels. Box can represent FLNG, FPSO, or FPU that has a large block coefficient which is the studied floating unit object of this thesis. The version of each software used in this study was MOSES 7.10 and ANSYS AQWA 15.0.

**Table 3-8 Geometry and Description**

		<b>MOSES</b>	<b>AQWA</b>
<b>LOA</b>	[m]	200	200
<b>Breadth</b>	[m]	40	40
<b>Depth</b>	[m]	28	28
<b>Draft</b>	[m]	28	28
<b>KG</b>	[m]	28	28
<b>Roll Gyration</b>	[m]	13.33	13.33
<b>Pitch Gyration</b>	[m]	50	50
<b>Yaw Gyration</b>	[m]	50	50
<b>Diffraction Type</b>		3D- Diffraction	3D- Diffraction
<b>Panels Number</b>		976	648
<b>Damping</b>		Tanaka	-
<b>Wave Periods</b>	[s]	3 to 25	3 to 25
<b>Wave Angles</b>			
• <b>Head/Following-seas</b>		√	√
• <b>Quarter-seas</b>		√	√
• <b>Beam-seas</b>		√	√
<b>Output to Compare</b>			
• <b>Translational RAO</b>	[m]	√	√
• <b>Rotational RAO</b>	[deg.]	√	√

### **3.4 Assessing the Outcome**

In order to validate the proposed numerical model as well as the hind cast data, some validations are to be sought with the available data. The extent of such variable data should be used as extensively as possible for cross checking. In case of the floating unit does not exist so it's recommended to try collecting existing data such marine logs and excursion monitoring system from existing unit in vicinity of the planned location of the project. More discussion of heading analysis outcome is presented in Section 4.

### **3.5 Mooring System Design**

The global analysis of the coupled Vessel-Lines system will be performed with several software packages and numerical tools, both in the time-domain and frequency-domain. The methodology presented in Figure 3-22 and software tools that will be employed for the global analyses have been extensively verified by model tests for other deep water turret moored vessels. For diffraction analysis, the diffraction program MOSES will be used to provide an accurate representation of the vessel wave-frequency response. This thesis will study an optimum mooring design layout by considering heading analysis result.

#### **3.5.1 Mooring System Characteristic**

The mooring system is to be designed as permanent external turret. The mooring system consist of 12 mooring legs split into three (3) groups of four (4) legs (3by4 system). The separation each group is 120deg. However, another thing is the Centre to Centre anchor pile clearance shall enough to minimize interaction between two adjacent anchors. The optimum separation angle ( $\alpha^\circ$ ) between the mooring legs within a group will investigate in this thesis, which is required a clearance between adjacent mooring legs of two groups shall no less than 90deg as can be seen in Figure 3-23.

Turret Center is located 40m forward of the Fore Perpendicular (FP), 33m above keel. Determination of turret location and elevation shall consider mooring system performance, enough clearance of mooring to touch vessel bow in extreme condition, and also prevent green water impact. General 3D view of mooring system are presented in Figure 3-24.

#### **3.5.2 Mooring Leg Components**

The mooring system will consist of top chain-steel wire-bottom chain configuration. Flash-welded studless chain will be used for both top and bottom chain segments. The chain segments and accessories will be designed, manufactured, and tested in accordance with the latest API Specification 2F Specification for Mooring Chain, DNV Offshore Standard for Offshore Mooring Chain, and ABS Guide for Certification of Offshore Mooring Chain. Spiral strand sheathed steel wire will be used for the wire segment. The spiral strand wire construction is torque-neutral and the sheathing adds some protection to the outer layer strands. The steel wire segments and accessories will be designed, manufactured, and tested in accordance with the latest API Specification 9A Specification for Wire Rope and DNV Offshore Standard for Offshore Mooring Steel Wire

Ropes. Mooring leg components and its properties is presented in Table 3-9, while mooring leg length is presented in Table 3-10.

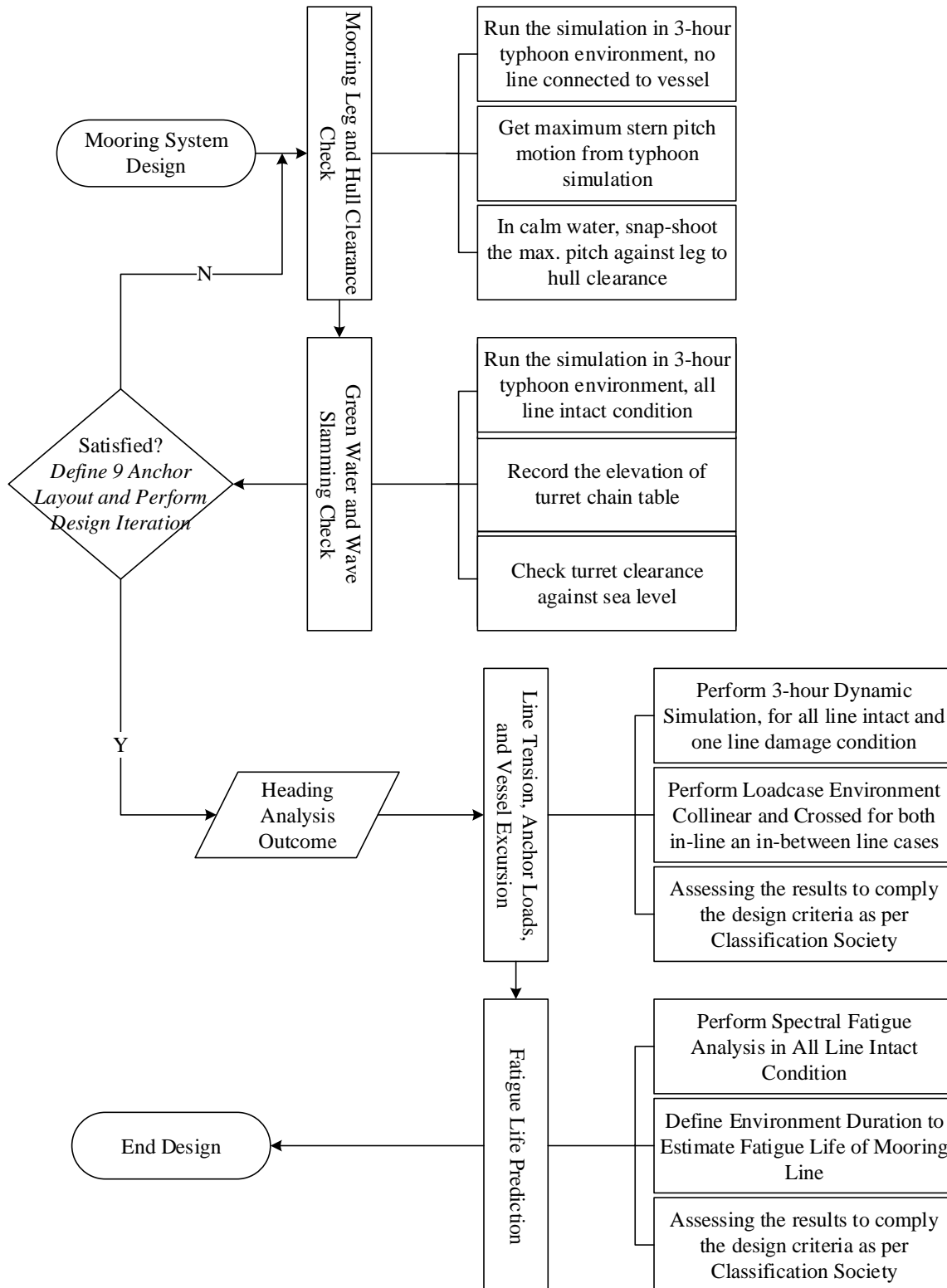


**Figure 3-22 External Turret Mooring System Design**



**Table 3-9 Mooring Leg Properties**

Title	Description	MBL (ton)	Weight (ton/m)
Top Chain	157mm Grade R4 Studless Chain	2163.04	0.4943
Steel Wire	131mm Spiral Strand sheated steel wire	1884.66	0.0688
Bottom Chain	170mm Grade R3 Studless Chain	2536.08	0.5796

**Table 3-10 Mooring Leg Lengths**

Mooring Group	Mooring Leg	Bottom Chain (m)	Steel Wire (m)	Top Chain (m)
G1	1	100	725	410
	2	100	725	410
	3	100	725	410
	4	100	725	410
G2	5	100	725	410
	6	100	725	410
	7	100	725	410
	8	100	725	410
G3	9	100	725	410
	10	100	725	410
	11	100	725	410
	12	100	725	410

Top Chain runs from the chain stopper on the chain table to the top end of the wire. Steel Wire segment is as strong as the chain segments, but is significantly lighter, thus serving to reduce top tensions and turret loads. Bottom Chain is quite heavy due to the strategic placement of this as a very heavy excursion limiter segment near the anchor leg touch down zone serves to improve the mooring system force-deflection characteristics, and significantly reduces turret offsets.

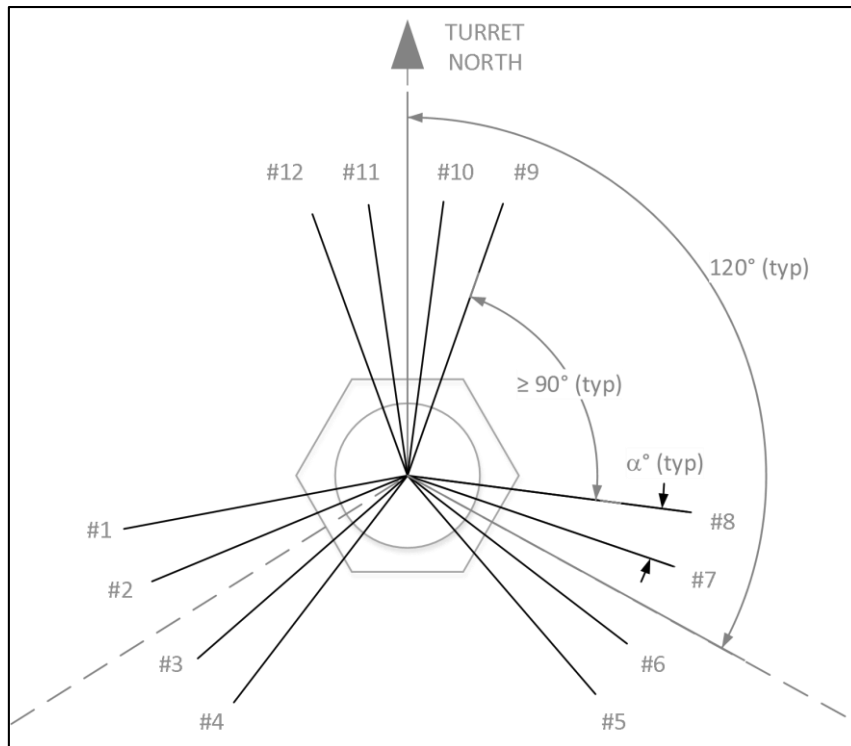


**Figure 3-23 Chain Table Layout**

### 3.5.3 Marine Growth and Corrosion

Marine growth essentially increases the drag diameter of the component and also increases the unit weight of the component. To account for the marine growth effects, the drag diameter should be increased to the diameter of the component plus the marine growth thickness. The unit weight of the component should also be adjusted for the marine growth.

Chain corrosion have a potential for increased in corrosion in the splash zone, wear allowance of it is 0.8mm/year. The lower chain and ground chain have a normal corrosion allowance of 0.4mm/year. All chain shall be manufactured, inspected, and tested in accordance with test the latest API Specification 2F Specification for Mooring Chain, and DNV Certification Notes No. 2.6 (1995).

However, the effect of marine growth and corrosion allowance on mooring lines and also risers will not be considered in this study.

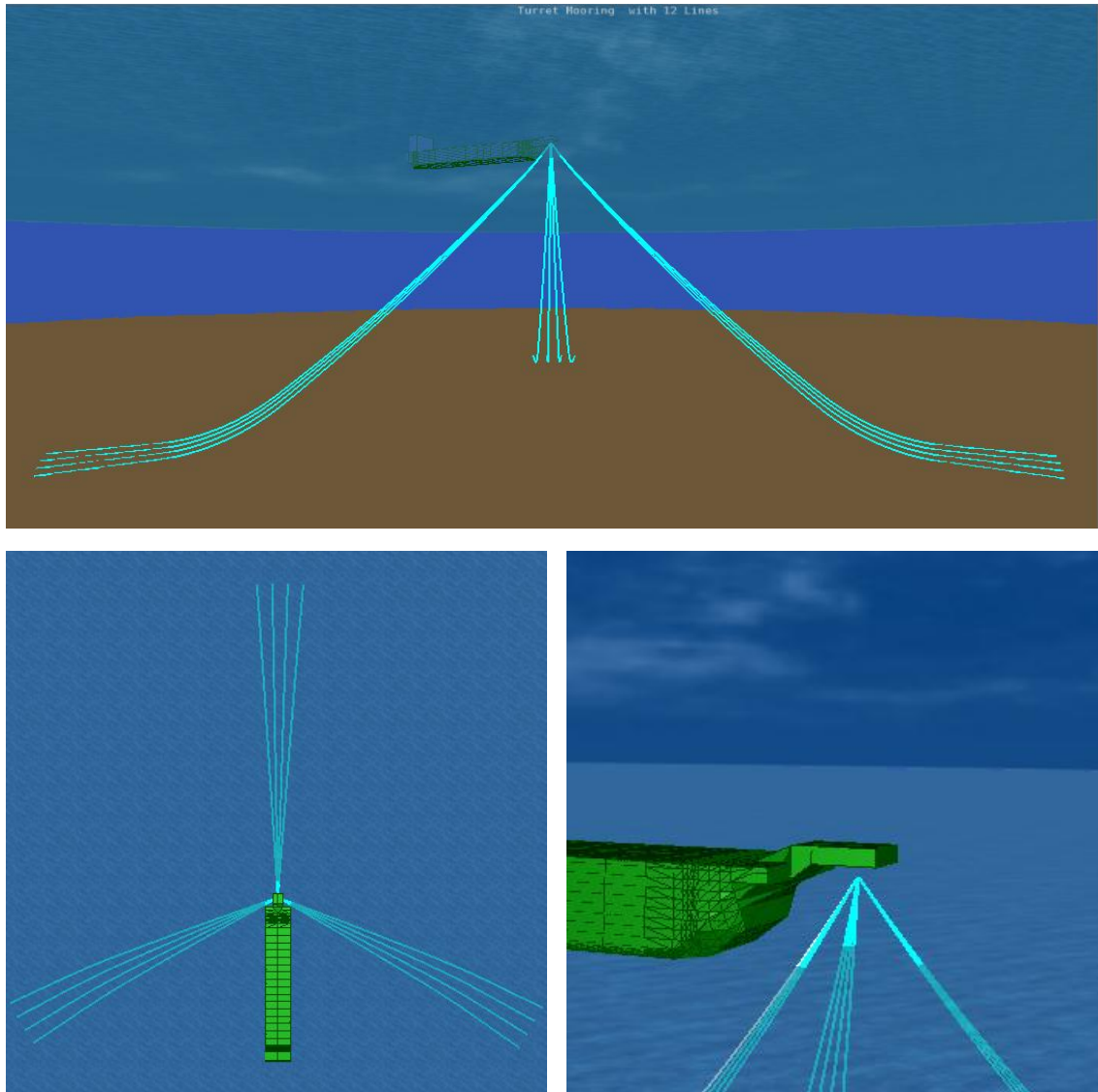


**Figure 3-24 Schematic View of Mooring System**

Note: Author is unable to make dual model i.e. earth fixed turret and rotating hull around the turret in MOSES due to its limitation. The computer model is one model and does not allow individual motion of turret and hull. The mooring lines are therefore connected to one point in center of turret to prevent yaw moment from the mooring lines.

### 3.5.4 Environmental Condition

Long term environment data was already describe at Section 3.1, which is the set of data are will be utilize for fatigue analysis of mooring system. For mooring strength performance the cyclonic environment data with specified return period is needed. Here is return period of 10-yr for mooring design performance check and 200-yr for extreme condition. The parameters of Omni-directional cyclonic environmental conditions with 10-yr and 200-yr RPs are reflected in Table 3-11 and Table 3-12m respectively. The environmental modelling will remain same as Section 3.2.5.

**Table 3-11 10-yr Return Period Environment Omni-Directional**

<b>Parameter</b>	<b>Unit</b>	<b>10-yr wave, 10-yr wind, and 10-yr current</b>
Wave		
Significant wave height	(m)	4.74
Spectral peak period	(s)	8.83
Jonswap peakedness parameter $\gamma$		1.24
Wind		
1-hour mean speed	(knots)	33.12
Current		
Surface current speed	(m/s)	0.74

**Table 3-12 200-yr Return Period Environment Omni-Directional**

<b>Parameter</b>	<b>Unit</b>	<b>200-yr wave, 200-yr wind, and 200-yr current</b>
Wave		
Significant wave height	(m)	7.28
Spectral peak period	(s)	10.74
Jonswap peakedness parameter $\gamma$		1.36
Wind		
1-hour mean speed	(knots)	47.37
Current		
Surface current speed	(m/s)	1.39

### 3.5.5 Analysis Matrix and Load Cases

The following limit states will be considered for analysis and design of the mooring system.

1. Fatigue limit state: long-term operational environmental condition with intact mooring system.
2. Ultimate limit state: 200-yr Return Period environmental with intact mooring system.
3. Accidental limit state: 200-yr Return Period environmental with one-line-damaged mooring system.

Long-term environmental data has been available as per Section 3.1, contains 29,208 data simultaneously combination of 1-hour mean wind speed, surface current speed, and wave/swell. This data set will be utilized for mooring system fatigue analysis. The fatigue damage will be calculated using DNV formulation “Accumulated Fatigue Damage” that stated in DNV-OS-E301 Position Mooring Section 2 F 100 (DNV, 2010).

A spectral approach requires a more comprehensive description of the environmental data and loads, and a more detailed knowledge of these phenomena. Using the spectral approach, the dynamic effects and irregularity of the waves may be more properly accounted for. This approach involves the following steps:

1. Selection of major wave directions,
2. For each wave direction, select a number of sea states and the associated duration, which adequately describe the long-term distribution of the wave,
3. For each sea state, calculate the short-term distribution of stress ranges using a spectral method.

Combine the results for all sea states in order to derive the long-term distribution of stress range. In the following, a formulation is used to further illustrate below.

Fatigue assessment approach by DNV is in line with the MOSES methodology to assess the fatigue damage (Nachlinger, 1989). The assessment of fatigue is normally expressed by a cumulative damage ratio. In other words, by Miner's Rule

$$CDR = \frac{T}{t} \int_0^{\infty} \frac{P(r)}{N(r)} dr \quad (3.5)$$

where  $CDR$  is the cumulative damage ratio,  $T$  is the duration of a process,  $t$  is the average period for a stress cycle,  $P$  is the probability density function of the stress range,

and  $N$  is the average number of cycles to failure at a given stress range. Notice that if a body is subjected to several different sea states, then the total damage ratio can be obtained by adding the CDR's for each sea state.

Notice that the frequency domain is an ideal place to consider the fatigue problem. Once the deformation response operators have been computed, the stress spectrum ( $S_s$ ) is simply

$$S_s = |S^*|^2 S_\eta \quad (3.6)$$

where  $S^*$  is the stress response operator and  $S_\eta$  is the sea spectrum. Combine the results for all sea states in order to derive the long-term distribution of stress range. A wave scatter diagram has been used to describe the wave climate for fatigue damaged assessment. The wave scatter diagram is represented by the distribution of  $H_s$  and  $T_p$ . The environmental wave spectrum  $S_\eta$  for the different sea states can be defined, i.e. applying the JONSWAP wave spectrum. Now, using the Raleigh distribution

$$P(r) = \frac{r}{4m_0} \exp\left(\frac{-r^2}{8m_0}\right)$$

$$t = 2\pi \left[ \frac{m_0}{m_2} (1 - \epsilon^2) \right]^{\frac{1}{2}}$$

$$\epsilon^2 = (m_0 m_4 - m_2^2) / m_0 m_4, \text{ and}$$

$$m_j = \int_0^{2\pi} \int_0^\infty S_s(\omega, \theta) \omega^j d\omega d\theta \quad (3.7)$$

Thus, the cumulative damage is easily computed from the stress response operators. Mathematically, Spectral-based Fatigue Analysis begins after the determination of the stress transfer function. Wave data are then incorporated to produce stress-range response spectra, which are used to describe probabilistically the magnitude and frequency of occurrence of local stress ranges at the locations for which fatigue strength is to be calculated. Wave data are represented in terms of a wave scatter diagram and a wave energy spectrum. The wave scatter diagram consists of sea-states, which are shortterm descriptions of the sea in terms of joint probability of occurrence of a significant wave height,  $H_s$ , and a characteristic period.

An appropriate method is to be employed to establish the fatigue damage resulting from each considered sea state. The damage resulting from individual sea states is referred to as “short-term”. The total fatigue damage resulting from combining the damage from

each of the short-term conditions can be accomplished by the use of a weighted linear summation technique (i.e., Miner's Rule).

The total expected damage for all seastates during the life of the structure is the sum of the damages for each individual seastate. Cumulative fatigue damage effect calculations are based on Miner's rule of linear accumulation with the appropriate S-N curve. The cumulative damage ratio (CDR), summed over all the various loads, shall not exceed 1.0. However, the Cumulative Damage Ratio (CDR) result computed by MOSES does not include the Design Fatigue Factors (DFF). Thus for corresponding targeted CDR is

$$CDR \leq \frac{1}{DFF} \quad (3.8)$$

The predicted fatigue life is then calculated as:

$$Predicted\ Fatigue\ Life\ (years) = \frac{Design\ Service\ Life}{CDR} \quad (3.9)$$

Moreover, Design Performance Limit State (10-yr RP environment) will not be included in this study as the extreme condition should be enough for ensure the reliable and efficient mooring system in term of mooring loads and vessel offsets for the riser design. The load cases for ultimate limit state and accidental limit state are defined using Omni-directional environment information as per Section 3.5.4 with 15deg resolution covering the entire 360deg. A number of environment alignment cases were created based on the DNV POSMOOR guidelines where the wind direction is modified up to a maximum of 30 degrees off the wave direction and the current up to a maximum of 45 degrees on the same side of the waves. The following combinations were used for the mooring analysis:

1. C1 - Collinear: Wind, wave and current from the same direction (aligned)
2. C2 - Crossed 1: Wind and current 30 degrees off the wave direction.
3. C3 - Crossed 2: Wind at 30 degrees off the waves, and current 45 degrees off the waves (on the same side as the wind).

Tension ratio is need to be considered at design of mooring configuration. Maximum tension should be limited by the tension ratio. It is defined as follow:

$$Tension\ Ratio = \frac{Applied\ Tension}{Minimum\ Breaking\ Load} \quad (3.10)$$

### 3.5.6 Design Criteria

The design criteria that will be considered in designing the mooring system are explained below:

1. Mooring system design life is 30 years. The mooring leg components will be designed as un-inspectable component and a minimum fatigue DFF of 10 (i.e.  $30 \times 10 = 300$ -yr fatigue life) as specified by ABS Rules for Classing and Building Floating Production Installations. (ABS, 2009)
2. Maximum ratio of maximum tension and breaking tension on anchor leg for an intact mooring system must be lower than 0.6 based on dynamic simulation.
3. Maximum ratio of maximum tension and breaking tension on anchor leg for a one-line-damage mooring system must be lower than 0.8 based on dynamic simulation.
4. Maximum vessel offsets for both intact and damaged mooring system must be restricted in consideration of riser system integrity (if any).

Allowable maximum tension and vessel offsets are presented in below:

**Table 3-13 Mooring System Design Criteria**

Limit State	Mooring System	Maximum Tension Ratio	Max Offset (%WD)
ULS (200-yr)	Intact	0.6	13%
ALS (200-yr)	One-Line-Damage	0.8	16%
DPLS (10-yr)	Intact	0.6	13%

5. No interference between anchor legs and vessel hull under any design storm conditions for intact or damaged mooring system.
6. No interference between anchor legs and risers under any design storm conditions for intact or damaged mooring system.
7. Mooring system must withstand loads from a carrier vessel up to a certain capacity in m<sup>3</sup> storage capacity, moored side-by-side to the storage vessel in the maximum loading environment.



## 4. RESULT AND DISCUSSION

### 4.1 Model Verification Result

The motion response operator were extracted and compared for both two computer program. All unit are based on metric system, meter and degree for translational and rotational RAO respectively. Both program use same theory when face a hydrodynamic problem i.e. linearized Bernoulli equation, the potential pressure functions beneath the water surface is given by:

$$P = -\rho\left(\frac{\partial\phi}{\partial t} + g_c z\right)$$

Where  $\rho$  is the fluid density,  $g_c$  is the gravity acceleration,  $z$  is the depth of submergence,  $\phi$  is the velocity potential for the flow.

The motion RAO for quarter-seas were plotted in Figure 4-1. From the comparison result following statements can be made:

1. The result mostly give a good agreement RAO graph between the two programs.
2. Since there are different method to solve the hydrodynamic problems, some of the result give a different solution. The supposed assumption for each program is listed below:

MOSES	AQWA
Fluid flow is inviscid and irrotational	Fluid flow is inviscid, irrotational, and incompressible
Body motion is small	Wave elevation is small
Water depth is infinite	Water depth is finite
Deformation acceleration is negligible	Boundary condition is solved by satisfying the body boundary condition (Timman-Newman relations)
Sea/structure interaction forces are independent of the deformation	Linearized free surface condition and radiation condition
	Long waves (low frequency) are depth limited while the short wave (high frequency) are limited by the mesh size.

3. It can be seen that in AQWA result give a larger result of motions due to ignored damping problem during preprocessing to solve the problem. In another side, MOSES

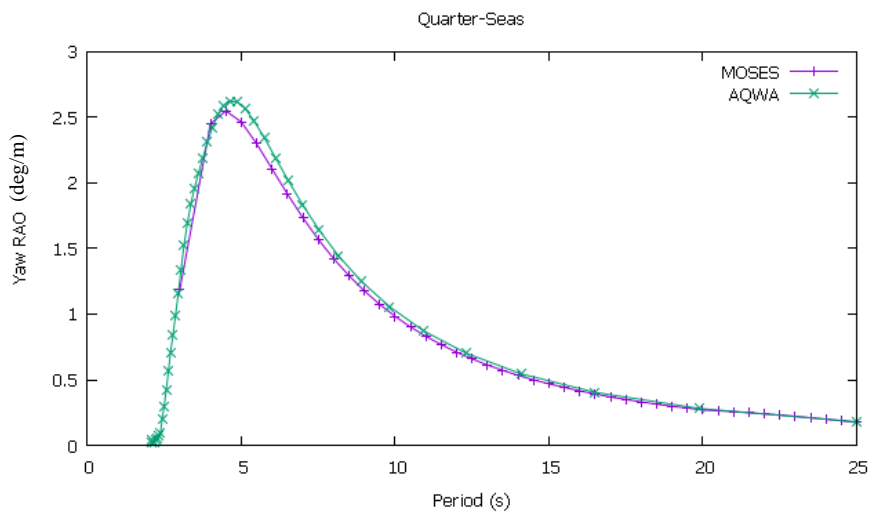
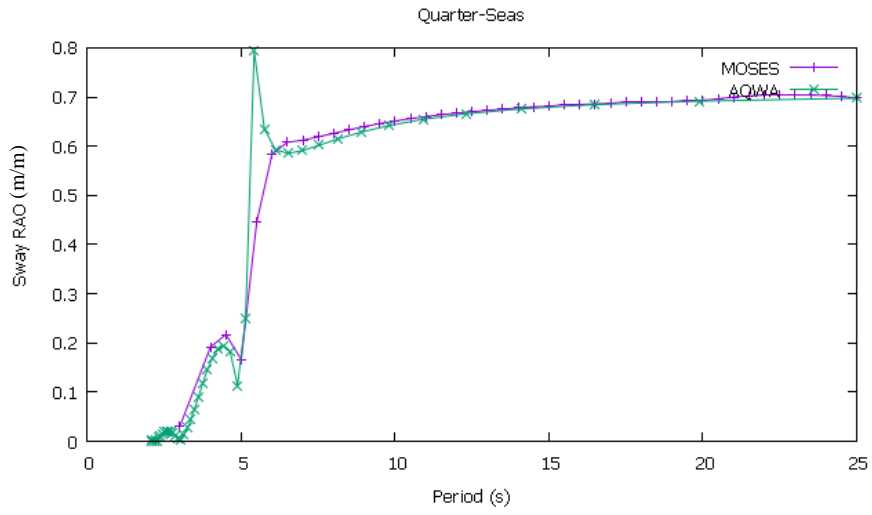
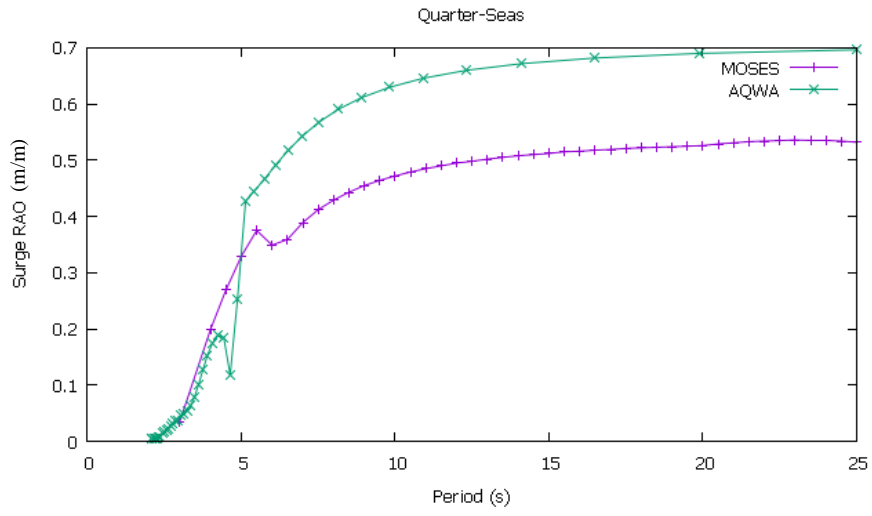
give a reasonable result since damping problem was set-up during preprocessing stage. As a sample, the peak pitch RAO given by AQWA is up to 35 since MOSES give only 15 of peak roll RAO.

4. For a simple geometry like a box, a resonance period should be not so critical and sensitive during solve the hydrodynamic problems. For this case, the absence of damping problem in AQWA give a significant result for motion response in resonance to high period.
5. Both programs give effective computing time to solve the hydrodynamic problems. But MOSES is more effective in time computing when left the unnecessary computing process.

For this study we can conclude MOSES is can be utilized for computing the hydrodynamic analysis. The comparison to AQWA give a satisfied result and it's convince that MOSES should be good and effective for heading analysis computation tool for this thesis.

Moreover to make it more convince with the proposed numerical calculation is also verified against existing publication by J.Ray McDermott in WAMIT-MOSES Hydrodynamic Analysis Comparison Study (McDermott, 2000). The added mass and damping coefficient is plotted in Figure 4-2 and Figure 4-3. As can be seen the proposed method resulted a pretty closed graph compare between MOSES to WAMIT. The wave periods used in the numerical calculation were selected from 2 second to 42 seconds in total of 20 period by increments of 2 seconds. Since the same of geometry and just slight different number of panels the consistent results is achieved between WAMIT and MOSES.

Finally we can now conclude that the extracted output of hydrodynamic coefficient in specific range period from low to high which cover a wide range of waves is resulting a good agreement between the three computer programs.



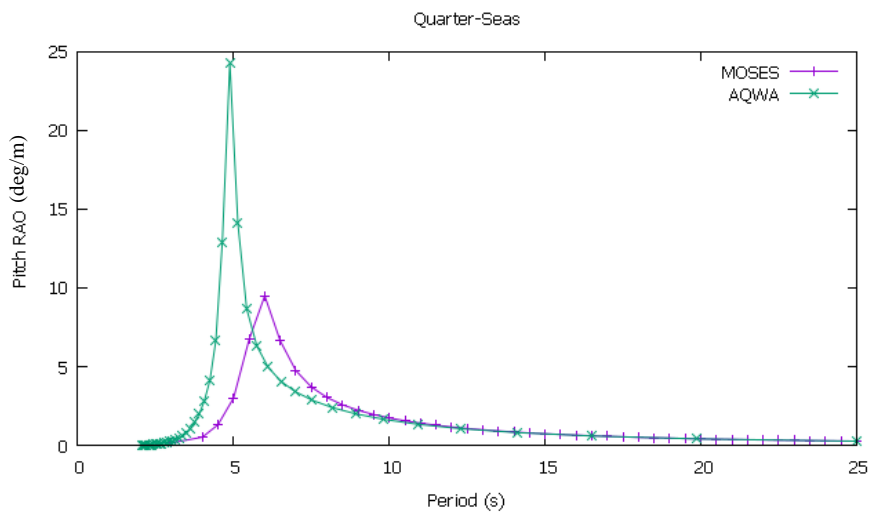
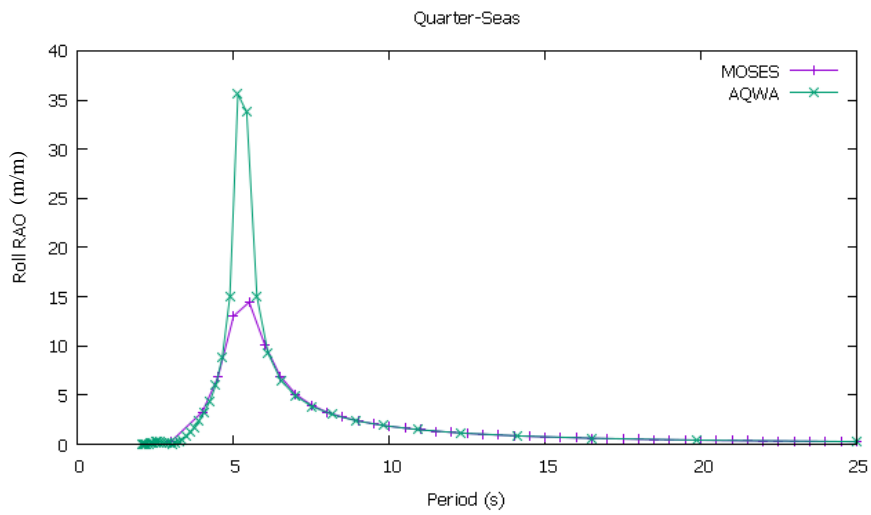
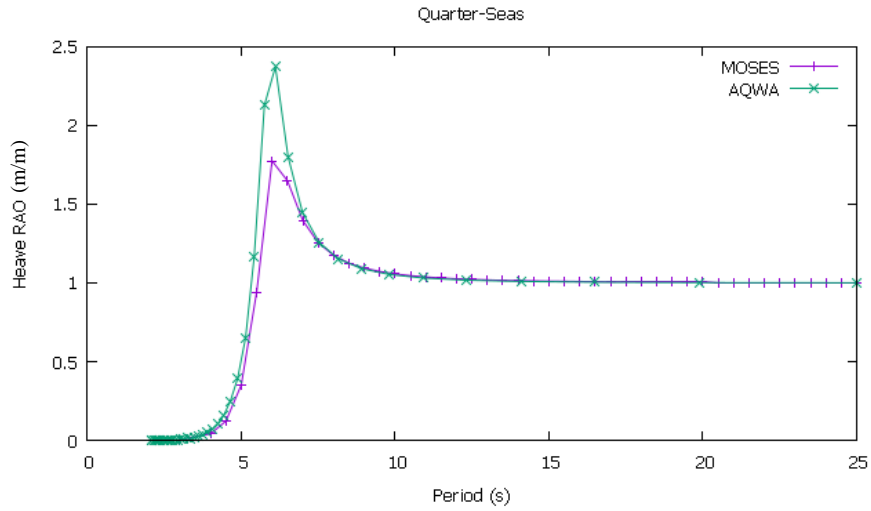


**Figure 4-1 Quarter-seas RAO Compare to AQWA**

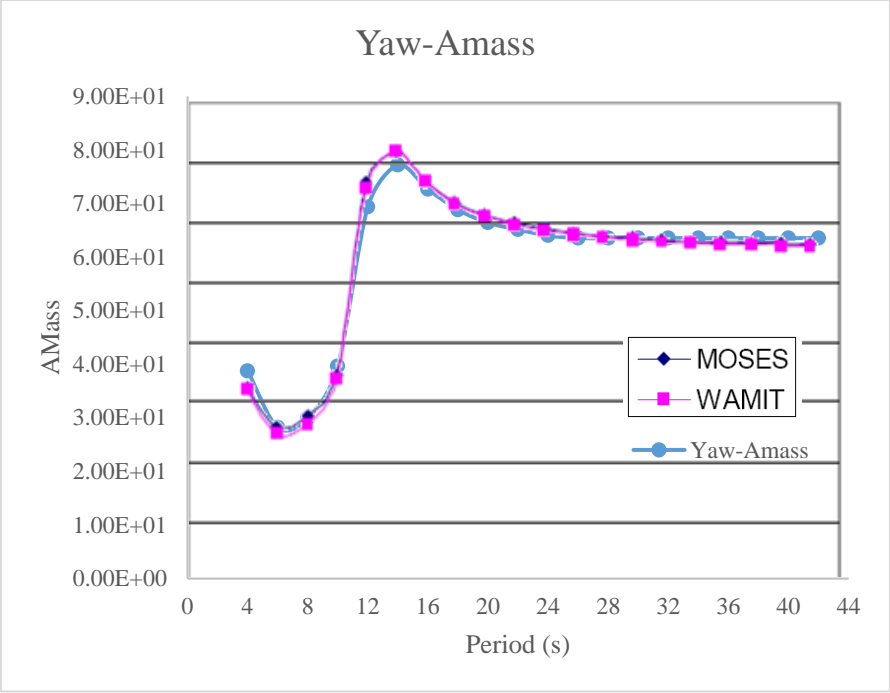
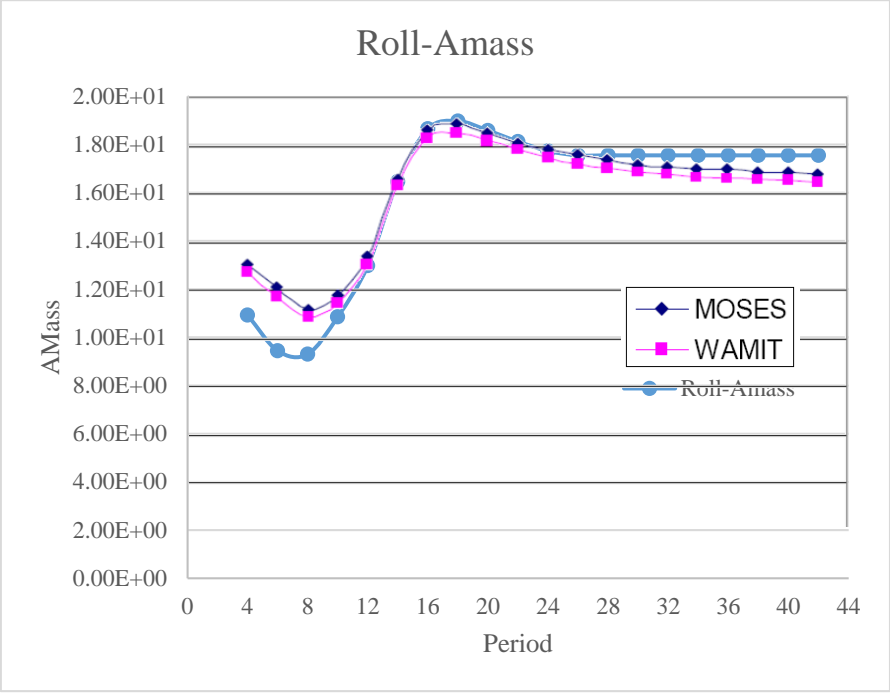


**Figure 4-2 Added Mass Compare to WAMIT**

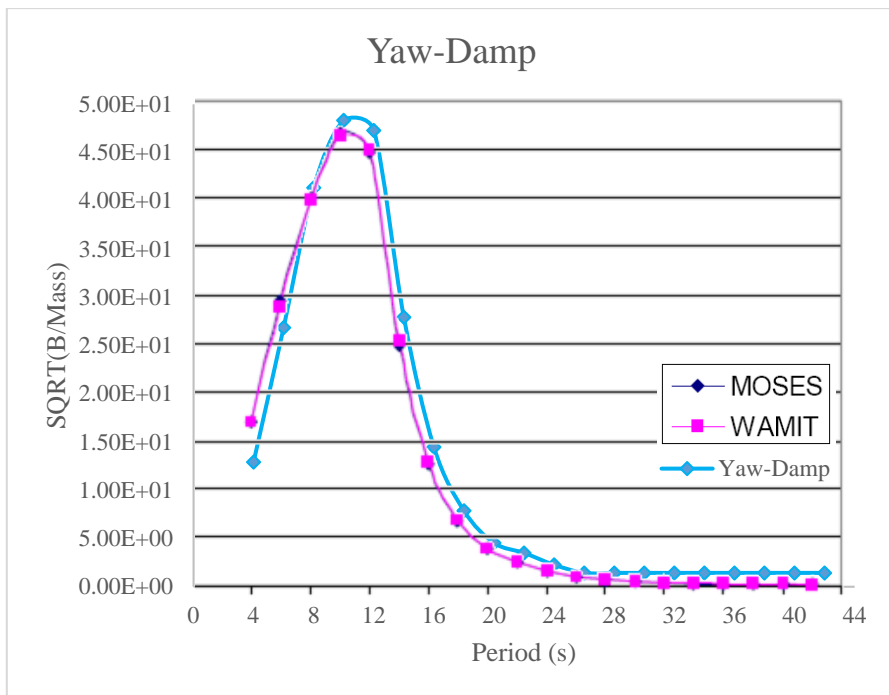
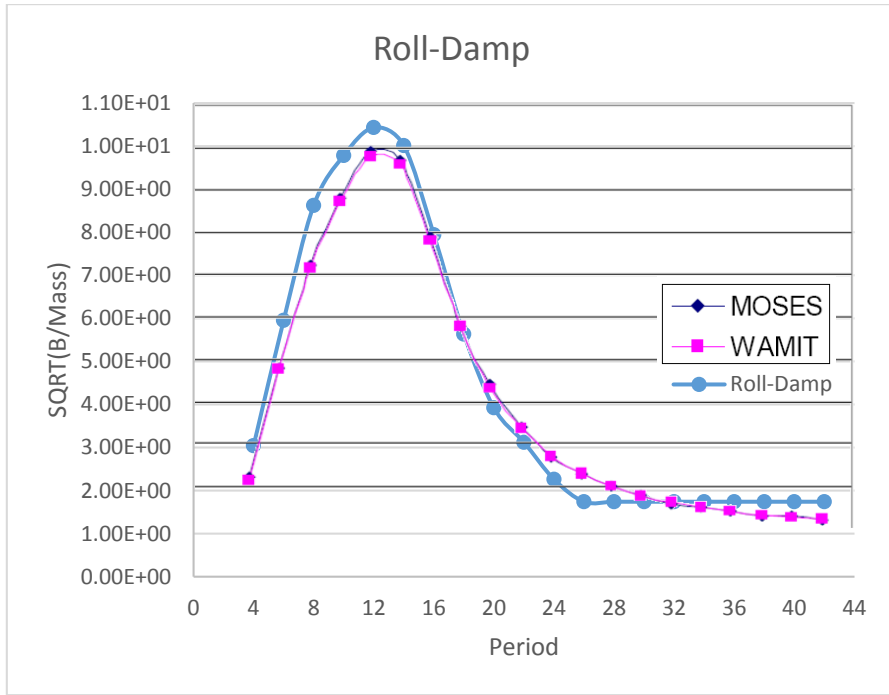


**Figure 4-3 Damping Compare to WAMIT**

## 4.2 Wave Heading Analysis

The long-term heading analysis is performed using the long-term fatigue load cases (10-year environmental conditions, 29208 cases). The analysis is performed for vessel in ballast draft but due to small variation of vessel draft the results for other drafts are reasonably close. The summary of vessel heading analysis is presented in Section 4.2.5. In this figure, the long-term probability distribution of vessel mean heading calculated in EFCS as well as the distribution of wind-vessel relative heading are presented. The vessel heading refers to the direction the vessel bow is heading towards and the relative wind-vessel heading is basically the wind heading measured with respect to the vessel heading (180deg. is head on and 90deg is beam on from starboard). Further detail of heading analysis result, for 29,208 load cases, is reported in Appendix A.

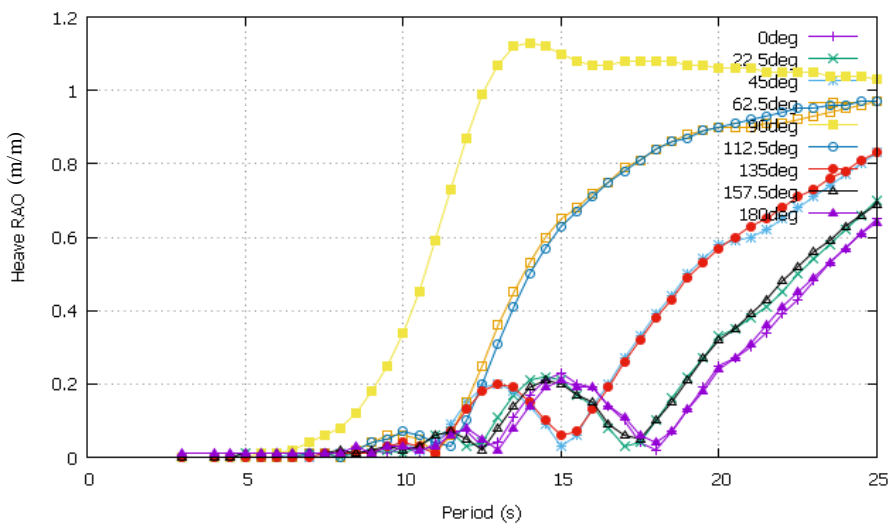
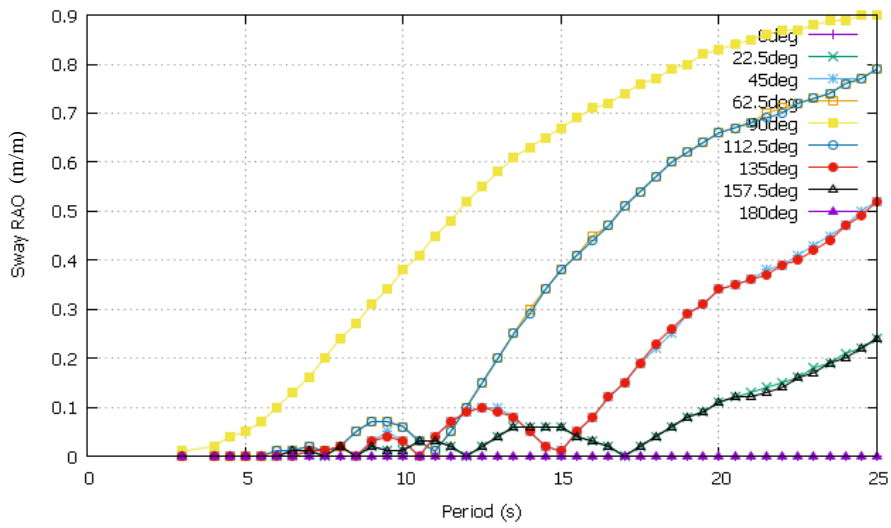
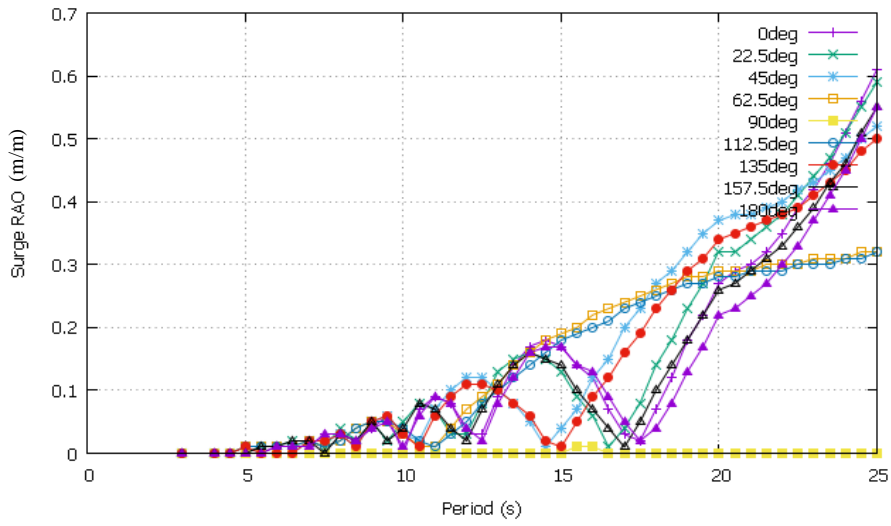
### 4.2.1 Response in Wave

Wetted surface of the vessel is discretized with 4500 panels, coordinate system as stated in Section 3.2.1. The x axis is positive in the direction of the vessel's bow, the y-axis point positive toward starboard side.  $\chi$  is the angle of incidence of a plane progressive wave relative to the positive x-axis, with  $\chi=180$  degrees defined as the head wave. The hydrodynamic forces are obtained by imposing boundary conditions on the wetted surface of the vessel.

Shown in Figure 4-4 are the RAOs for six degrees of freedom of the vessel in regular waves along with combined inclination of roll and pitch, calculated by integrating hydrodynamic forces on the wetted surface. Surge, sway, and heave motions are described per unit wave amplitude, and roll, pitch, and yaw are described per unit wave slope.

Pitch motion, quite small compared to roll motion, will have substantially no influence on the operability of the vessel. On the other hand, roll motion will cause significant inclination only in limited wave conditions near-natural period wave and near-beam wave.

Mean wave drift force for the vessel is presented in Figure 4-5. There are three wave drift component of surge force, sway force, and yaw force. As can be seen the sway force and yaw force is have zero value when wave coming from bow for all wave period. Moreover the surge force is remain constant for all wave period during wave coming from bow.





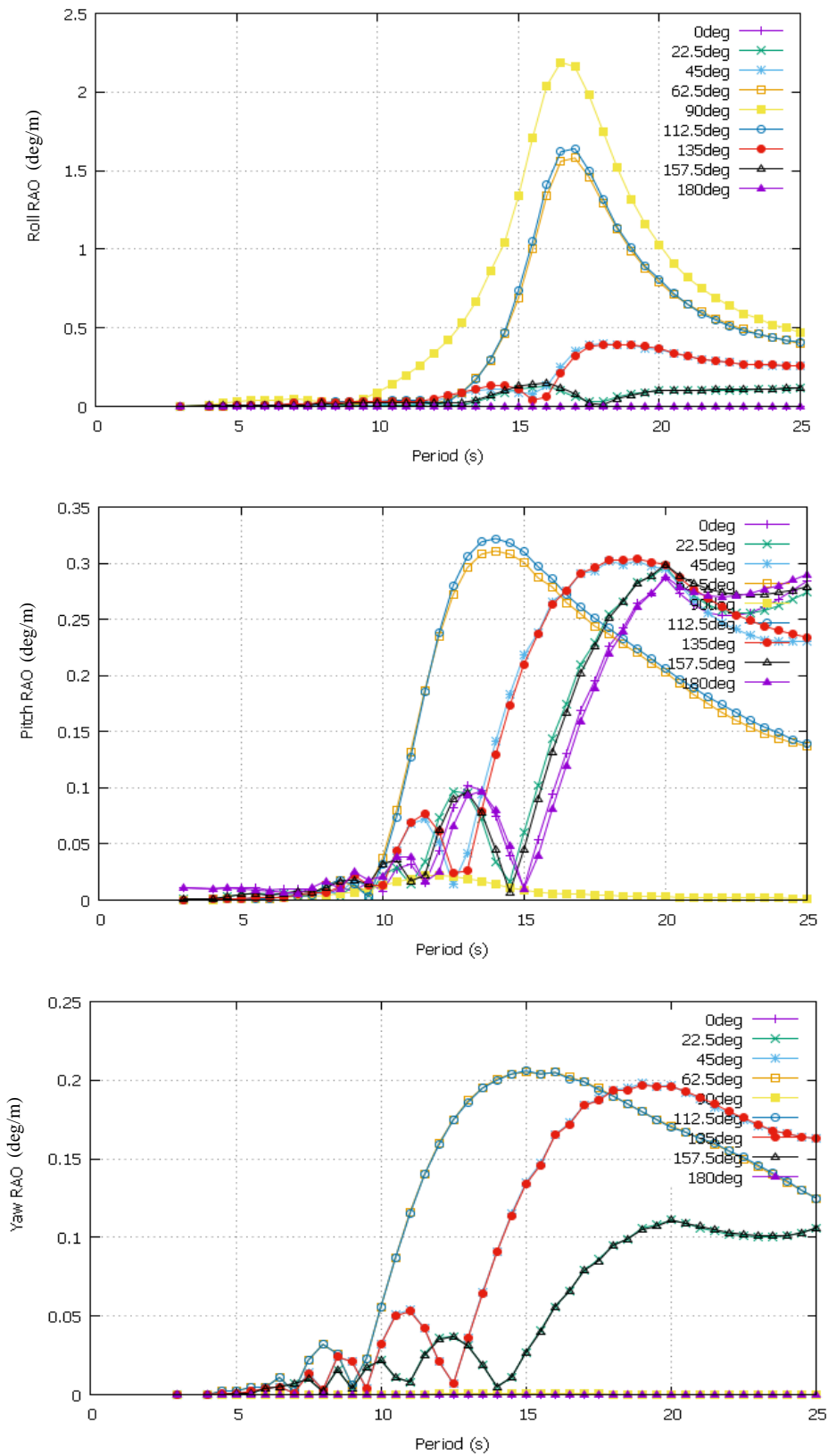


**Figure 4-4 Vessel Motion Response Operator**

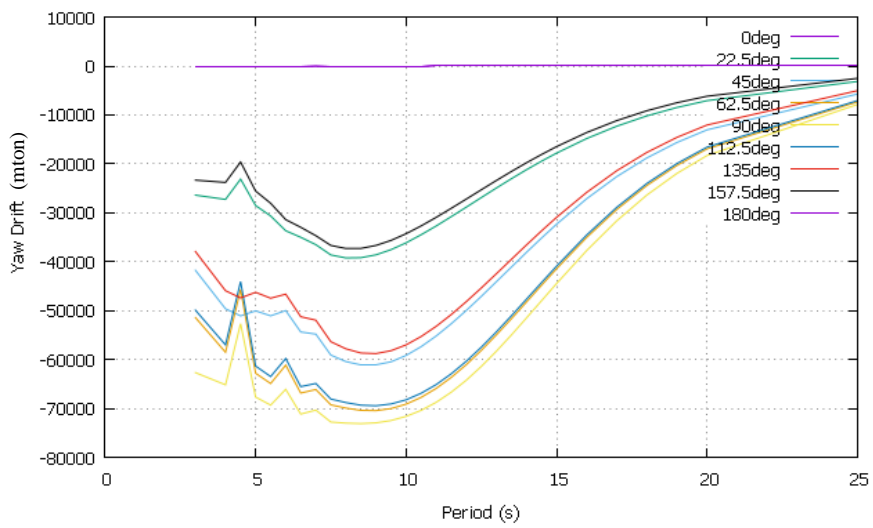
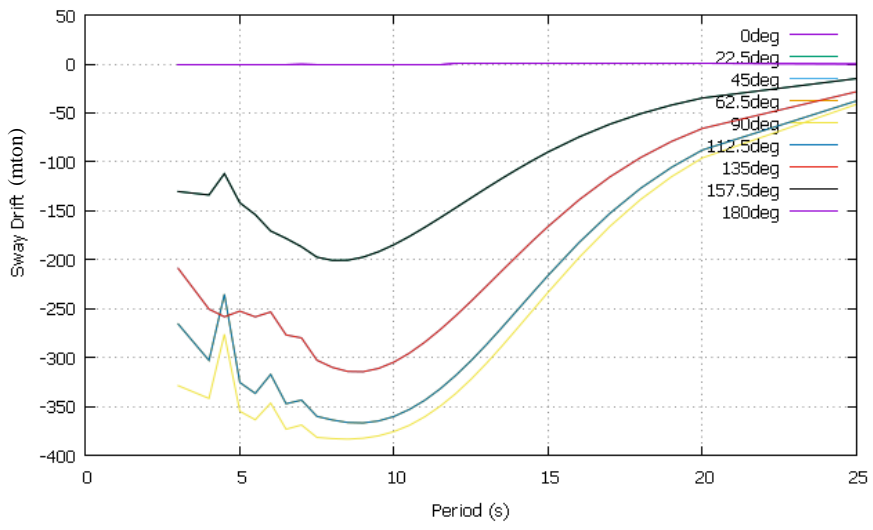


**Figure 4-5 Mean Drifting Forces**

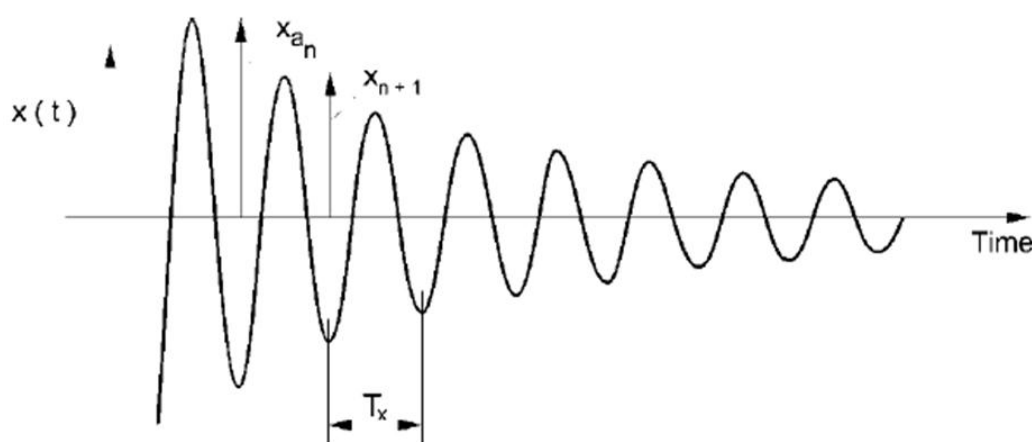
#### 4.2.2 Free Decay Test

Free decay test are performed in time domain with MOSES to estimate natural periods and the damping of the three oscillation motion from the six degree of freedom. The results are provided in Table 4-1 and the time histories of motion, used to estimate these values, are reported respectively in Figure 4-6 through Figure 4-8.

**Table 4-1 Natural Period and Critical Damping**

Motion	Natural Period (s)	Damping (% of Critical Damping)
Heave	10	21.5%
Roll	16	3.4%
Pitch	9	6.2%

Natural periods can be obtained from the recorded decay curves of the various decay/free excitation test the damping coefficients may be derived from the decrease of motion amplitude for two successive oscillations. Also natural the natural periods may be derived from the test.



Where

$x(t)$  = time history of motion  $x$

$x_{an}$  = motion amplitude of  $n$ -th oscillation

$T_\phi$  = natural period of motion  $x$

The free decay test are performed in free floating and calm seas condition. The contribution of mooring line is not consider at this stage. The natural period is taken as the average over the firs cycles which is 5 to 10 cycles are considered.

The damping is calculated as:

$$\zeta = \frac{\delta}{\sqrt{4\pi^2 + \delta^2}}$$

Where  $\delta$  is the logarithmic decrement defined as:

$$\delta = \ln \frac{(X_i)}{(X_{i+1})}$$

Where  $x_i$  is the  $i$ -th maximum from the free decay test result.

In MOSES the customized parameter to solve damping problem are coefficient parameter of Tanaka and Current. How the problem solved is further explained in MOSES Manual (Ultramarine, 2012). Either customized parameter shall not use in a same time, then if it so will cause over damped result. Since there are no model test experiment to determine the correct damping coefficient value, sensitivity study on damping calculation to get a reasonable damping value is observed. As can be seen in Figure 4-6 and Figure 4-7 it is a slight difference between both damping parameter used in calculation. But in Figure 4-8 for pitch motion the effect of difference method is clearly seen. Both method has used damping coefficient of 1.0. The “Tanaka” damping is supposed to be a result of eddy formation at the bilge and the “current” panel integration is simply due to pressure drag over the bottom. The damping problem should be verified against field measurements or model test that to be tune-in onto hydrodynamic model. Since the absence on model test result this study was utilize the “current” damping method to perform further hydrodynamic problem.

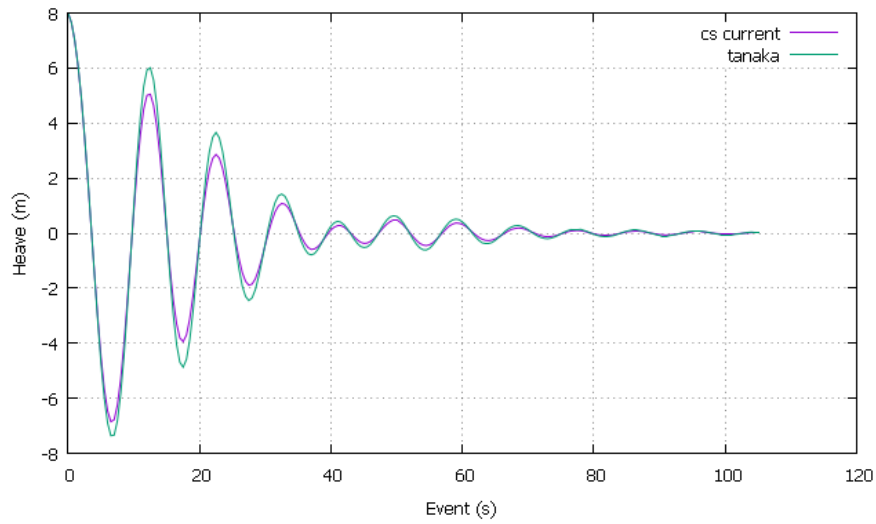


**Figure 4-6 Heave Free Decay Test: Maximum for Each Cycles**

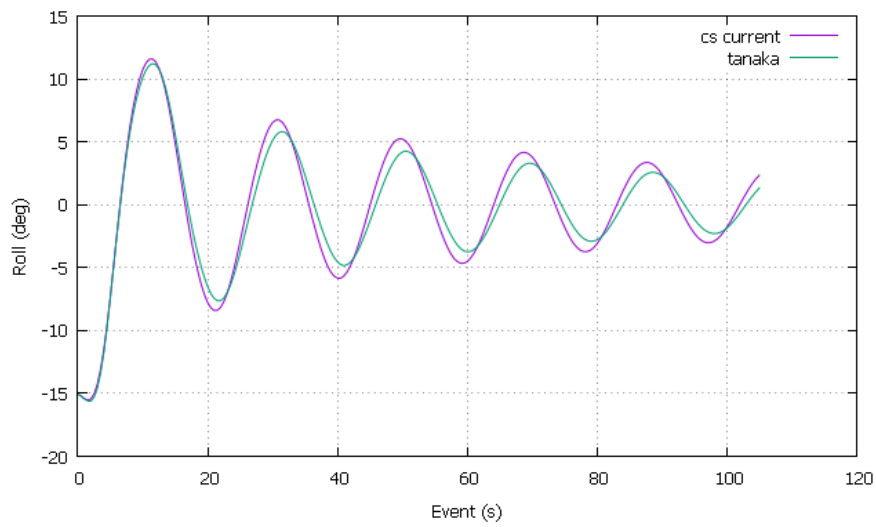


**Figure 4-7 Roll Free Decay Test: Maximum for Each Cycles**

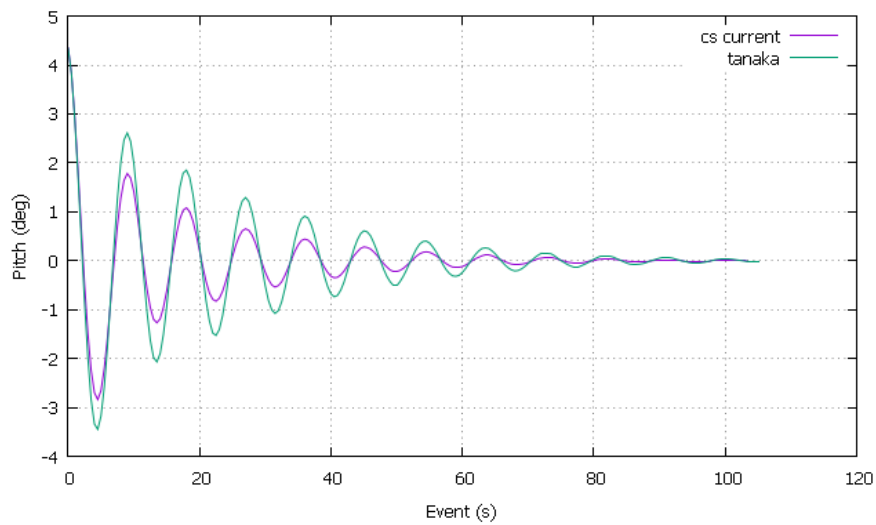


**Figure 4-8 Pitch Free Decay Test: Maximum for Each Cycles**

### 4.2.3 Hydrodynamic Coefficient

Three dimensional diffraction/radiation analysis is performed using MOSES to compute the hydrodynamic coefficients, such as added mass, radiation damping, linear wave force, and QTF. Using available vessel documents the following sample result are as follow:

#### 1. Added mass and damping

Frequency	0.2513	Period	25.0000		
Added Mass					
5.30864E-02	0.00000E+00	0.00000E+00	0.00000E+00	-1.32716E+00	8.50456E-10
0.00000E+00	7.06747E-01	2.94800E-04	-1.11925E+00	8.43235E-05	2.58724E-01
0.00000E+00	-3.22944E-04	2.54670E+00	1.10660E-02	1.99234E+01	-2.83352E-04
0.00000E+00	-1.11925E+00	1.10660E-02	4.96935E+02	3.84590E+00	9.66995E-01
-1.32716E+00	8.43235E-05	1.99234E+01	-1.99841E+00	5.35814E+04	4.70997E+01
8.50456E-10	2.58724E-01	-2.83352E-04	-3.67407E+00	-4.66145E+01	1.38142E+04
Damping					
1.17696E-02	0.00000E+00	0.00000E+00	0.00000E+00	-2.94239E-01	1.88551E-10
0.00000E+00	8.06999E-02	1.95601E-04	9.25084E-01	4.27550E-06	-1.24520E+01
0.00000E+00	4.27495E-06	7.95628E-01	5.44590E-03	3.68950E+01	-4.99487E-05
0.00000E+00	9.25084E-01	5.44590E-03	9.25522E+01	1.21044E+00	-3.11672E+02
-2.94239E-01	4.27550E-06	3.68950E+01	1.90987E-01	3.29788E+04	1.25504E+01
1.88551E-10	-1.24520E+01	-4.99487E-05	-3.11748E+02	-1.64801E+01	8.27194E+03
Frequency	0.2565	Period	24.5000		
Added Mass					
5.30864E-02	0.00000E+00	0.00000E+00	0.00000E+00	-1.32716E+00	8.50456E-10
0.00000E+00	7.08200E-01	2.81257E-04	-1.08037E+00	8.74001E-05	2.59293E-01
0.00000E+00	-3.26971E-04	2.51569E+00	1.08238E-02	1.97001E+01	-2.82149E-04
0.00000E+00	-1.08037E+00	1.08238E-02	4.96499E+02	3.78639E+00	9.85656E-01
-1.32716E+00	8.74001E-05	1.97001E+01	-2.00174E+00	5.29330E+04	4.65503E+01
8.50456E-10	2.59293E-01	-2.82149E-04	-3.51491E+00	-4.57208E+01	1.38426E+04
Damping					
1.16414E-02	0.00000E+00	0.00000E+00	0.00000E+00	-2.91034E-01	1.86497E-10
0.00000E+00	8.58031E-02	1.97281E-04	9.14101E-01	4.63279E-06	-1.26350E+01
0.00000E+00	2.90027E-06	7.96162E-01	5.46784E-03	3.71547E+01	-5.03455E-05
0.00000E+00	9.14101E-01	5.46784E-03	9.36654E+01	1.23025E+00	-3.16294E+02
-2.91034E-01	4.63279E-06	3.71547E+01	1.75206E-01	3.31673E+04	1.27792E+01
1.86497E-10	-1.26350E+01	-5.03455E-05	-3.16353E+02	-1.67150E+01	8.48743E+03

## 2. Linearized Wave Frequency Forces

+++ L I N E A R I Z E D W A V E F R E Q U E N C Y F O R C E S +++

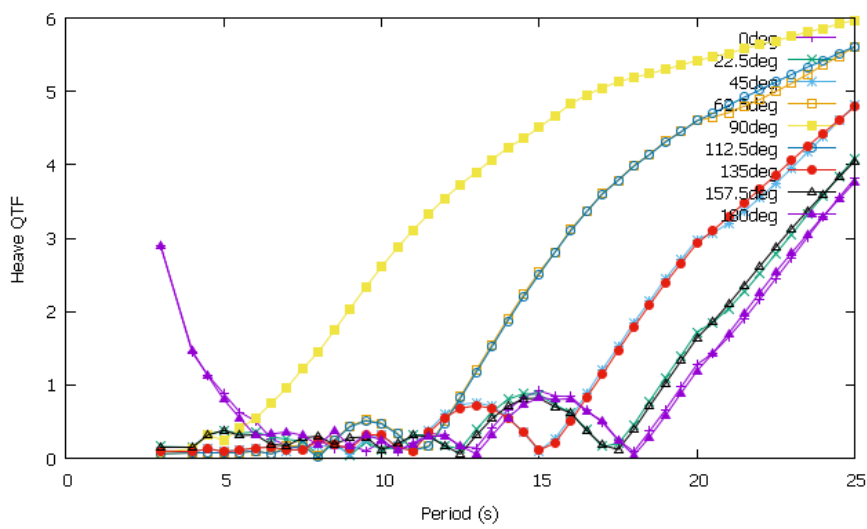
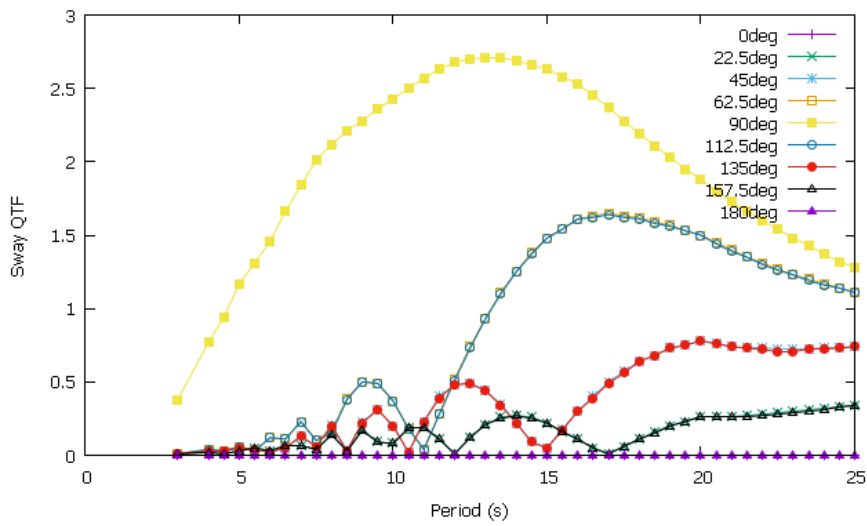
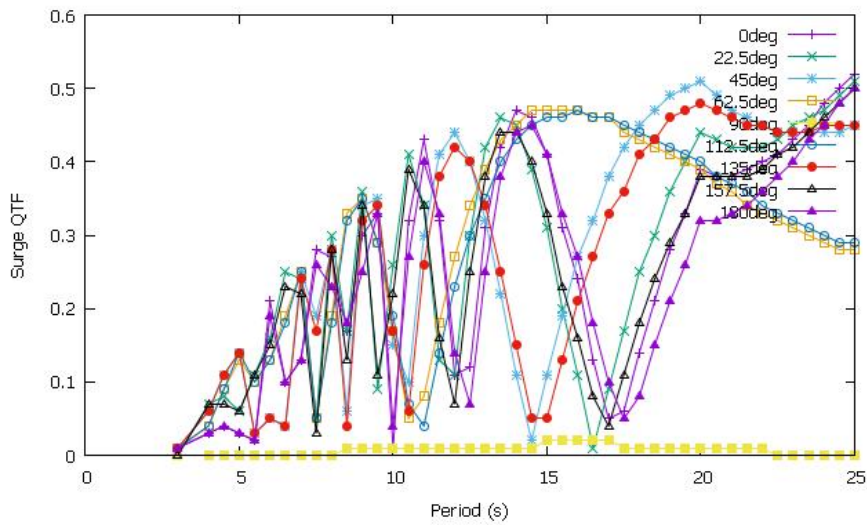
Results are in Body System

Of Point On Body TANKER At X = 257.1 Y = 0.0 Z = 25.0

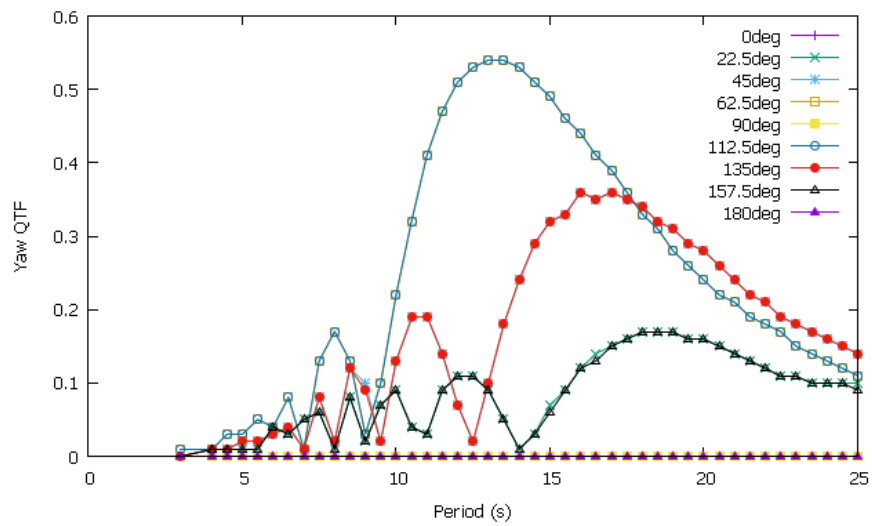
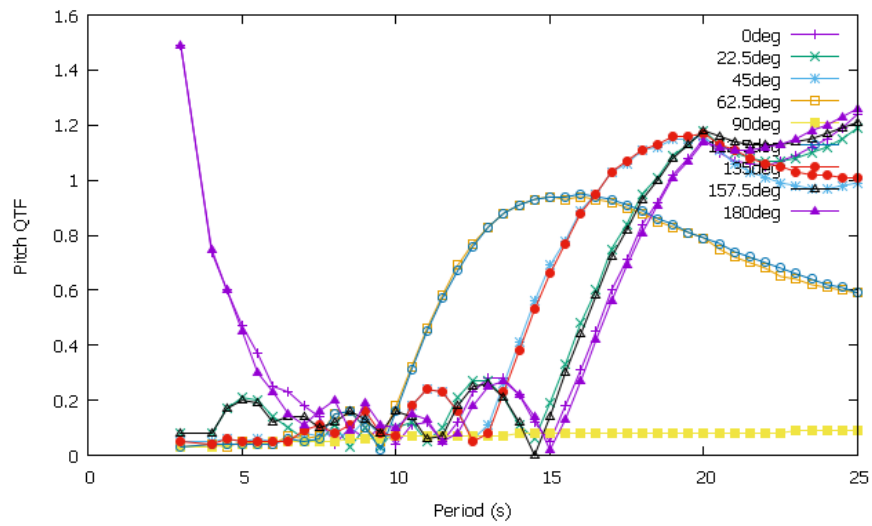
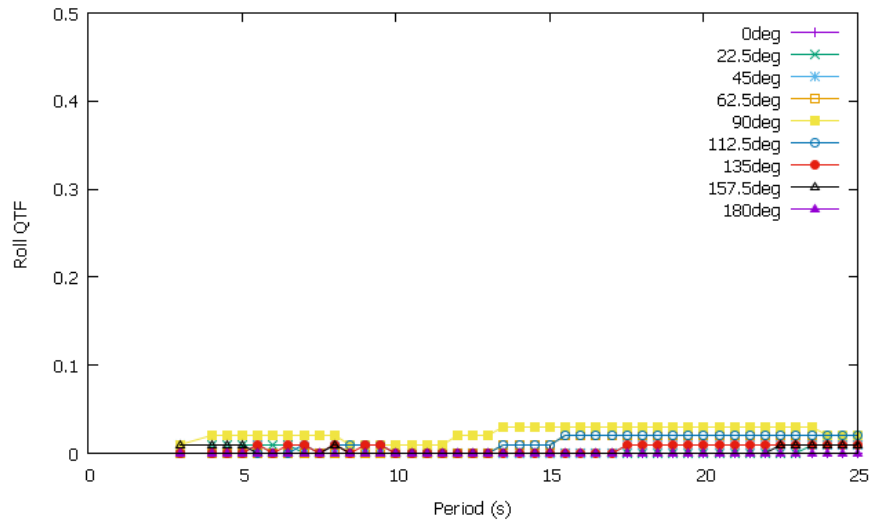
Process is DEFAULT: Units Are Degrees, Meters, and M-Tons Unless Specified

E N C O U N T E R		Surge Force /		Sway Force /		Heave Force /		Roll Moment /		Pitch Moment /		Yaw Moment /	
-----		Wave Ampl.		Wave Ampl.		Wave Ampl.		Wave Ampl.		Wave Ampl.		Wave Ampl.	
Frequency	Period	/-----/		/-----/		/-----/		/-----/		/-----/		/-----/	
-(Rad/Sec)-	-(Sec)-	Ampl.	Phase	Ampl.	Phase	Ampl.	Phase	Ampl.	Phase	Ampl.	Phase	Ampl.	Phase
0.2513	25.00	2284	22	3722	-163	24097	-41	34508	36	2528199	45	363460	103
0.2565	24.50	2260	19	3671	-167	23196	-43	33653	34	2539163	43	380299	98
0.2618	24.00	2241	16	3630	-170	22278	-44	32852	32	2554606	40	401464	92
0.2674	23.50	2230	12	3602	-174	21344	-46	32084	30	2575226	38	426762	87
0.2732	23.00	2226	9	3589	-178	20392	-48	31345	28	2601701	35	455984	83
0.2793	22.50	2231	5	3592	177	19426	-50	30647	25	2634826	33	488898	78
0.2856	22.00	2247	1	3614	173	18452	-53	29991	22	2675295	30	525341	75
0.2922	21.50	2274	-2	3656	168	17478	-56	29410	18	2724053	28	565140	71
0.2992	21.00	2314	-6	3721	164	16516	-60	28932	14	2782089	25	608143	68
0.3065	20.50	2367	-10	3809	160	15587	-64	28601	10	2850563	22	654259	65
0.3142	20.00	2436	-13	3922	156	14718	-69	28461	5	2930812	20	703342	63
0.3222	19.50	2357	-19	3773	150	13363	-73	26252	1	2912330	16	738831	57
0.3307	19.00	2299	-24	3659	144	12003	-78	23974	-3	2907862	12	783900	51
0.3396	18.50	2161	-30	3407	137	10502	-82	21068	-6	2847310	7	812610	44
0.3491	18.00	2046	-37	3196	130	8986	-88	17878	-11	2802552	2	854727	37
0.3590	17.50	1832	-43	2820	123	7381	-93	14379	-13	2683043	-2	867998	29
0.3696	17.00	1641	-51	2486	114	5753	-100	10464	-16	2579002	-8	899905	21
0.3808	16.50	1338	-57	1974	107	4153	-105	7366	-12	2382297	-15	884788	12
0.3927	16.00	1047	-67	1487	95	2497	-116	3931	-5	2202270	-22	894682	2
0.4054	15.50	666	-67	872	94	1037	-117	2608	34	1924136	-29	834687	-8
0.4189	15.00	259	-69	238	82	543	62	4216	90	1657401	-39	806796	-20
0.4333	14.50	270	44	449	-127	1788	43	6785	95	1322664	-48	720830	-33
0.4488	14.00	750	46	1119	-138	2765	31	8622	92	956870	-59	601653	-47
0.4654	13.50	1241	33	1730	-153	3396	18	9360	87	576152	-70	447612	-62
0.4833	13.00	1685	16	2210	-170	3623	5	9059	86	203285	-82	260883	-79
0.5027	12.50	2011	-3	2472	170	3414	-8	8400	89	134639	79	50497	-92
0.5236	12.00	2125	-26	2420	149	2769	-23	8439	98	405426	65	165949	55
0.5464	11.50	1918	-52	1982	125	1738	-39	9101	103	572568	49	355066	32
0.5712	11.00	1308	-81	1151	99	479	-46	8858	106	596828	31	473011	5
0.5984	10.50	322	-109	77	118	778	87	7612	123	456156	12	470882	-25
0.6283	10.00	841	19	1024	-153	1585	69	10308	150	177515	2	316942	-59
0.6614	9.50	1700	-25	1565	166	1605	44	16018	146	196342	108	39632	-81
0.6981	9.00	1588	-79	1131	120	676	28	15286	128	407199	87	238221	24
0.7392	8.50	205	-138	156	-150	934	116	9749	158	277743	55	294079	-29
0.7854	8.00	1387	-41	1017	171	1186	77	19566	160	198294	132	44289	-75
0.8378	7.50	875	-133	293	105	537	146	10494	155	265390	91	195968	-1
0.8976	7.00	1221	-68	641	172	623	107	18000	170	215353	154	18672	-37
0.9666	6.50	191	-30	245	-136	756	158	14454	-157	123682	179	92402	-29
1.0472	6.00	253	154	95	-126	682	-166	12509	-134	135523	-157	80663	8
1.1424	5.50	137	-75	200	-105	546	-133	13157	-110	137450	-130	60872	12
1.2566	5.00	725	166	245	-153	442	-70	10931	-87	126710	-70	42762	80
1.3963	4.50	537	121	144	-138	640	-9	6130	-17	163232	-12	27287	88
1.5708	4.00	301	95	154	-70	448	60	8390	71	110641	58	17796	113
2.0944	3.00	58	160	33	36	484	13	6421	32	125257	13	9841	-131

### 3. QTF (Quadratic Transfer Function)







#### 4.2.4 Weathervaning Analysis

Weathervaning analysis is performed to find the low frequency dynamic behavior of the vessel in waves. In Figure 4-9 is shown dynamic behavior of the vessel during a 3hr simulation. Time step is 0.4s, and that gives 27000 time iterations. The yaw motion is represent by blue line (RZ vessel). This initial weathervaning analysis is performed by single environmental load case in order to validate proposed numerical model. It can be seen that the vessel initial heading of 0deg then change gradually from event 0s up to 1,200s till heading of 20deg. This event is on transient state of the simulation. Then going to steady state at event above 1,200s till the simulation finish at event 10,800s, weathervane effect is seen. Therefore the proposed weathervane model is verified to utilize for further analysis.

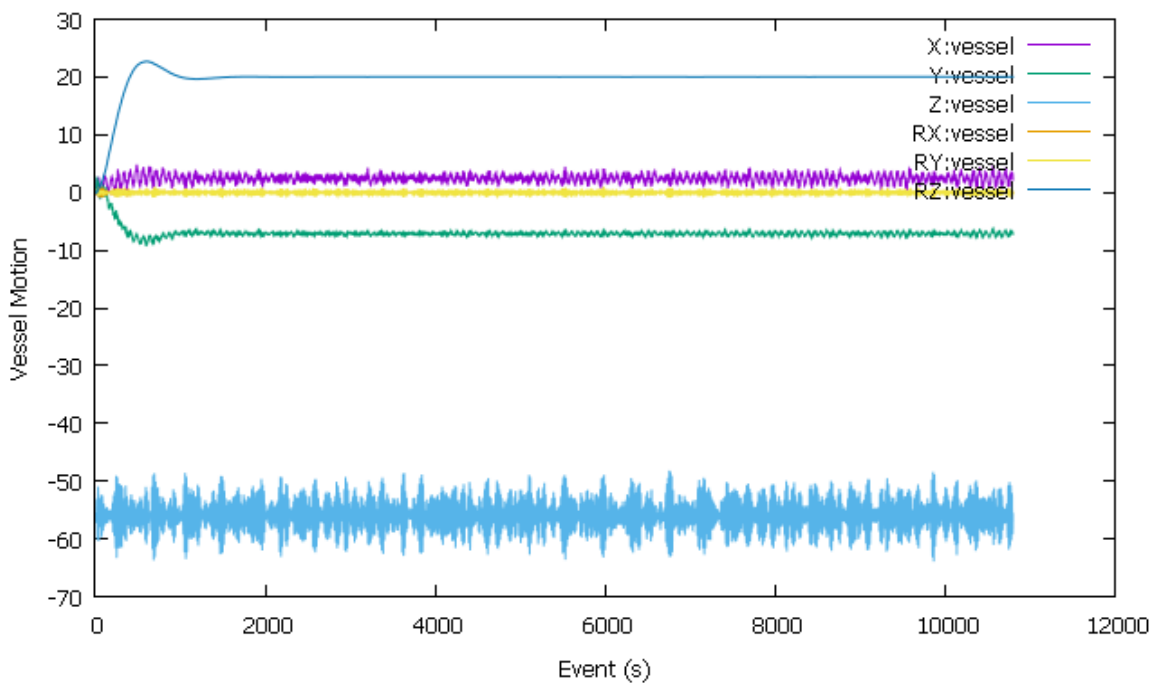


**Figure 4-9 Weathervaning Analysis**

#### 4.2.5 Heading Analysis Outcome

The outcomes of heading analysis in this study are presented in Figure 4-10 as occurrence probability, where vessel's bow facing to north is defined as 0 degree. As shown in Figure 14.1, the vessel heads towards South East-East sector (from 105deg to 135deg) for more than 60% of time. Secondly, vessel heads towards the North West – West sector (270deg to 300deg) for about 28% of time.

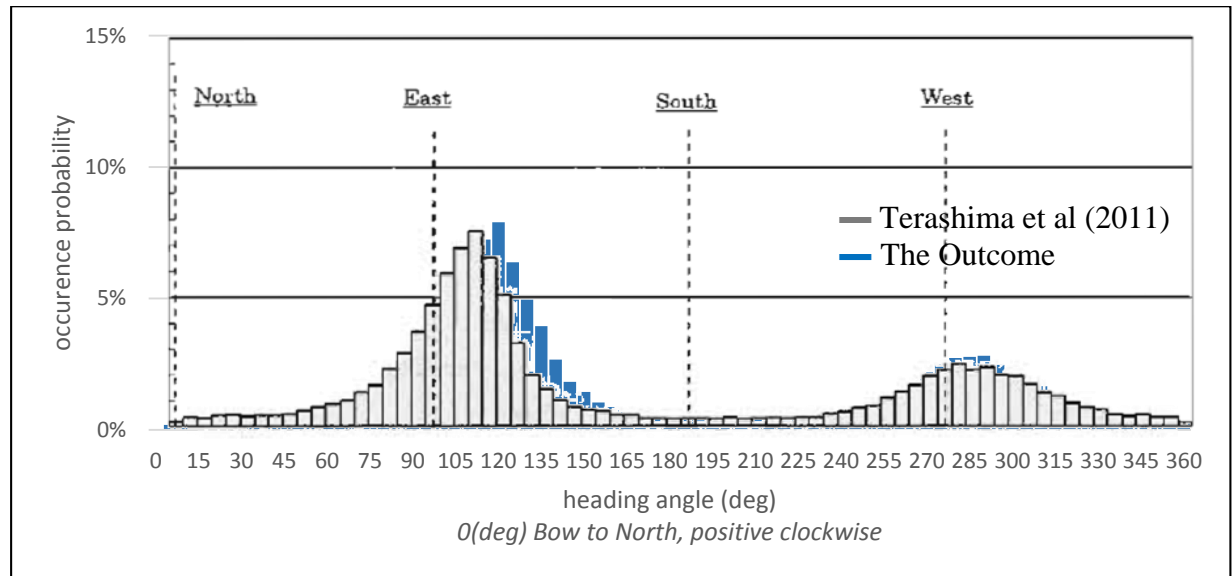


**Figure 4-10 Occurrence Probability of vessel's Heading Angles**

Figure 4-11 shows relations of incident wind direction and wind speed for all cases. Weathervane effect is seen for strong winds. Occurrence probability of incident wind direction is shown in Figure 4-12. It is seen that the vessel has a tendency to turn to incoming wind direction but the most frequent wind direction is shifted 15 degree to starboard side, which implies that current predominantly incomes from the opposite side, i.e. port side. Heading with current is shown in Figure 4-13 and Figure 4-14 in the same manner as for wind. As expected, current port side is predominant.

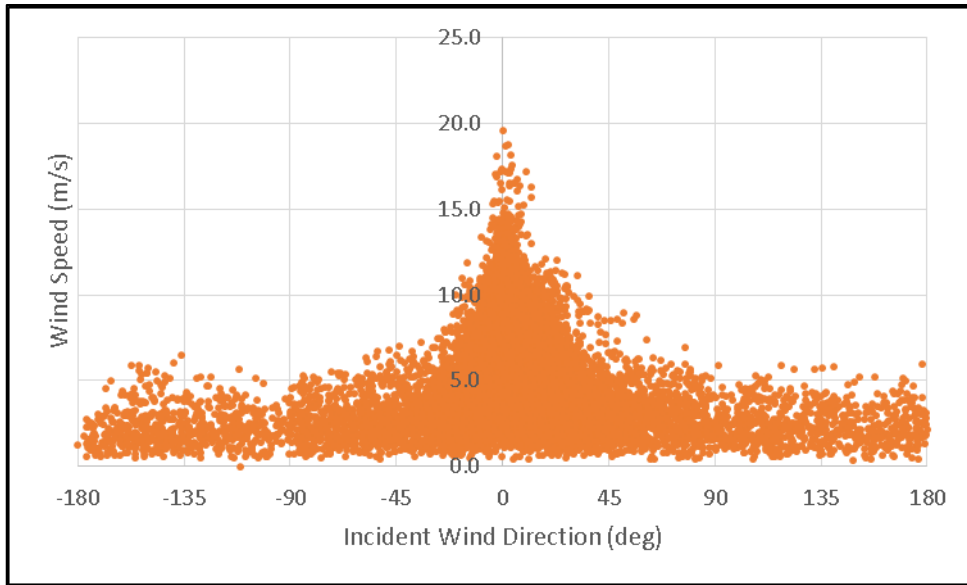


**Figure 4-11 Relation between Wind Speed and Incident Wind Direction**

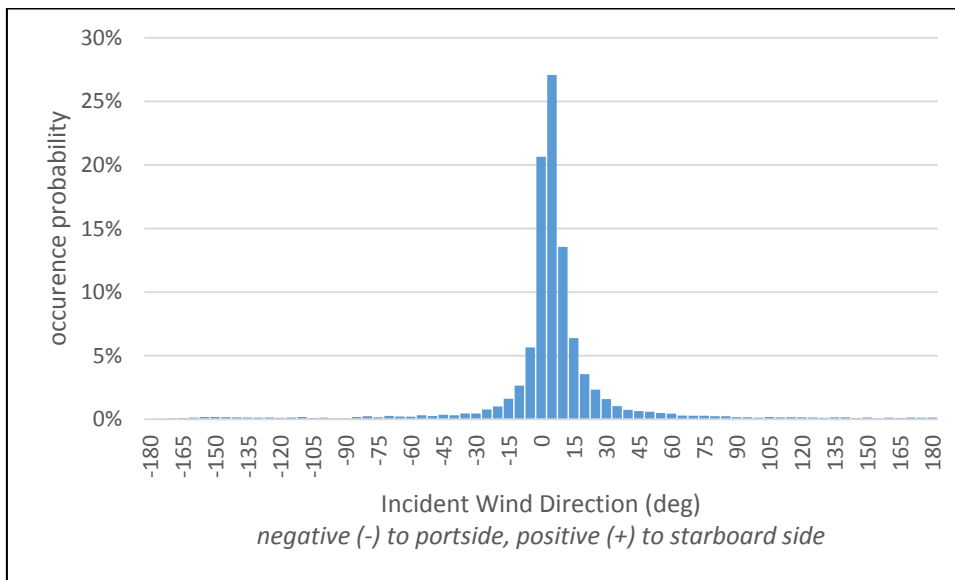


**Figure 4-12 Occurrence Probability of Wind Direction**

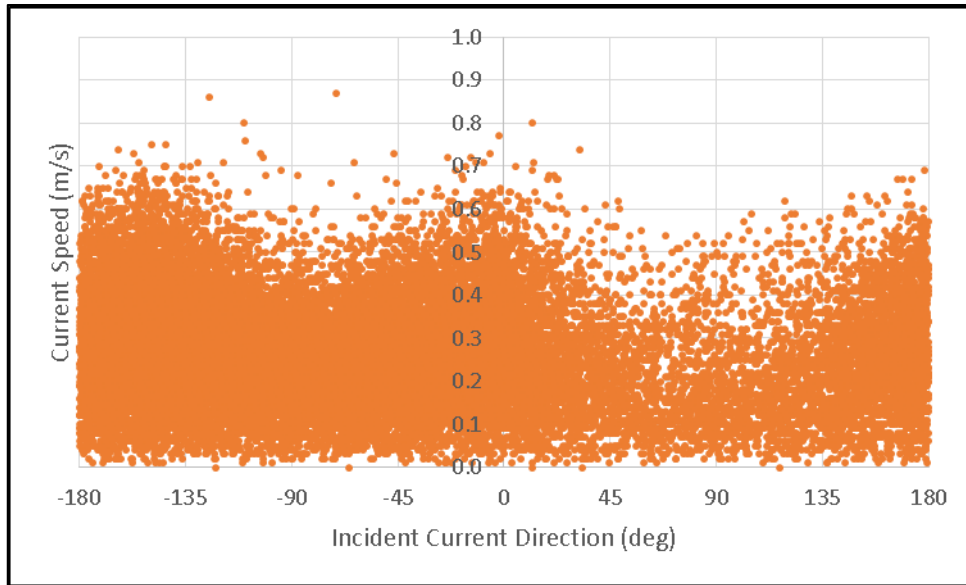


**Figure 4-13 Relation between Current Speed and Incident Current Direction**

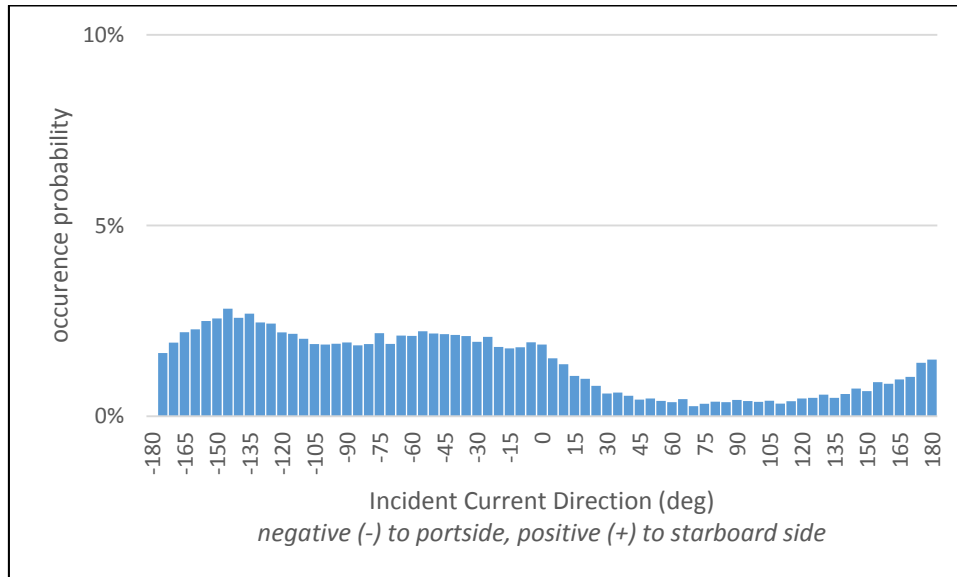


**Figure 4-14 Occurrence Probability of Incident Current Direction**

Heading with wave is shown in Figure 4-15 and Figure 4-16. Weathervane effect is seen, probably because wave direction is usually close to wind direction. One lump of occurrence probability is seen on the port side, which will be considered NE waves to the vessel, heading ESE wind and wave. Different from wind results, high waves sometimes come in from side or oblique directions.

Heading with swell is shown in Figure 4-17 and Figure 4-18. Frequency of swell occurrence is predominant in stern port side direction, where the vessel heading is to ESE wind and wave with NE swell. High swell comes in from 45 degree starboard side.

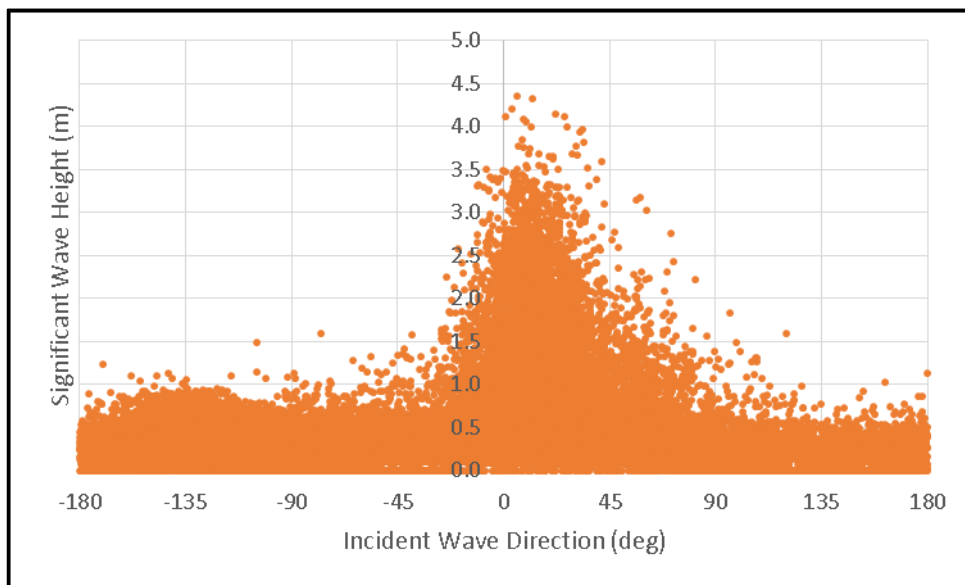


**Figure 4-15 Relation between Significant Wave Height and Incident Wave Direction**

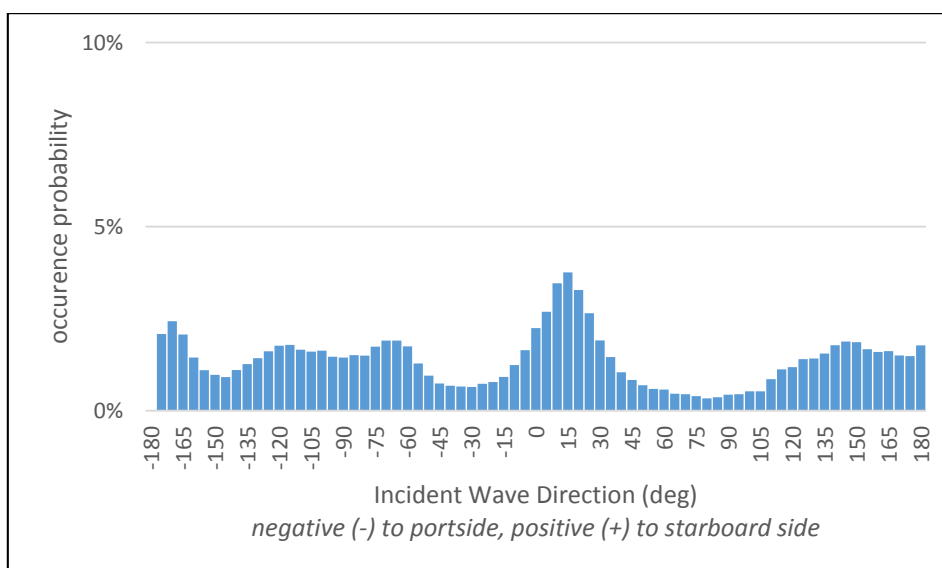


**Figure 4-16 Occurrence Probability of Incident Wave Direction**

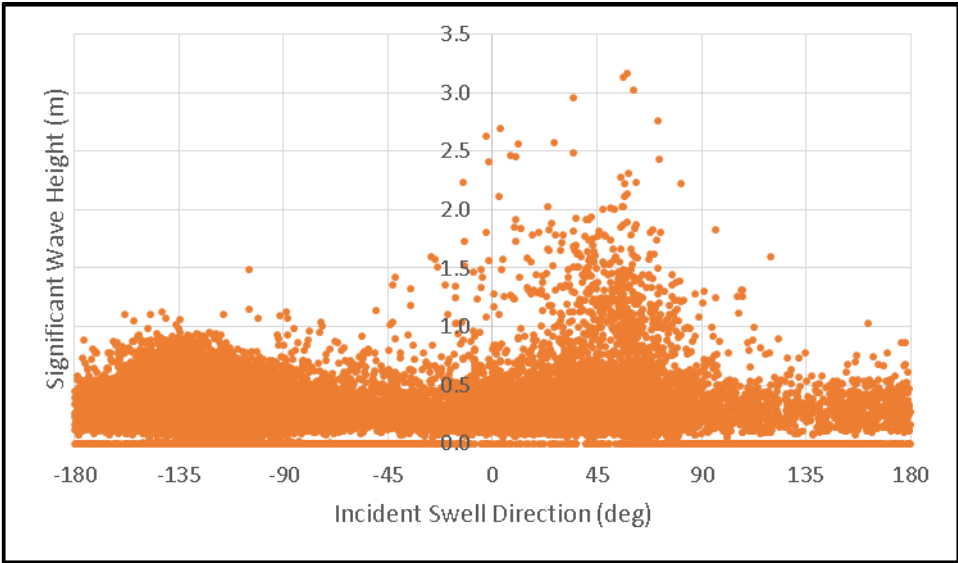


**Figure 4-17 Relation between Significant Wave Height and incident Swell Direction**

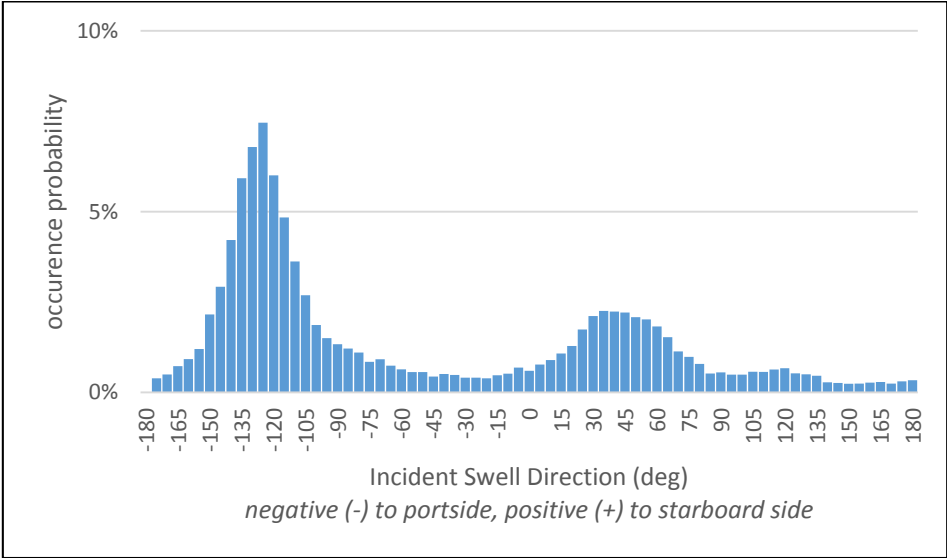
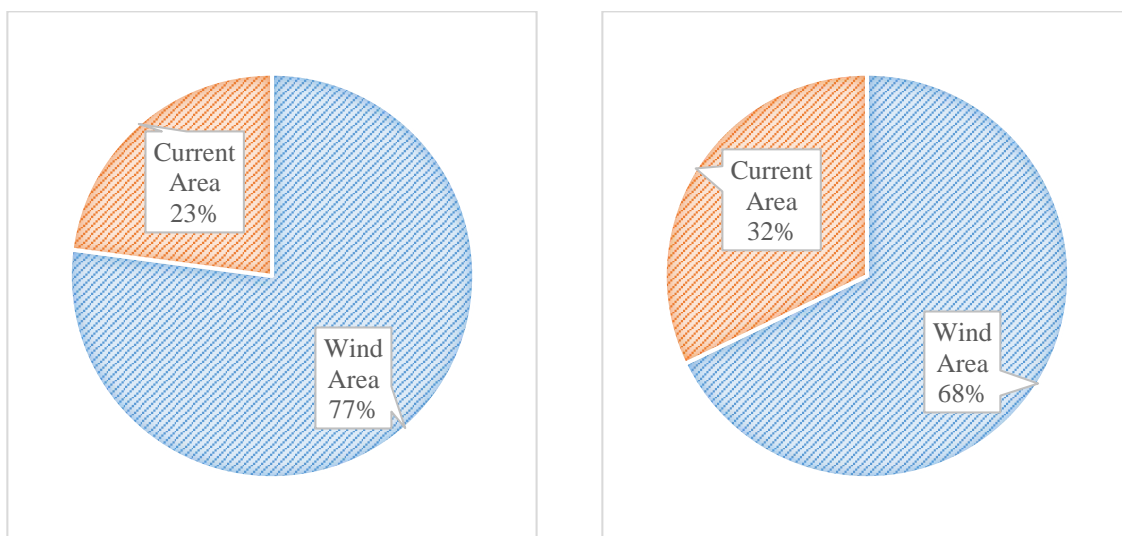


**Figure 4-18 Occurrence Probability of Incident Swell Direction**

The result of vessel heading angles is on a good agreement with proposed method by Terashima (2011) in a same vessel principle dimension. Moreover it should be noted that dynamic equilibrium by time domain simulation in minimum 10,800s (3hrs) is still believed the most accurate, but time demanding consequences. So in this study the static approach by double check static equilibrium which is faster and easier way to get the heading angles result. A double check static equilibrium approach is believed can speed up computation without compromising the quality outcomes. Comparison study between dynamic and double static approach insist the double static approach give 99% accuracy rather than 100% for dynamic approach on his 1414 cases. (Ardhiansyah, 2016).

The result of heading analysis calculation indicated that the most affected external forces that causing vessel mean heading is dedicated by wind, it is seen the relative heading between wind and vessel heading is quite small (<10degree) with large occurrence probability (up to 45%). This probably due to the wind force coefficient is larger than current coefficient and also the wind age area is larger than hydrodynamic drag area. As can be seen in Figure 4-19 wind area is have a larger portion than current area for both lateral and longitudinal projected area. As expected the wind effect will take dominant impact to the system by consider 16.2 m vessel draft and 21m freeboard plus topside area above the main hull. The wind dominance also strength up by the value of wind and current force coefficient that has been adopted to this study. Moreover the biggest impact of a large windage area not only on vessel heading probability but also will be on the mooring system performance.



(a) Lateral Area

(b) Longitudinal Area

**Figure 4-19 Wind and Current Area Comparison**



### 4.3 Mooring System Design

To design a mooring system there are several step to be considered in mooring study.. The stage is start from mooring leg and hull clearance check, and fatigue life estimation in the final stage. The mooring system is not only design to withstand in rough environment but also to prevent any contact between mooring leg and vessel hull since the object study is external turret moored unit. Turret location should be located in safe elevation to avoid green water and slamming from sea water that could possibility of mooring fairlead structural integrity failure. The maximum surge and sway motion due to mooring lines effect as known as a low frequency vessel offset is also need take into account in design of mooring system. The detailed of mooring design consideration is presented in Section 4.3.1 through Section 4.3.5.

**Table 4-2 Layout of Mooring Pattern**

<b>Layout No.</b>	<b>Within Group (deg)</b>	<b>One Group (deg)</b>	<b>Between Adjacent Groups (deg)</b>	<b>Remark</b>
<b>1</b>	3	9	111	Group
<b>2</b>	4	12	108	Group
<b>3</b>	5	15	105	Group
<b>4</b>	6	18	102	Group
<b>5</b>	7	21	99	Group
<b>6</b>	8	24	96	Group
<b>7</b>	9	27	93	Group
<b>8</b>	10	30	90	Group
<b>9</b>	-	-	-	30deg Equally space

The static characteristic of mooring lines as extracted by MOSES as seen below. Mooring line segmented by three (3) segment with specified properties as described in Section 3. The properties of mooring lines is quiet useful to measure of the stiffness of the line as a function of distance from the anchor in keeping the vessel from moving very far.

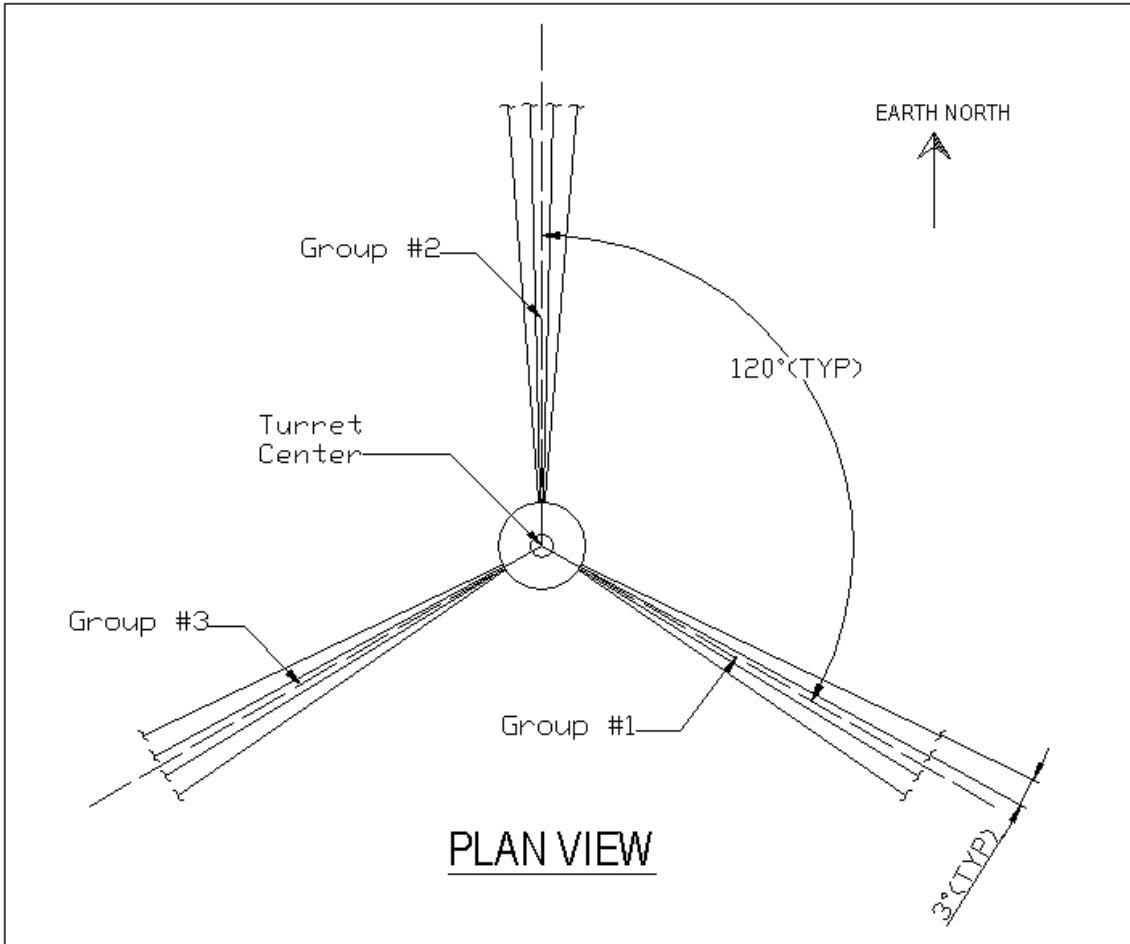


**Figure 4-20 Mooring Pattern Layout #1**

Mooring layout #1, as seen in Figure 4-20, is divided into three bundle, each group consist of four (4) lines which is separate by 3 degree angle. The angle between groups remain the same i.e. 120 degree. By considering the maximum environment condition and heading analysis outcome, mooring bundle group #2 will be located coincident to North. The maximum wind wave, wind, current, and swell is coming from NW even the probability occurrence is less than from SE. A bundle mooring group is designed to reduce fatigue damage due to environment load which align to the maximum probability of vessel heading to SEE. Moreover mooring layout #2 to #9 that will be investigated in this study is reported in Appendix B. According to Section 3.5, there are nine (9) investigated layouts in this study as seen in Table 4-2. Total number of 8,425 load cases design MOSES syntax will be reported on Appendix C. And also the mooring fatigue cases are reported in Appendix D.

```

*****
*                                     *** MOSES ***
*                                     -----
*                                     30 September, 2016
*
* Turret Mooring with 12 Lines
*
*****

```

+++ M O O R I N G L I N E C L A S S E S +++

Process is DEFAULT: Units Are Degrees, Meters, and M-Tons Unless Specified

Type Name	Water Depth	Slope of Bottom	Clump weight	/-----/ Length	Segment w/L	Data AE	-----/ Break
~CAT	600.0	0.0000	0.0	160.00	0.2888	1.13E+05	1263.66
			0.0	725.00	0.0688	1.35E+05	1884.66
			0.0	410.00	0.5796	2.27E+05	2536.08

```

*****
*                                     *** MOSES ***
*                                     -----
*                                     30 September, 2016
*
* Turret Mooring with 12 Lines
*
*****

```

+++ P R O P E R T I E S O F L I N E C A T 1 +++

Process is DEFAULT: Units Are Degrees, Meters, and M-Tons Unless Specified

Line Class = ~CAT Water Depth = 601 Length of First Segment = 161

H. Dist. X	Horizontal		Tension				Anchor		Line on Bottom	Height Anchor	Ab Net Force Applied
	Force	DF/DX	---/ Ten Top	---/ Max T/TB	---/ Cri Break	---/ Crit. Seg	V. Pull	H. Pull			
677.69	0.01	0.01	77.76	0.062	1263.66	1	0.00	0.01	676.50	458.42	0.00
780.56	3.02	0.05	80.71	0.064	1263.66	1	0.00	3.02	634.50	458.67	0.00
897.52	12.06	0.12	89.15	0.071	1263.66	1	0.00	12.06	523.04	461.43	0.00
981.31	27.14	0.30	102.83	0.081	1263.66	1	0.00	27.14	404.74	468.46	0.00
1022.64	48.25	0.86	125.09	0.099	1263.66	1	0.00	48.25	376.77	477.36	0.00
1044.89	75.39	1.67	156.17	0.124	1263.66	1	0.00	75.39	339.95	485.60	0.00
1060.80	108.56	2.53	194.89	0.154	1263.66	1	0.00	108.56	296.71	492.74	0.00
1074.09	147.76	3.39	240.47	0.190	1263.66	1	0.00	147.76	248.65	498.85	0.00
1085.92	193.00	4.28	292.48	0.231	1263.66	1	0.00	193.00	196.79	504.23	0.00
1096.74	244.26	5.22	350.66	0.277	1263.66	1	0.00	244.26	141.88	509.03	0.00
1106.77	301.56	6.23	414.83	0.328	1263.66	1	0.00	301.56	84.44	513.36	0.00
1116.12	364.88	7.33	484.89	0.384	1263.66	1	0.00	364.88	24.86	517.32	0.00
1124.44	434.24	10.25	561.09	0.444	1263.66	1	21.59	434.24	0.00	520.86	0.00
1130.41	509.63	15.53	644.53	0.510	1263.66	1	60.85	509.63	0.00	523.77	0.00
1134.79	591.05	22.22	735.21	0.582	1263.66	1	103.53	591.05	0.00	526.13	0.00
1138.17	678.50	29.99	833.03	0.659	1263.66	1	149.56	678.50	0.00	528.06	0.00
1140.92	771.98	38.31	937.90	0.742	1263.66	1	198.90	771.98	0.00	529.66	0.00
1143.26	871.50	46.56	1049.75	0.831	1263.66	1	251.49	871.50	0.00	530.99	0.00
1145.36	977.04	54.20	1168.55	0.925	1263.66	1	307.28	977.04	0.00	532.11	0.00
1147.30	1088.62	60.89	1294.24	1.024	1263.66	1	366.25	1088.62	0.00	533.06	0.00
1149.14	1206.22	66.50	1426.80	1.129	1263.66	1	428.35	1206.22	0.00	533.87	0.00
1150.94	1329.86	71.04	1566.19	1.239	1263.66	1	493.56	1329.86	0.00	534.56	0.00
1152.71	1459.53	74.65	1712.39	1.355	1263.66	1	561.83	1459.53	0.00	535.16	0.00
1154.50	1595.23	77.46	1865.37	1.476	1263.66	1	633.15	1595.23	0.00	535.68	0.00
1156.30	1736.96	79.63	2025.12	1.603	1263.66	1	707.46	1736.96	0.00	536.13	0.00
1158.14	1884.72	81.29	2191.62	1.734	1263.66	1	784.76	1884.72	0.00	536.53	0.00
1160.01	2038.52	82.55	2364.85	1.871	1263.66	1	865.00	2038.52	0.00	536.87	0.00
1161.93	2198.34	83.51	2544.79	2.014	1263.66	1	948.16	2198.34	0.00	537.18	0.00
1163.91	2364.20	84.23	2731.42	2.162	1263.66	1	1034.19	2364.20	0.00	537.44	0.00
1165.94	2536.08	84.76	2924.73	2.314	1263.66	1	1123.08	2536.08	0.00	537.68	0.00

### 4.3.1 Mooring Leg and Hull Clearance Analysis

The proposed mooring system design is effective in a) reducing vessel offset, and b) preventing contact between the anchor leg and the vessel hull. Clearance between the anchor legs and hull becomes smallest when the vessel drifts upstream of its calm water position, resulting in a decrease in fairlead declination angle (from horizontal) of the downstream legs. Anchor leg/hull clearance also decreases with decreasing vessel draft.

Figure 4-21 shows the above-water, calm water, intact system configuration of a single anchor leg relative to the vessel bow. Figure 4-22 shows the results of a conservative quasi-static leg/hull clearance analysis with the maximum upstream offset associated with 200-yr Typhoon conditions. This figure represents a snapshot at the point in time where the vessel is experiencing its maximum upward pitch motion. As can be seen, the anchor leg does not come into contact with the vessel bow.

This analysis is conservative because the upstream offset utilized corresponds to the largest upstream offset realized when either current or wind was set to zero strength, thus reducing the total mean force that would otherwise prevent the vessel from drifting further upstream. In addition, it is not likely that the maximum pitch motion would occur at the vessel's largest upstream position. The present, extremely conservative analysis resulted in a minimum clearance of approximately 3 meters between the anchor leg and bow cut.

Since the mooring legs component is similar for 9 layouts, therefore this legs and hull clearance analysis result is applicable for all mooring layout stated in Table 4-2. From the yield result indicated that the proposed turret location is acceptable according to mooring hull clearance analysis.

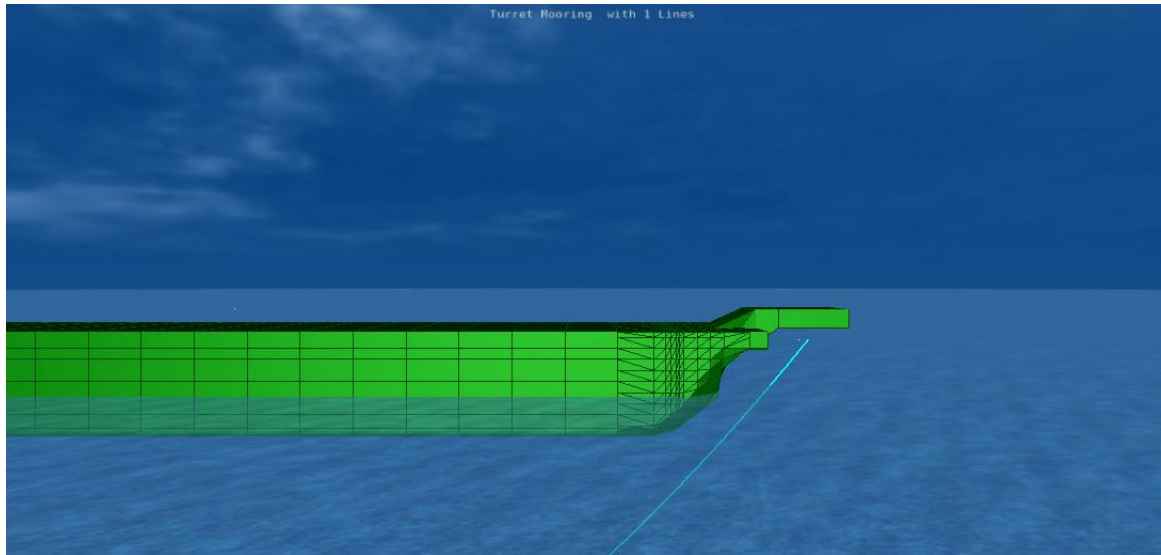


**Figure 4-21 Elevation View of Vessel Bow and Anchor Leg: Calm Water.**

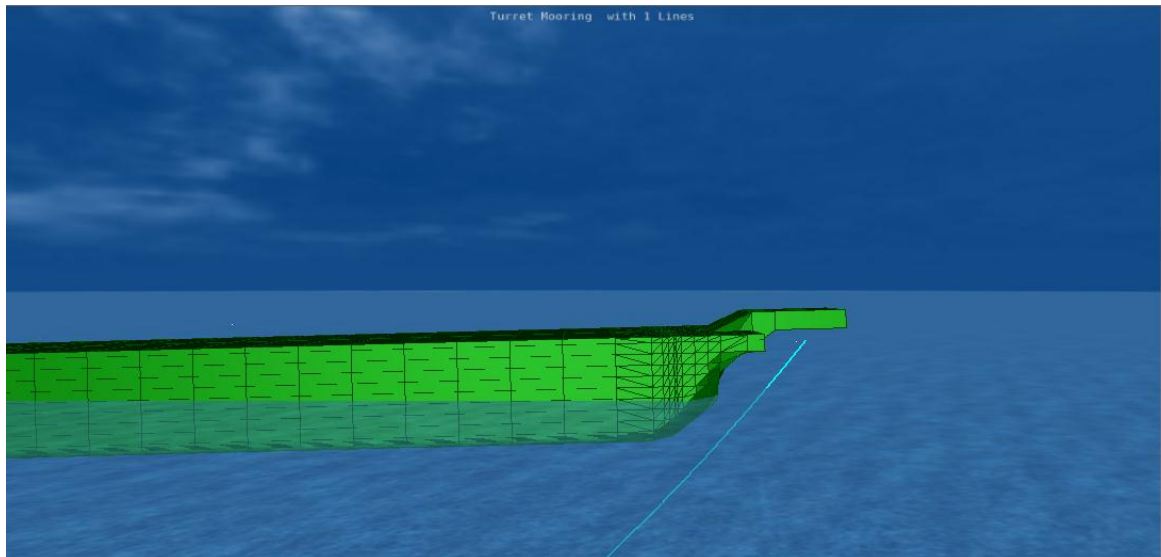


**Figure 4-22 200-yr Maximum Upstream Offset and Maximum Bow-Up Pitch.**

### 4.3.2 Green Water and Chain Table Slamming Analysis

Relative vertical “air gap” between the sea surface and any pre-specified point on the vessel is obtained by simulating the dynamic behavior in 3-hour simulation. MOSES will reports air gap for a 3-hour storm duration for the point of interest.

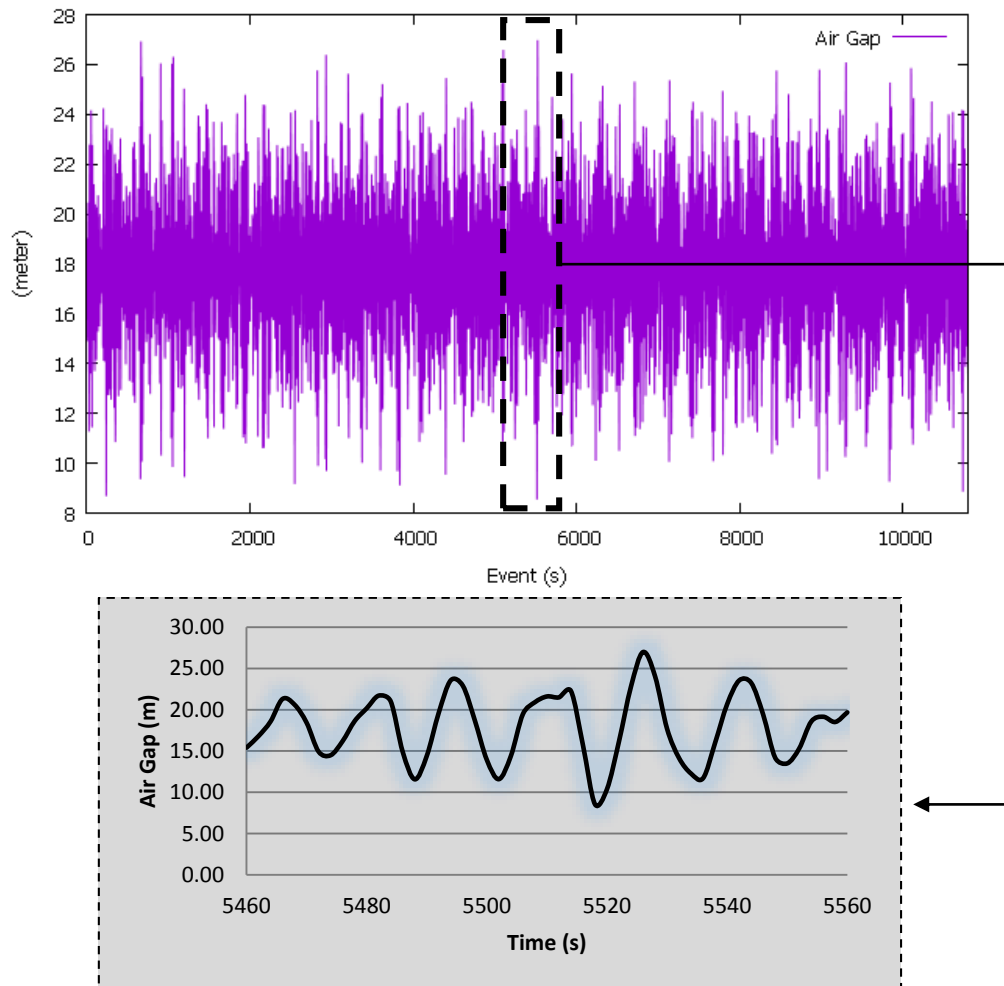


**Figure 4-23 3-Hour Simulation Relative Wave Elevation**

Figure 4-23 show the simulation-estimated 3-hr maximum relative wave elevation distributions for head-on 200-yr Typhoon wave conditions. As can be seen, the turret and riser inspection platform remain well above the sea surface. Minimum air gap is 8.54 meter occur at simulation time of 5,518 second, and the maximum air gap is 26.98 meter occur at simulation time of 5,526 second.

Again same as mooring leg and hull clearance analysis, since the mooring legs component is similar for 9 layouts, therefore this legs and hull clearance analysis result is applicable for all mooring layout stated earlier in Table 4-2. From the yield result indicated that the proposed turret location is acceptable according to air gap clearance analysis.

### 4.3.3 Mooring Line and Anchor Loads

The extreme intact and damaged mooring system anchor leg component loads, safety factors and turret offsets resulting from the global analysis of the vessel for the environments discussed in Section 3 are presented in Table 4-3. Anchor design loads are summarized in Table 4-4. Maximum values listed are the 3-hour predicted maximum.

The calculated maximum mooring line tension in ultimate limit state 200-yr Return Period condition for all lines intact and one line damage are presented in Figure 4-24. Those figures also present the allowable tension that should be satisfied as outlined in Classification Society.

The overall maximum tension for intact condition gives tension ratio which is satisfies the design criteria, shall less than 0.6, for intact condition. Moreover for one line damage condition the maximum tension gives tension ratio which is satisfies the design criteria, shall less than 0.8, for damage condition. Therefore the design criteria according to API RP 2SK for line tension are satisfied, except equally space mooring type in Layout 9.

Weathervane effect can be seen on tension result because of the environmental level are nearly the same from all directions. The maximum line tension occurs when the environments are in line with one mooring line bundle when almost all the loads are taken by this bundle.

The present proposal contains line-item offers for both suction embedded pile-type anchors, and drag-embedded fluke-type anchors. Although the difference in material cost for each type is noticeable, there may be additional benefits to using suction piles.

Suction piles may be installed separately from the anchor leg if an optional subsea connector is included in the configuration. As such, the vessels installing the suction piles for the subsea equipment could also install the suction piles for the anchor legs. This would prevent two installation contractors from mobilizing similar equipment for a similar task, thus resulting in potentially significant savings for the project as a whole. In addition, because suction piles do not require proof loading, the installation vessels do not need to have large bollard pull capacities. This allows for a wider range of available vessels to be considered for this task. Therefore, it is recommended that further discussions take place during the study stage to determine how best to reduce the installed cost of all subsea and mooring components. The selection of mooring system anchor type will be integral to these discussions.

**Table 4-3 Mooring Loads Summary Result**

Layout			1		2		3	
Env. Condition			200-yr	200-yr	200-yr	200-yr	200-yr	200-yr
Mooring System			Intact	Damage	Intact	Damage	Intact	Damage
Line 1	Max. Tension	(ton)	468	789	474	784	477	769
	Ratio		0.25	0.42	0.25	0.42	0.25	0.41
	Line on Bottom	(m)	30	0	25	0	23	0
	Vertical pull	(ton)	0	147	0	145	0	137
Line 2	Max. Tension	(ton)	462	818	466	826	466	824
	Ratio		0.25	0.43	0.25	0.44	0.25	0.44
	Line on Bottom	(m)	34	0	31	0	31	0
	Vertical pull	(ton)	0	161	0	165	0	164
Line 3	Max. Tension	(ton)	461	852	463	880	463	908
	Ratio		0.24	0.45	0.25	0.47	0.25	0.48
	Line on Bottom	(m)	35	0	34	0	34	0
	Vertical pull	(ton)	0	178	0	192	0	206
Line 4	Max. Tension	(ton)	460	867	462	916	463	949
	Ratio		0.24	0.46	0.25	0.49	0.25	0.50
	Line on Bottom	(m)	36	0	34	0	33	0
	Vertical pull	(ton)	0	186	0	209	0	226
Line 5	Max. Tension	(ton)	443	910	446	971	447	1026
	Ratio		0.24	0.48	0.24	0.52	0.24	0.54
	Line on Bottom	(m)	49	0	47	0	47	0
	Vertical pull	(ton)	0	207	0	236	0	264
Line 6	Max. Tension	(ton)	442	885	445	934	445	981
	Ratio		0.23	0.47	0.24	0.50	0.24	0.52
	Line on Bottom	(m)	50	0	48	0	48	0
	Vertical pull	(ton)	0	194	0	219	0	241
Line 7	Max. Tension	(ton)	443	836	445	866	445	886
	Ratio		0.23	0.44	0.24	0.46	0.24	0.47
	Line on Bottom	(m)	50	0	48	0	48	0
	Vertical pull	(ton)	0	170	0	185	0	195
Line 8	Max. Tension	(ton)	443	793	447	807	448	810
	Ratio		0.24	0.42	0.24	0.43	0.24	0.43
	Line on Bottom	(m)	49	0	46	0	45	0
	Vertical pull	(ton)	0	149	0	156	0	157
Line 9	Max. Tension	(ton)	462	615	462	610	462	602
	Ratio		0.24	0.33	0.25	0.32	0.24	0.32
	Line on Bottom	(m)	35	0	34	0	35	0
	Vertical pull	(ton)	0	62	0	60	0	56
Line 10	Max. Tension	(ton)	467	631	469	629	469	622
	Ratio		0.25	0.33	0.25	0.33	0.25	0.33
	Line on Bottom	(m)	30	0	29	0	29	0
	Vertical pull	(ton)	0	70	0	69	0	66
Line 11	Max. Tension	(ton)	472	636	476	634	477	628
	Ratio		0.25	0.34	0.25	0.34	0.25	0.33
	Line on Bottom	(m)	27	0	24	0	23	0
	Vertical pull	(ton)	0	72	0	72	0	68
Line 12	Max. Tension	(ton)	476	995	481	1067	483	1126
	Ratio		0.25	0.53	0.26	0.57	0.26	0.60
	Line on Bottom	(m)	23	0	20	0	18	0
	Vertical pull	(ton)	0	248	0	283	0	312

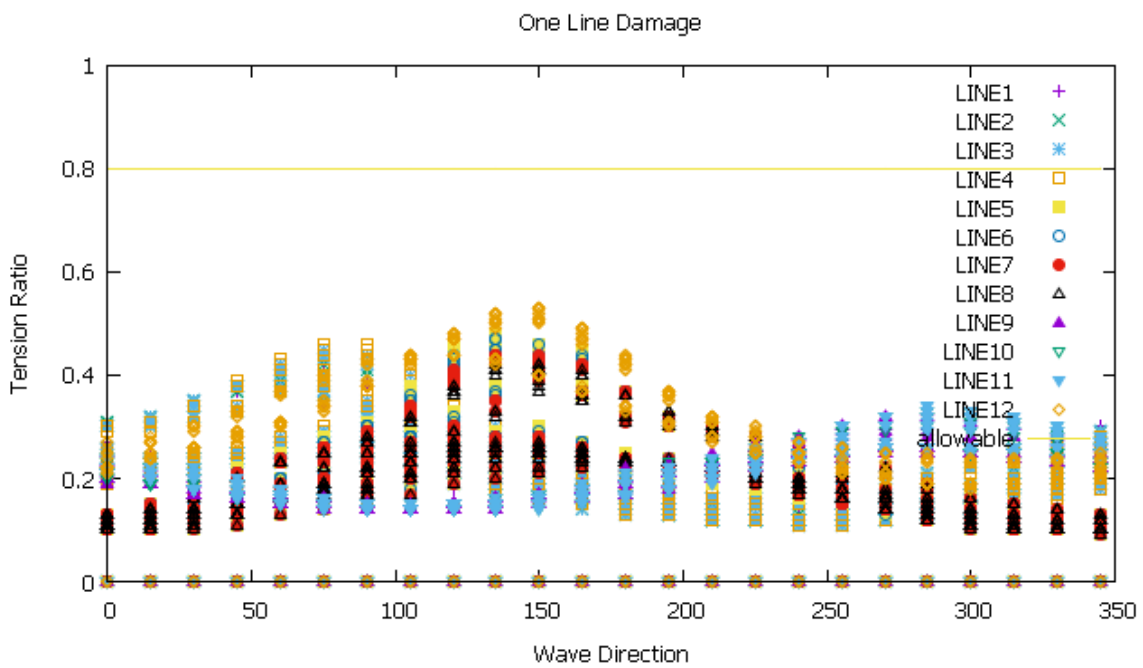
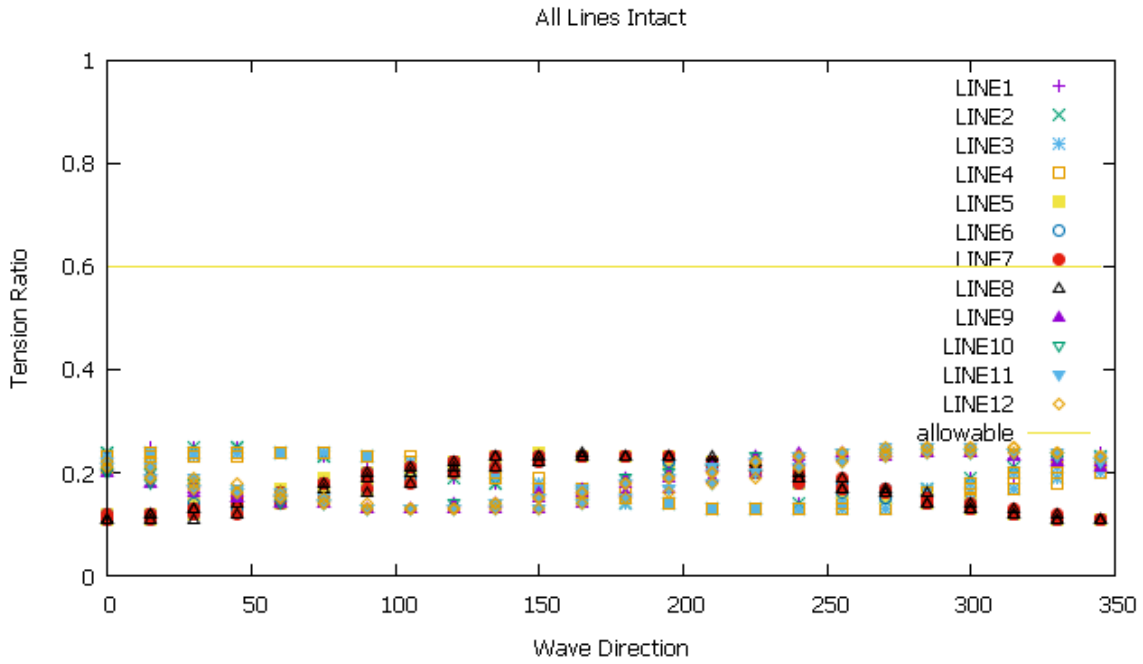


Layout			4		5		6	
Env. Condition			200-yr	200-yr	200-yr	200-yr	200-yr	200-yr
Mooring System			Intact	Damage	Intact	Damage	Intact	Damage
Line 1	Max. Tension	(ton)	480	751	483	732	482	712
	Ratio		0.25	0.40	0.26	0.39	0.26	0.38
	Line on Bottom	(m)	21	0	18	0	19	0
	Vertical pull	(ton)	0	129	0	119	0	110
Line 2	Max. Tension	(ton)	468	822	469	819	467	816
	Ratio		0.25	0.44	0.25	0.43	0.25	0.43
	Line on Bottom	(m)	30	0	29	0	30	0
	Vertical pull	(ton)	0	163	0	162	0	161
Line 3	Max. Tension	(ton)	463	935	463	962	461	993
	Ratio		0.25	0.50	0.25	0.51	0.24	0.53
	Line on Bottom	(m)	33	0	33	0	35	0
	Vertical pull	(ton)	0	219	0	232	0	247
Line 4	Max. Tension	(ton)	464	987	464	1023	463	1066
	Ratio		0.25	0.52	0.25	0.54	0.25	0.57
	Line on Bottom	(m)	33	0	32	0	34	0
	Vertical pull	(ton)	0	244	0	262	0	283
Line 5	Max. Tension	(ton)	447	1079	448	1140	446	1194
	Ratio		0.24	0.57	0.24	0.60	0.24	0.63
	Line on Bottom	(m)	46	0	46	0	47	0
	Vertical pull	(ton)	0	289	0	319	0	346
Line 6	Max. Tension	(ton)	445	1029	445	1075	443	1126
	Ratio		0.24	0.55	0.24	0.57	0.24	0.60
	Line on Bottom	(m)	48	0	47	0	49	0
	Vertical pull	(ton)	0	265	0	288	0	313
Line 7	Max. Tension	(ton)	446	902	446	916	444	928
	Ratio		0.24	0.48	0.24	0.49	0.24	0.49
	Line on Bottom	(m)	47	0	47	0	49	0
	Vertical pull	(ton)	0	203	0	210	0	215
Line 8	Max. Tension	(ton)	449	810	450	806	447	801
	Ratio		0.24	0.43	0.24	0.43	0.24	0.43
	Line on Bottom	(m)	45	0	44	0	46	0
	Vertical pull	(ton)	0	157	0	156	0	153
Line 9	Max. Tension	(ton)	461	596	462	593	460	589
	Ratio		0.24	0.32	0.25	0.31	0.24	0.31
	Line on Bottom	(m)	35	0	34	0	36	0
	Vertical pull	(ton)	0	53	0	51	0	50
Line 10	Max. Tension	(ton)	468	616	468	612	464	608
	Ratio		0.25	0.33	0.25	0.32	0.25	0.32
	Line on Bottom	(m)	29	0	30	0	33	0
	Vertical pull	(ton)	0	63	0	60	0	58
Line 11	Max. Tension	(ton)	478	621	478	615	476	611
	Ratio		0.25	0.33	0.25	0.33	0.25	0.32
	Line on Bottom	(m)	22	0	22	0	23	0
	Vertical pull	(ton)	0	65	0	62	0	60
Line 12	Max. Tension	(ton)	485	1188	488	1255	487	1322
	Ratio		0.26	0.63	0.26	0.67	0.26	0.70
	Line on Bottom	(m)	17	0	14	0	15	0
	Vertical pull	(ton)	0	343	0	376	0	408

Layout			7		8		9	
Env. Condition			200-yr	200-yr	200-yr	200-yr	200-yr	200-yr
Mooring System			Intact	Damage	Intact	Damage	Intact	Damage
Line 1	Max. Tension	(ton)	488	700	490	688	504	722
	Ratio		0.26	0.37	0.26	0.37	0.27	0.38
	Line on Bottom	(m)	14	0	13	0	3	0
	Vertical pull	(ton)	0	104	0	98	0	115
Line 2	Max. Tension	(ton)	471	816	472	814	502	767
	Ratio		0.25	0.43	0.25	0.43	0.27	0.41
	Line on Bottom	(m)	28	0	27	0	4	0
	Vertical pull	(ton)	0	160	0	160	0	137
Line 3	Max. Tension	(ton)	464	1021	465	1055	488	1015
	Ratio		0.25	0.54	0.25	0.56	0.26	0.54
	Line on Bottom	(m)	33	0	32	0	15	0
	Vertical pull	(ton)	0	261	0	278	0	258
Line 4	Max. Tension	(ton)	465	1125	466	1184	478	1457
	Ratio		0.25	0.60	0.25	0.63	0.25	0.77
	Line on Bottom	(m)	32	0	31	0	22	0
	Vertical pull	(ton)	0	312	0	341	0	475
Line 5	Max. Tension	(ton)	449	1243	449	1293	467	1726
	Ratio		0.24	0.66	0.24	0.69	0.25	0.92
	Line on Bottom	(m)	45	0	45	0	31	166
	Vertical pull	(ton)	0	370	0	394	0	0
Line 6	Max. Tension	(ton)	446	1175	446	1219	456	1861
	Ratio		0.24	0.62	0.24	0.65	0.24	0.99
	Line on Bottom	(m)	47	0	47	0	39	311
	Vertical pull	(ton)	0	336	0	358	0	0
Line 7	Max. Tension	(ton)	446	940	447	949	453	1632
	Ratio		0.24	0.50	0.24	0.50	0.24	0.87
	Line on Bottom	(m)	47	0	46	0	42	79
	Vertical pull	(ton)	0	221	0	226	0	0
Line 8	Max. Tension	(ton)	452	794	453	786	456	1279
	Ratio		0.24	0.42	0.24	0.42	0.24	0.68
	Line on Bottom	(m)	42	0	41	0	39	0
	Vertical pull	(ton)	0	150	0	146	0	387
Line 9	Max. Tension	(ton)	464	587	466	584	467	829
	Ratio		0.25	0.31	0.25	0.31	0.25	0.44
	Line on Bottom	(m)	33	0	32	0	31	0
	Vertical pull	(ton)	0	48	0	47	0	167
Line 10	Max. Tension	(ton)	467	603	466	599	479	627
	Ratio		0.25	0.32	0.25	0.32	0.25	0.33
	Line on Bottom	(m)	31	0	31	0	21	0
	Vertical pull	(ton)	0	56	0	54	0	68
Line 11	Max. Tension	(ton)	480	607	481	605	492	617
	Ratio		0.25	0.32	0.26	0.32	0.26	0.33
	Line on Bottom	(m)	21	0	20	0	12	0
	Vertical pull	(ton)	0	58	0	57	0	63
Line 12	Max. Tension	(ton)	494	1393	496	1462	501	2205
	Ratio		0.26	0.74	0.26	0.78	0.27	1.17
	Line on Bottom	(m)	10	0	9	0	5	800
	Vertical pull	(ton)	0	443	0	477	0	0

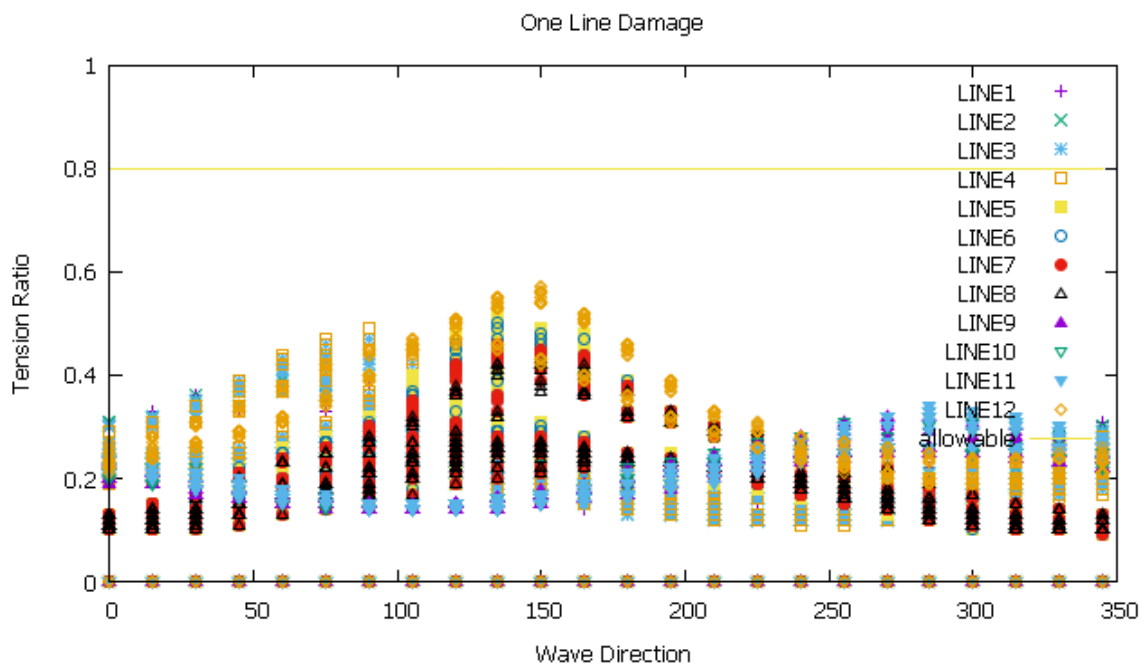
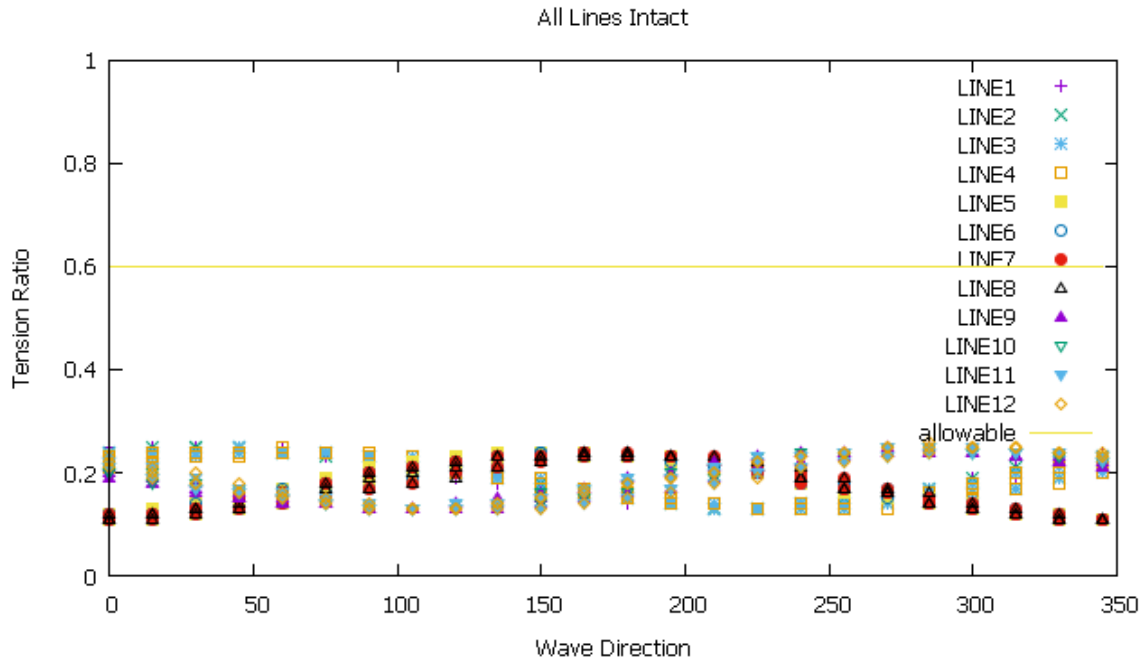
**Table 4-4 Pile Anchor and Drag Anchor Design Load**

Layout	Required Capacity (ton)			
	Pile Type		Drag Type	
	= 2.0xintact; 1.50xdamage		= 1.5xintact; 1.25xdamage	
1	Intact	953		715
	Damage		1493	1244
	Max. Load	1493		1244
2	Intact	962		722
	Damage		1600	1333
	Max. Load	1600		1333
3	Intact	966		725
	Damage		1689	1408
	Max. Load	1689		1408
4	Intact	970		728
	Damage		1782	1485
	Max. Load	1782		1485
5	Intact	977		732
	Damage		1883	1569
	Max. Load	1883		1569
6	Intact	975		731
	Damage		1982	1652
	Max. Load	1982		1652
7	Intact	987		740
	Damage		2090	1742
	Max. Load	2090		1742
8	Intact	992		744
	Damage		2193	1828
	Max. Load	2193		1828
9	Intact	1008		756
	Damage		3307	2756
	Max. Load	3307		2756



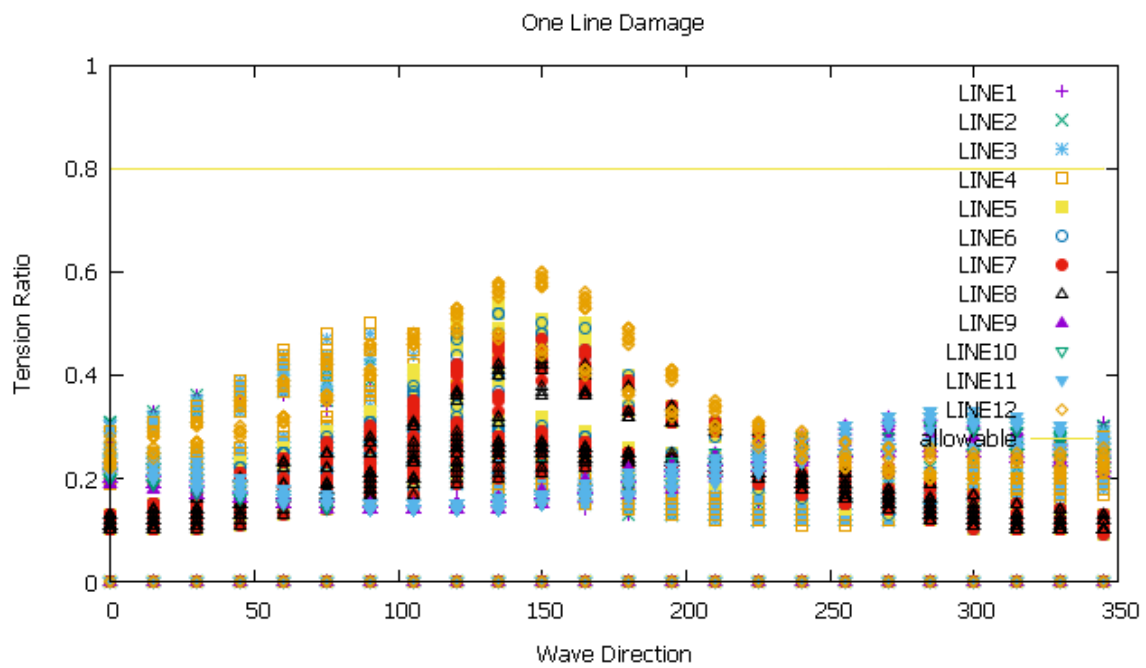
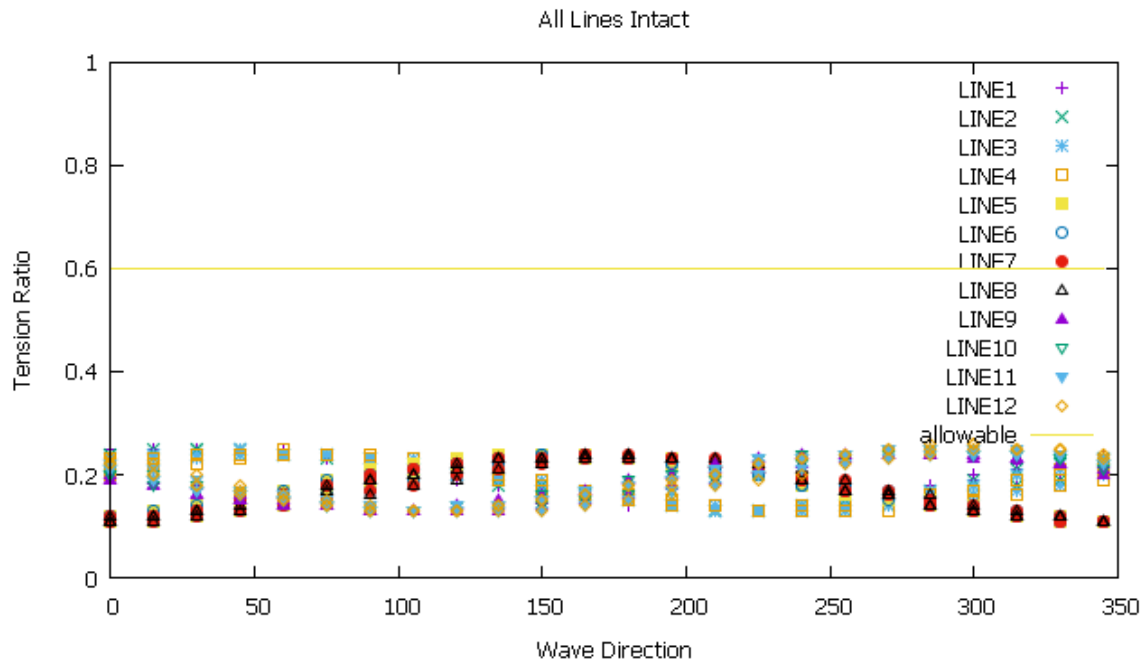
### Tension Result for Layout 1

The maximum tension result for both intact and damage cases indicated that the mooring system is satisfy the design criteria. Maximum tension ratio allowed for intact and damage case is 0.6 and 0.8 respectively. The result show maximum tension ratio is 0.253 for intact case and 0.528 for damage case.



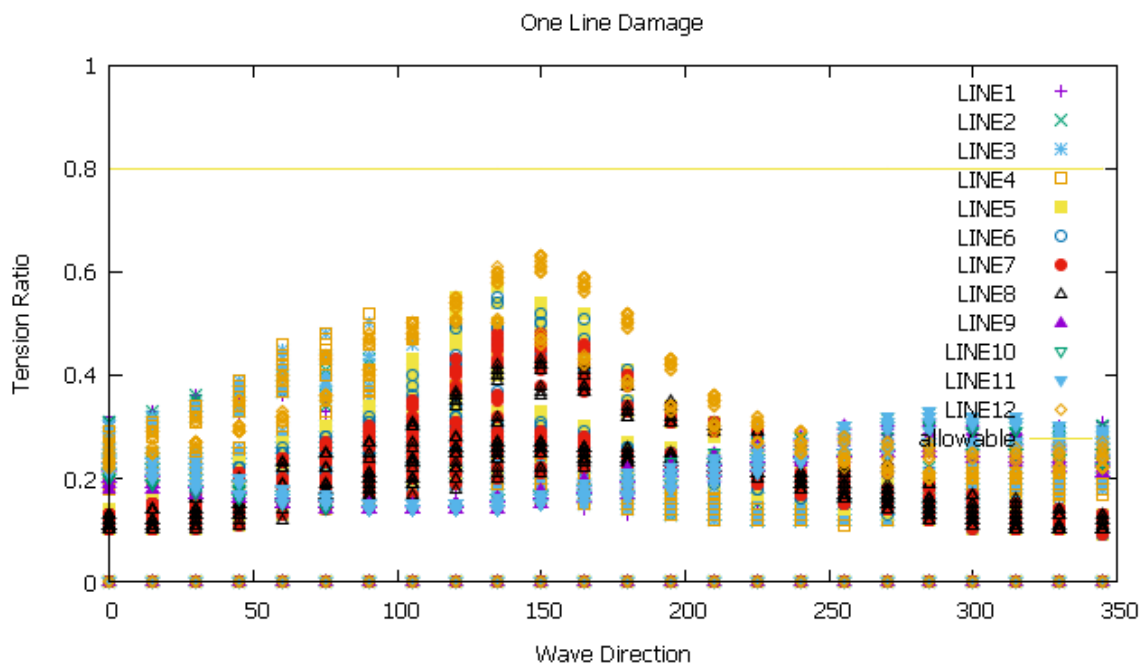
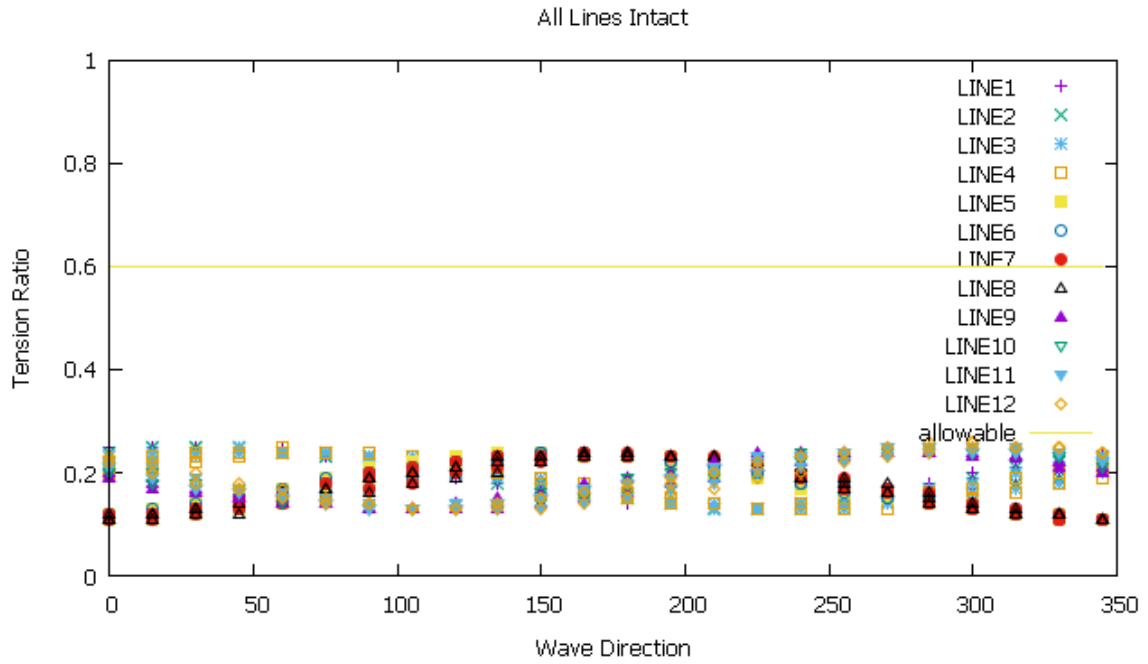
### Tension Result for Layout 2

The maximum tension result for both intact and damage cases indicated that the mooring system is satisfy the design criteria. Maximum tension ratio allowed for intact and damage case is 0.6 and 0.8 respectively. The result show maximum tension ratio is 0.255 for intact case and 0.566 for damage case.



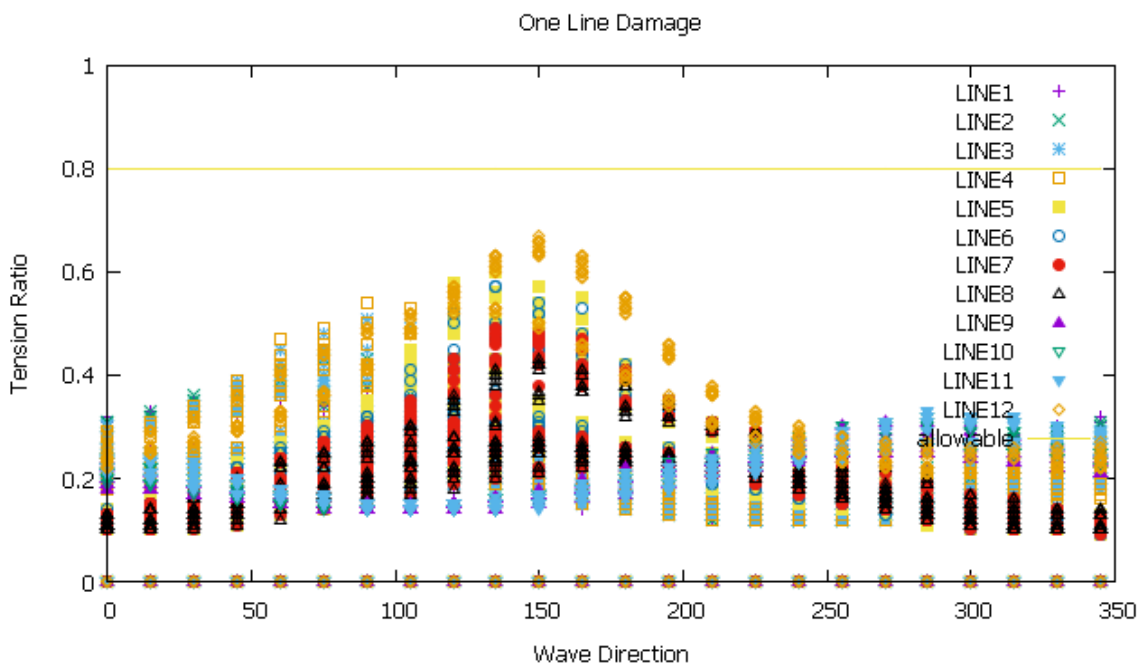
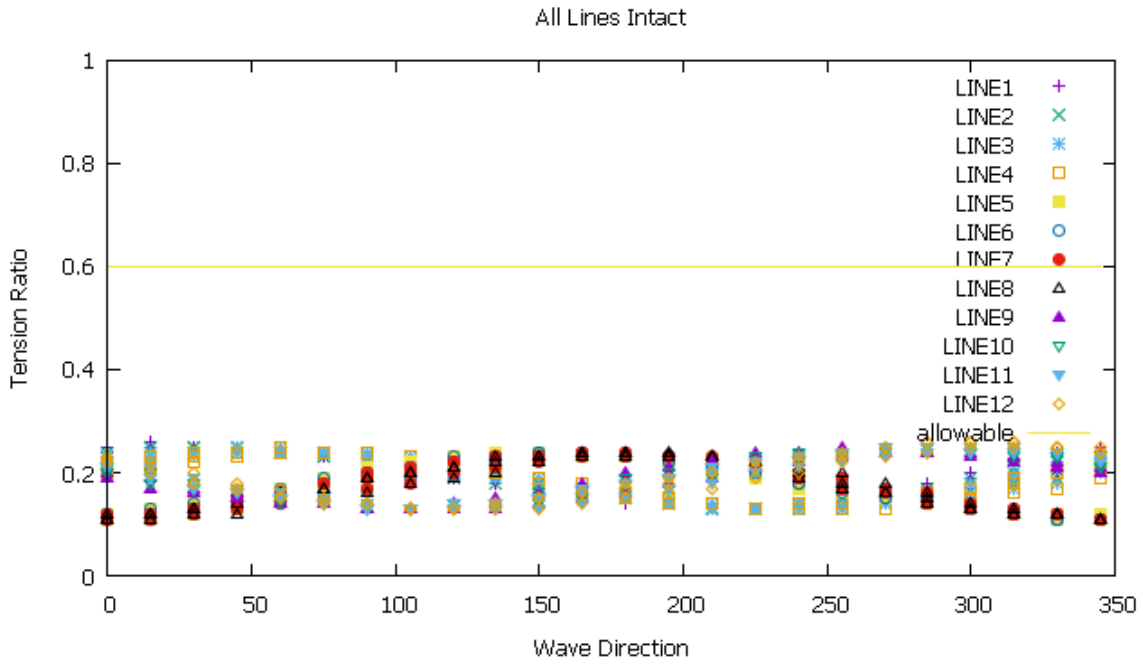
### Tension Result for Layout 3

The maximum tension result for both intact and damage cases indicated that the mooring system is satisfy the design criteria. Maximum tension ratio allowed for intact and damage case is 0.6 and 0.8 respectively. The result show maximum tension ratio is 0.256 for intact case and 0.597 for damage case.



#### Tension Result for Layout 4

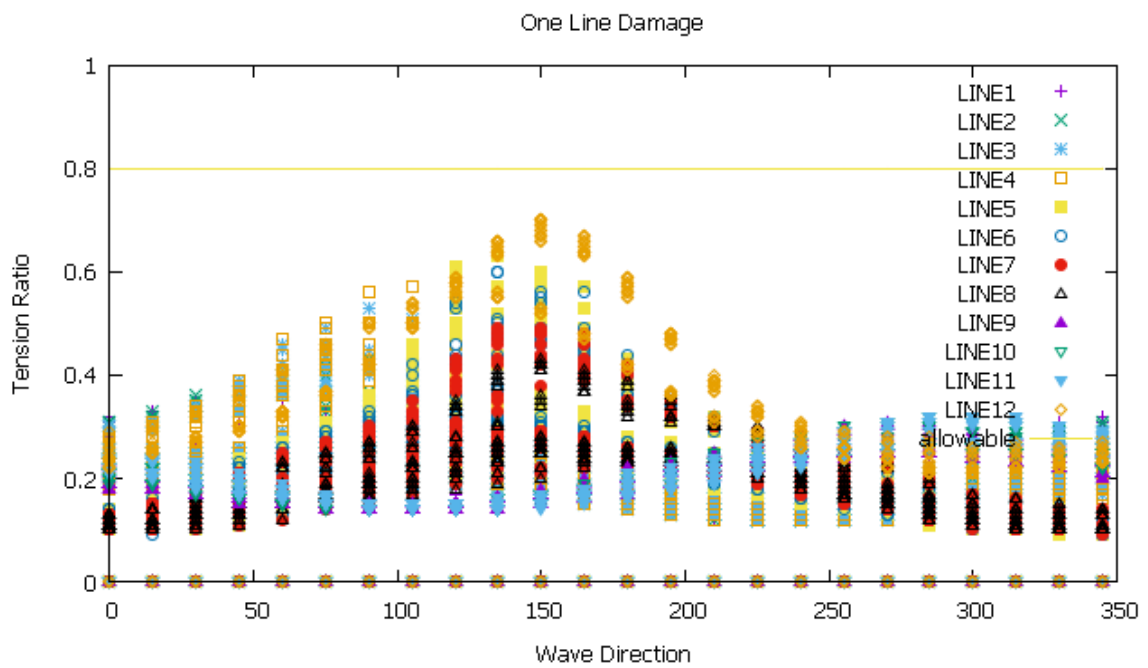
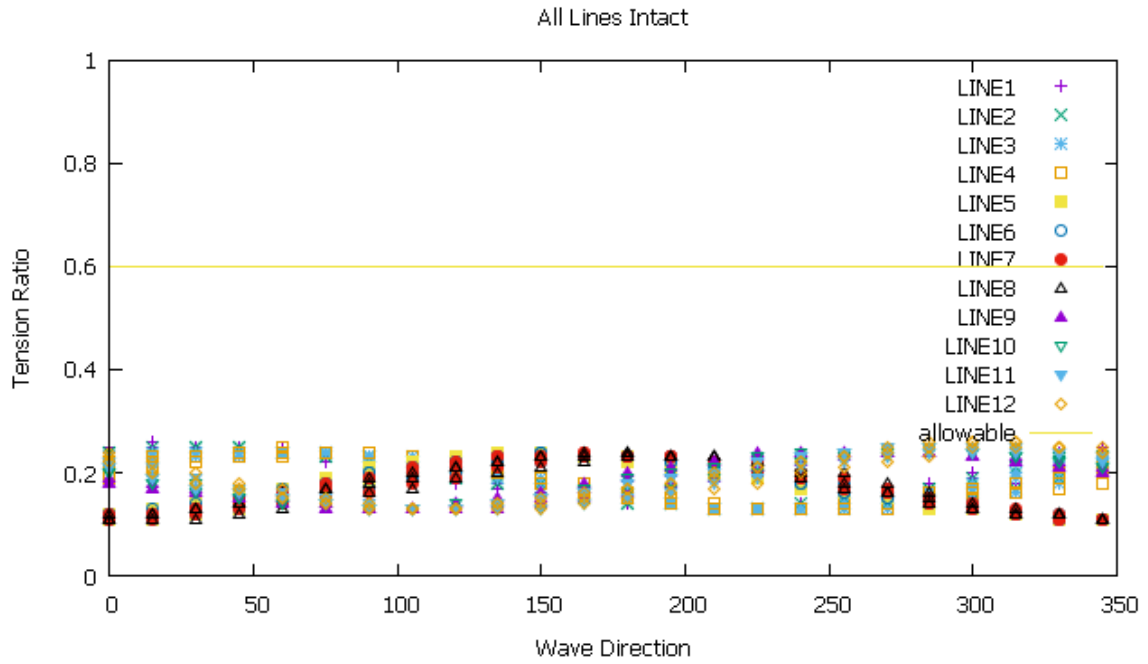
The maximum tension result for both intact and damage cases indicated that the mooring system is satisfy the design criteria. Maximum tension ratio allowed for intact and damage case is 0.6 and 0.8 respectively. The result show maximum tension ratio is 0.257 for intact case and 0.630 for damage case.



### Tension Result for Layout 5

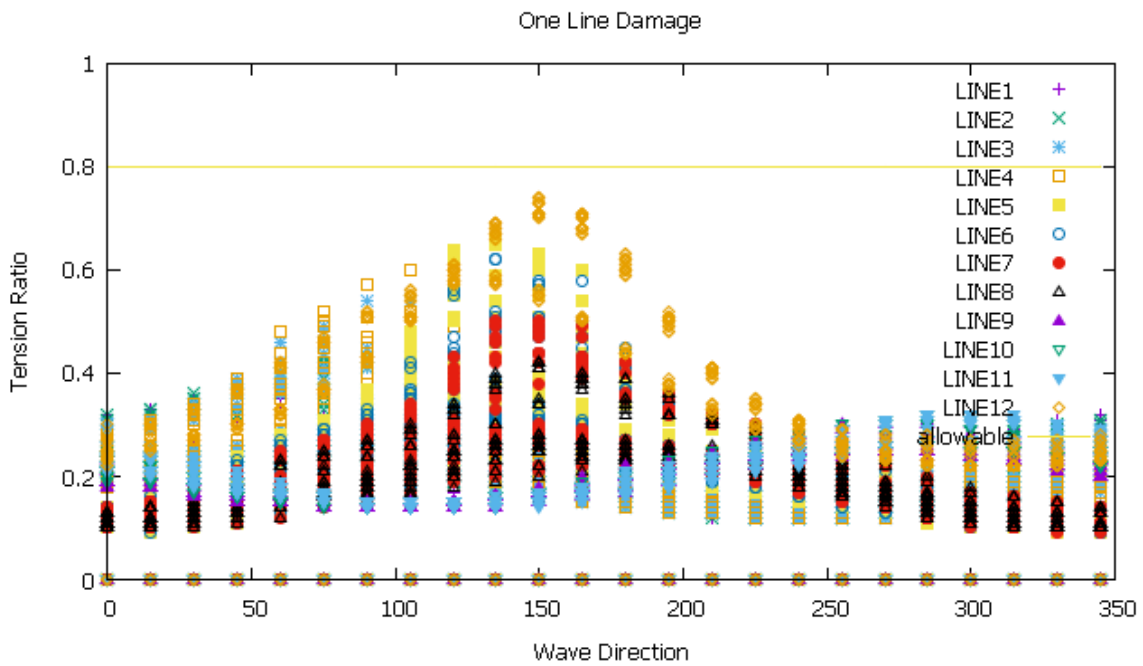
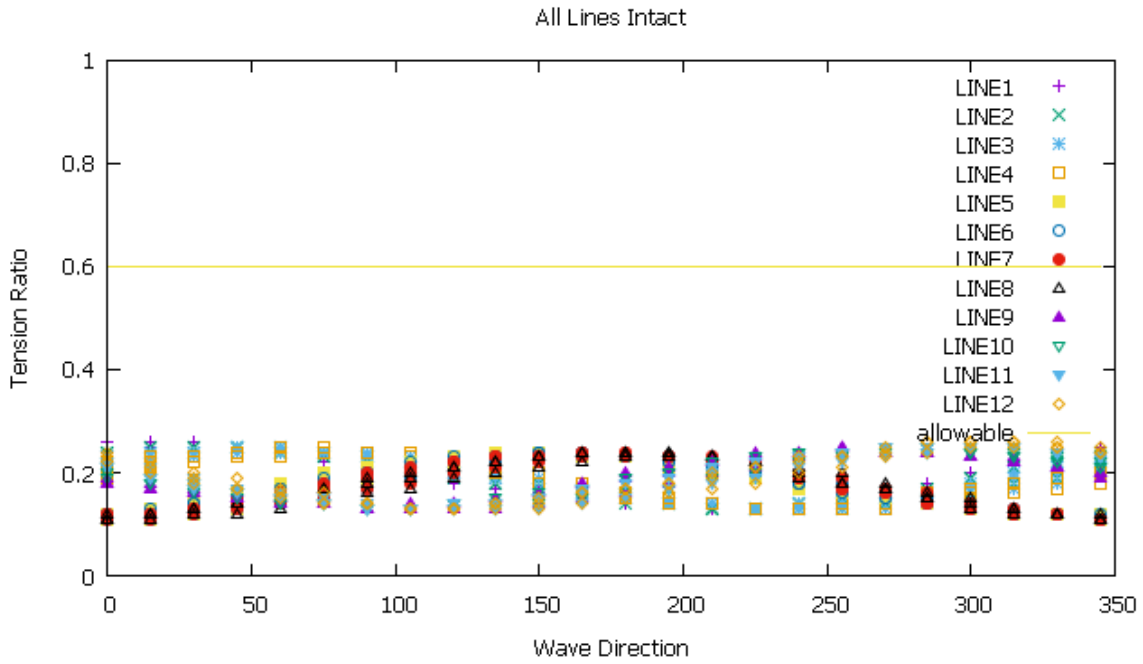
The maximum tension result for both intact and damage cases indicated that the mooring system is satisfy the design criteria. Maximum tension ratio allowed for intact and damage case is 0.6 and 0.8 respectively. The result show maximum tension ratio is 0.259 for intact case and 0.666 for damage case.





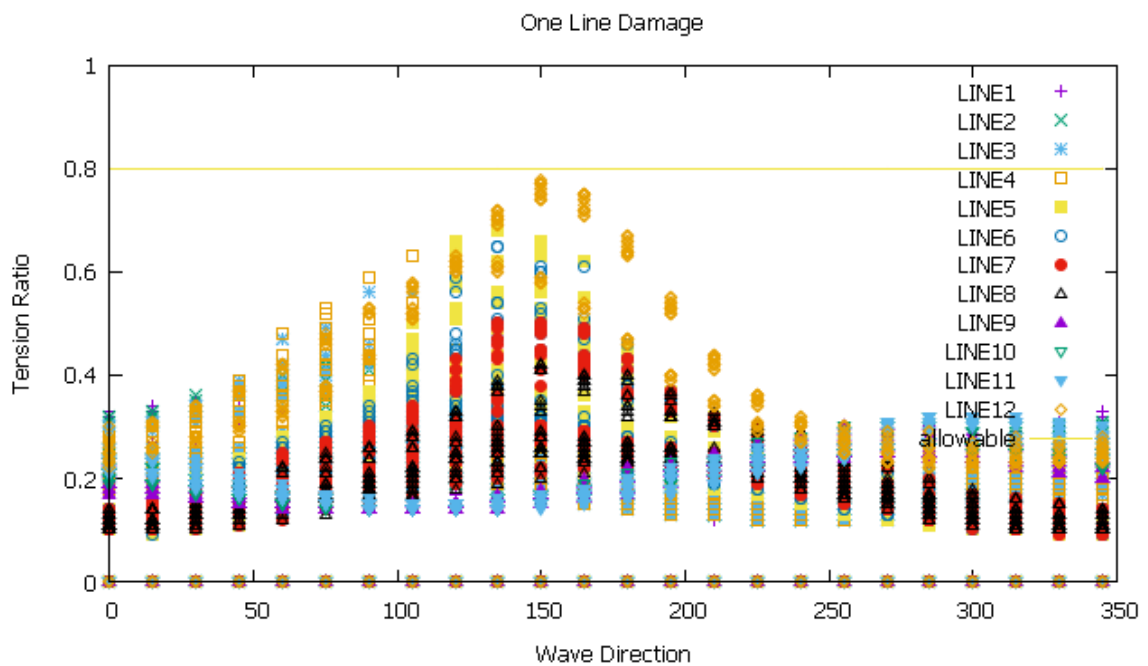
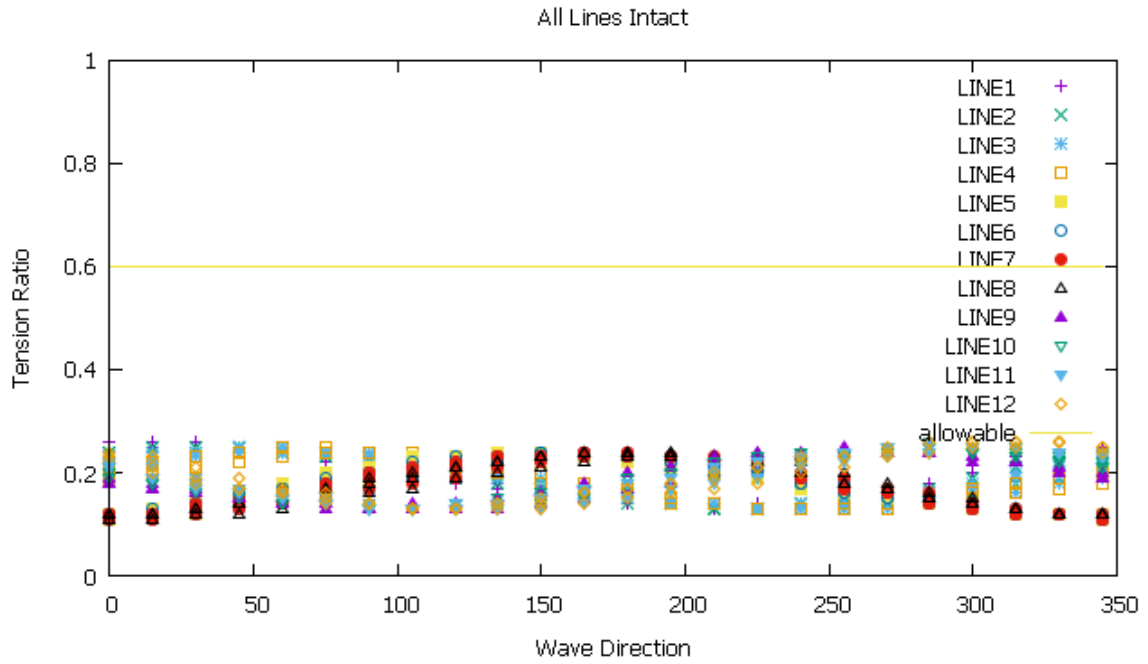
### Tension Result for Layout 6

The maximum tension result for both intact and damage cases indicated that the mooring system is satisfy the design criteria. Maximum tension ratio allowed for intact and damage case is 0.6 and 0.8 respectively. The result show maximum tension ratio is 0.259 for intact case and 0.701 for damage case.



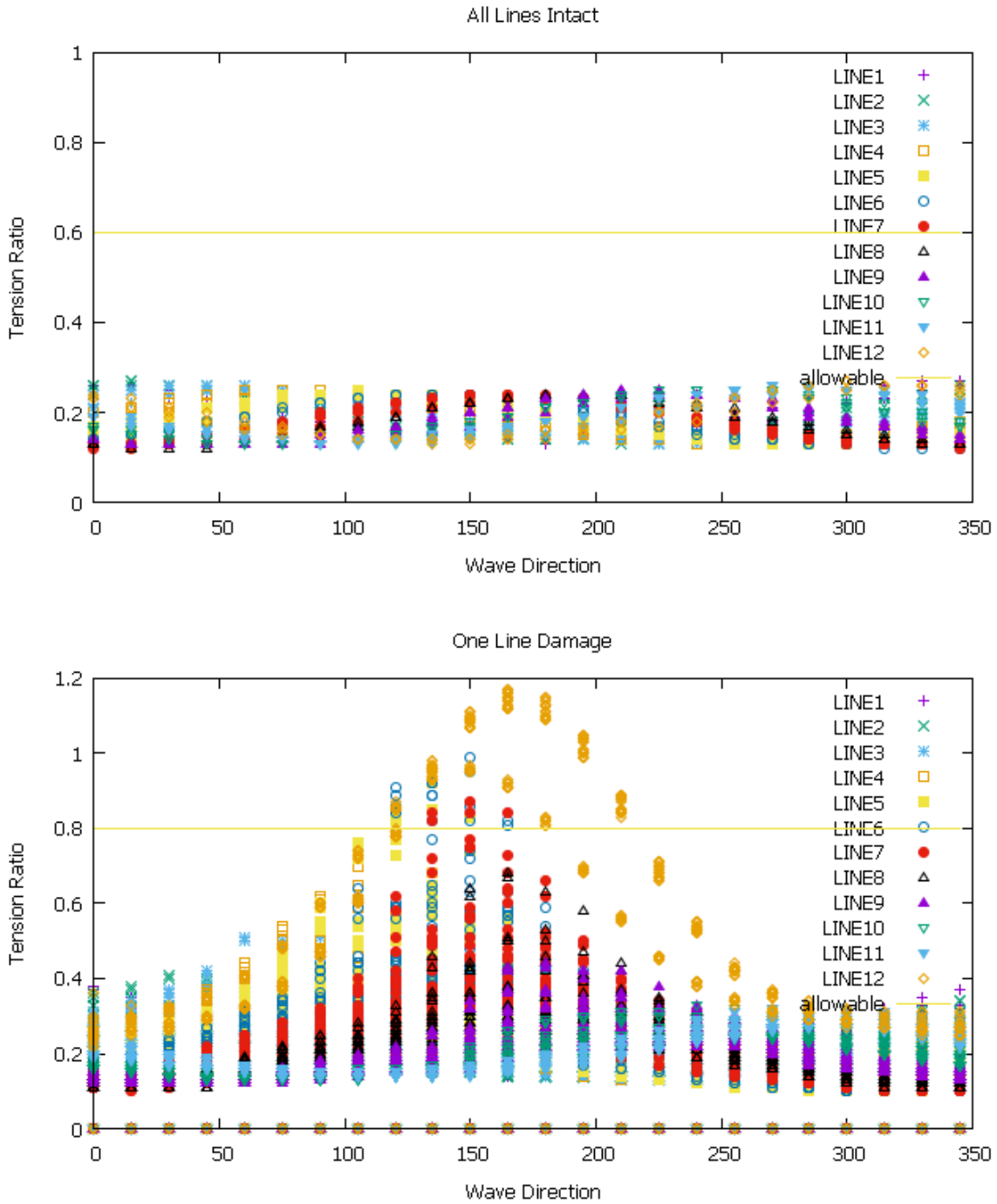
### Tension Result for Layout 7

The maximum tension result for both intact and damage cases indicated that the mooring system is satisfy the design criteria. Maximum tension ratio allowed for intact and damage case is 0.6 and 0.8 respectively. The result show maximum tension ratio is 0.262 for intact case and 0.739 for damage case.



### Tension Result for Layout 8

The maximum tension result for both intact and damage cases indicated that the mooring system is satisfy the design criteria. Maximum tension ratio allowed for intact and damage case is 0.6 and 0.8 respectively. The result show maximum tension ratio is 0.263 for intact case and 0.776 for damage case.



**Tension Result for Layout 9**

**Figure 4-24 Maximum Mooring Tension Load in Intact and Damage Cases**

The maximum tension result for intact cases indicated that the mooring system is satisfy the design criteria but no for damage case. Maximum tension ratio allowed for intact and damage case is 0.6 and 0.8 respectively. The result show maximum tension ratio is 0.267 for intact case and 1.170 for damage case.

Mooring line tension, anchor loads, and vessel offset is depend on the environment applied to the turret unit. Not only case of co-linear environment but also crossed environment is investigated in this study. We first consider wind, wave, and current aligned from bow with respect to the vessel ( $\psi_w=\psi_c=\psi_\zeta=180^\circ$ ). And second we consider two crossed cases, crosses-1 at an angle ( $\psi_w=\psi_c=210^\circ$ ,  $\psi_\zeta=180^\circ$ ), crossed-2 at an angle ( $\psi_w=210^\circ$ ,  $\psi_c=225^\circ$ ,  $\psi_\zeta=180^\circ$ ).

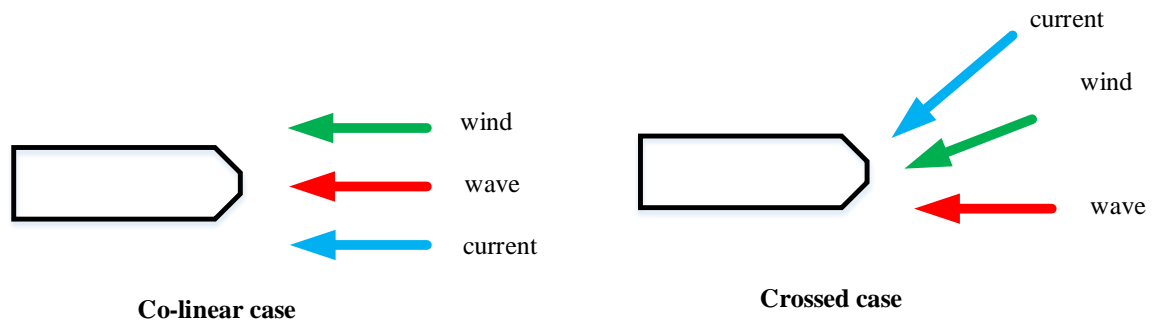


**Figure 4-25 Environment Loadcase**

The dynamic analysis is carried out to verify the maximum line tensions in typhoon environment condition for both all line intact and one line damage condition. Mooring line tension result indicated that maximum tension for crossed case is higher than co-linear cases (up to 6%). This is due to a large windage area exposed by wind when wind blowing from beam of the vessel rather than below water hull area that pay role in current hydrodynamic force. The maximum tension for both intact and damage line is occurred at crossed cases value of 504 ton and 2,200 ton respectively.

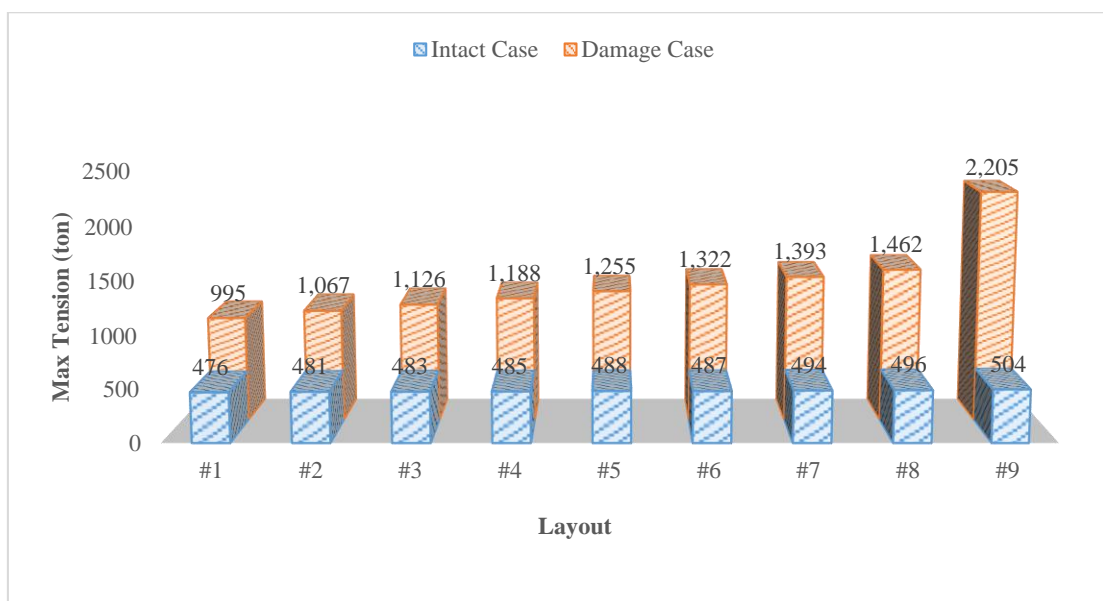


**Figure 4-26 Mooring Line Loads Summary**

From maximum tension in all nine (9) anchor layouts shows that layout number #1 which is a group type with have smallest angle within group have the smallest maximum tension compare to another eight (8) layouts. The results indicated that mooring pattern with smaller angle within group will have smaller tension as well. The bigger maximum tension is occurred in layout number #9 which have biggest angle within group. Summary of mooring line loads is presented in Figure 4-26

In co-linear environment case the difference of maximum tension for all nine (9) layouts have no big differences. In the opposite side in crossed environment case, the maximum tension for each layout have a significant difference in maximum line tension. There is up to 10% gradually increase of tension ratio when angle within group is increase in group mooring pattern type, angle within group is gradually increase from 3° to 10°. The tension ratio is jump up to 30% when in equally space mooring pattern type, which is angle between mooring legs is 30°

#### 4.3.4 Low Frequency Vessel Offset

The vessel low-frequency offsets obtained from all simulations ran for Ultimate Limit State are provided in Figure 4-27. As shown in this figure, the difference between the results of cases for each layout is quite significant. The data shown in Figure 4-27 indicate that the vessel offset remains within the required 16% of water depth envelope for one-line-damage condition and the required 13% of water depth envelope for intact condition. In general, the numerical model found to be reasonably conservative resulting in larger vessel offsets, larger loads on the turret, and larger mooring lines.

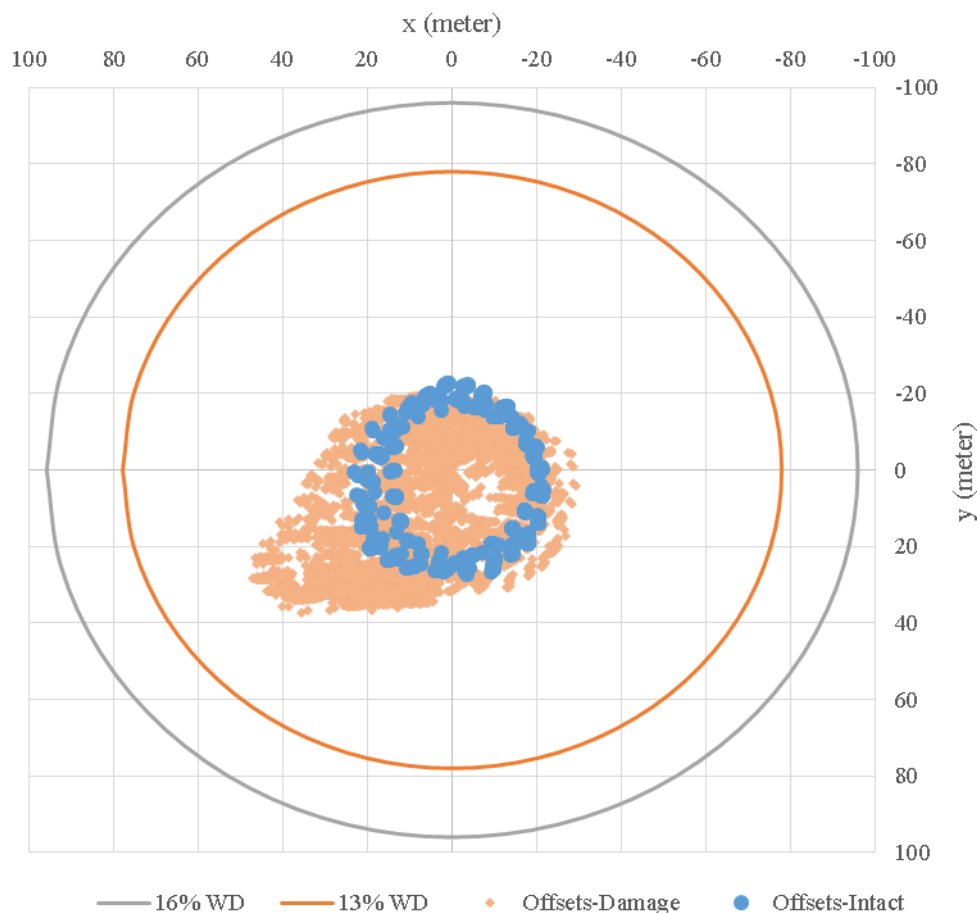


**Figure 4-27 Vessel Low Frequency Offset: All Cases**

The maximum vessel offset for all line intact condition in Ultimate Limit State condition is 27 meter (4.5% of water depth) based on dynamic time domain simulation. The proposed mooring system of the vessel is to be safe to maintain 5% coverage of water depth up to Ultimate Limit State 200-yr environment condition.

### 4.3.5 Fatigue Life

Fatigue analysis is performed to estimate the fatigue life of the major mooring components according to recommended practice that stated in DNV-OS-E301 Position Mooring Section 2 F 100. Unfortunately MOSES cannot get mooring line fatigue results at different locations along the line, such as the interfaces for a chain/wire/chain line makeup. Only fatigue at the most highly stressed location in the line. All of the analysis is performed within the frequency response analysis.

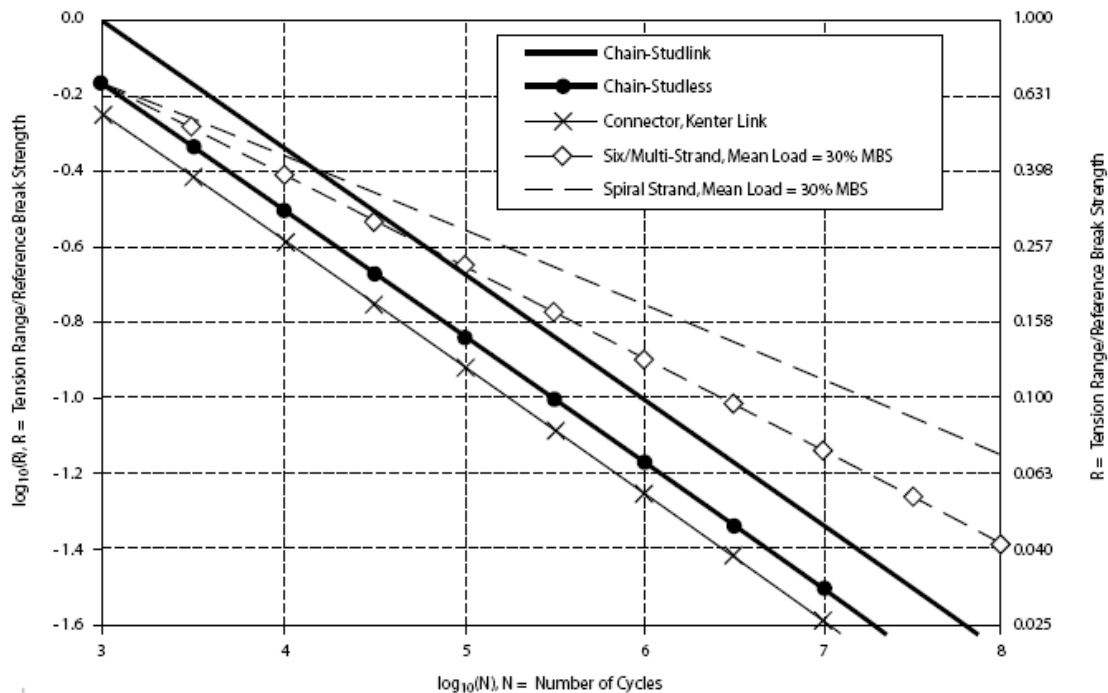


**Figure 4-28 Mooring Fatigue Design Curves**

The T-N curves extracted from API RP2SK 3<sup>rd</sup> edition is presented in Figure 4-28, as can be seen the lowest tension range graph is refer to studless-chain since the studied mooring system configuration is make-up from chain-wire-chain. That's mean the highly stress tension should be occurred in location of chain entire the lines.

Since the slope of the above T-N curve for studless chains lies outside the 95% confidence range from a regression analysis on the available test data, the T-N curves based on regression analysis of the test data presented in 2 chain fatigue test JIP Noble Denton & Associates, Inc. in reports Corrosion Fatigue Testing of 76mm Grade R3 & R4 Studless Mooring Chain (Noble Denton & Associates, Inc., 2002)



Below were extracted typically the MOSES output tension cycles to estimate fatigue damage ratio for each mooring lines. The tension cycles is calculate for duration of 10,950 days which is equal to 30 years as the designed life of the mooring system.

```
*****
*                                     *** MOSES ***                                     *
*                                     -----                                     30 September, 2016 *
*
* Environment is to estimate fatigue damage layout4
* Draft = 16.2 Meters Trim Angle = -0.00 Deg. GMT = 8.8 Meters *
* Roll Gy. Radius = 24.4 Meters Pitch Gy. Radius = 119.6 Meters Yaw Gy. Radius = 118.7 Meters *
* Multi-Spectrum Height = 2.2 Meters *
*
*****
```

+++ T E N S I O N C Y C L E S +++

=====

For a Duration of 10950.00 Days

/-- Tensions ---/		Connectors								
Starting	Ending	CAT1	CAT10	CAT11	CAT12	CAT2	CAT3	CAT4	CAT5	
0.0	10.0	5549375	13106493	16288389	20724976	5032989	4737340	4659815	43173092	
10.0	20.0	11904752	21312786	23057350	24622868	11285065	10910904	10726629	24964356	
20.0	30.0	12988545	13765786	13618299	13029860	12406972	12038265	11873564	6935090	
30.0	40.0	10609263	7083305	6680194	5893326	10323184	10094750	9966922	2492873	
40.0	50.0	7386946	3787957	3439799	2871901	7361085	7295640	7237024	1134690	
50.0	60.0	4702578	2290026	1993605	1591438	4831465	4880856	4878512	607591	
60.0	70.0	2817469	1494953	1242945	949029	3000283	3101659	3129878	345413	
70.0	80.0	1597040	999845	792942	579631	1763981	1868264	1905269	197102	
80.0	90.0	856568	670228	507493	356994	977963	1059857	1092439	112316	
90.0	100.0	436297	448051	325731	222545	511953	566035	589348	64942	
100.0	110.0	212682	299185	211157	141798	254759	286099	300609	38664	
110.0	120.0	100267	200474	139386	93107	121655	137977	146151	23708	
120.0	130.0	46311	135641	94263	63150	56329	64061	68353	14772	
130.0	140.0	21304	93311	65482	44058	25553	28882	31034	9190	
140.0	150.0	9966	65690	46674	31358	11473	12743	13795	5630	
150.0	160.0	4855	47554	33994	22565	5146	5538	6049	3369	
160.0	170.0	2512	35474	25149	16295	2325	2384	2634	1960	
170.0	180.0	1392	27236	18779	11749	1064	1021	1145	1108	
180.0	190.0	819	21435	14073	8436	494	436	499	607	
190.0	200.0	502	17195	10539	6026	232	186	219	323	
200.0	220.0	512	25424	13690	7318	163	113	138	251	
220.0	240.0	202	17149	7426	3660	36	20	26	60	
240.0	260.0	76	11555	3899	1835	8	3	5	13	
260.0	280.0	27	7690	1973	935	2	0	1	3	
280.0	300.0	9	5043	960	487	0	0	0	0	
300.0	320.0	3	3265	448	258	0	0	0	0	
320.0	340.0	1	2096	200	137	0	0	0	0	
340.0	360.0	0	1338	85	72	0	0	0	0	
360.0	380.0	0	852	34	37	0	0	0	0	
380.0	400.0	0	542	13	18	0	0	0	0	
400.0	450.0	0	636	7	14	0	0	0	0	
450.0	500.0	0	194	0	2	0	0	0	0	
500.0	550.0	0	54	0	0	0	0	0	0	
550.0	600.0	0	13	0	0	0	0	0	0	
600.0	650.0	0	3	0	0	0	0	0	0	
650.0	700.0	0	1	0	0	0	0	0	0	
700.0	750.0	0	0	0	0	0	0	0	0	
750.0	800.0	0	0	0	0	0	0	0	0	

**Table 4-5 Summary of Fatigue Analysis**

Cumulative Damage Ratio	Lines												Max. CDR (per year)	
	#1	#2	#3	#4	#5	#6	#7	#8	#9	#10	#11	#12		
Layout	#1	0.0E+00	0.0E+00	0.0E+00	0.0E+00	0.0E+00	1.0E-04	3.0E-04	6.0E-04	6.0E-03	3.3E-03	1.7E-03	8.0E-04	6.0E-03
	#2	0.0E+00	0.0E+00	0.0E+00	0.0E+00	0.0E+00	1.0E-04	3.0E-04	7.0E-04	7.5E-03	3.3E-03	1.2E-03	6.0E-04	7.5E-03
	#3	0.0E+00	0.0E+00	0.0E+00	0.0E+00	0.0E+00	1.0E-04	3.0E-04	9.0E-04	8.7E-03	3.5E-03	1.1E-03	5.0E-04	8.7E-03
	#4	0.0E+00	0.0E+00	0.0E+00	0.0E+00	0.0E+00	1.0E-04	3.0E-04	1.2E-03	1.4E-02	4.2E-03	9.0E-04	5.0E-04	1.4E-02
	#5	0.0E+00	0.0E+00	0.0E+00	0.0E+00	0.0E+00	0.0E+00	4.0E-04	1.5E-03	1.8E-02	4.0E-03	9.0E-04	5.0E-04	1.8E-02
	#6	0.0E+00	0.0E+00	0.0E+00	0.0E+00	0.0E+00	0.0E+00	4.0E-04	1.9E-03	2.4E-02	4.1E-03	8.0E-04	6.0E-04	2.4E-02
	#7	0.0E+00	0.0E+00	0.0E+00	0.0E+00	0.0E+00	0.0E+00	4.0E-04	2.2E-03	3.0E-02	4.2E-03	6.0E-04	6.0E-04	3.0E-02
	#8	0.0E+00	0.0E+00	0.0E+00	0.0E+00	0.0E+00	0.0E+00	4.0E-04	2.6E-03	3.4E-02	3.7E-03	5.0E-04	7.0E-04	3.4E-02
	#9	6.0E-04	0.0E+00	0.0E+00	0.0E+00	0.0E+00	0.0E+00	3.0E-04	3.2E-03	2.2E-02	7.0E-02	4.3E-03	1.3E-03	7.0E-02

Fatigue Life Prediction	Lines												Fatigue Life (hundred Years)	
	#1	#2	#3	#4	#5	#6	#7	#8	#9	#10	#11	#12		
Layout	#1	inft	inft	inft	inft	inft	3000	1000	500	50	91	176	375	50.00
	#2	inft	inft	inft	inft	inft	3000	1000	429	40	91	250	500	40.00
	#3	inft	inft	inft	inft	inft	3000	1000	333	34	86	273	600	34.48
	#4	inft	inft	inft	inft	inft	3000	1000	250	22	71	333	600	21.90
	#5	inft	inft	inft	inft	inft	inft	750	200	16	75	333	600	16.30
	#6	inft	inft	inft	inft	inft	inft	750	158	13	73	375	500	12.50
	#7	inft	inft	inft	inft	inft	inft	750	136	10	71	500	500	9.90
	#8	inft	inft	inft	inft	inft	inft	750	115	9	81	600	429	8.77
	#9	500	inft	inft	inft	inft	inft	1000	94	14	4	70	231	4.29

The summary results of fatigue analysis obtained from the simulation is provided in Table 4-5 and Figure 4-29. In this table, the expected life of mooring chain components, of all 12 mooring legs is presented. The results of all studied conditions are presented in this table. The CDR in this table is estimated as the ratio of the expected life by the design life of the system of 30 years. As seen here, the maximum CDR of grouping mooring pattern and equally space type mooring pattern are respectively 0.034 in Layout 8 and 0.070 in Layout 9 which are lower than the required value of 0.1.

It should be note there are many methodology to calculate the mooring fatigue life by considering each case condition, e.g. Spectral Simply Summation, Combined Spectrum, Dual-Narrow Banded Correction Factor, and Time Domain Cycle Counting. They have each advantages and disadvantages depend on the mooring system condition. In this study is focuses on the most optimum mooring layout and configuration, so author perform the fatigue analysis calculation with the simplest method in reason detail fatigue analysis

needed and time effective consideration. This make the fatigue life prediction seen significantly overestimate than the actual fatigue damage. As a further apart study, it is suggested to assess the mooring fatigue analysis method and identify the suitable method to satisfy the fatigue limit state design criteria for a box-shaped turret moored units.

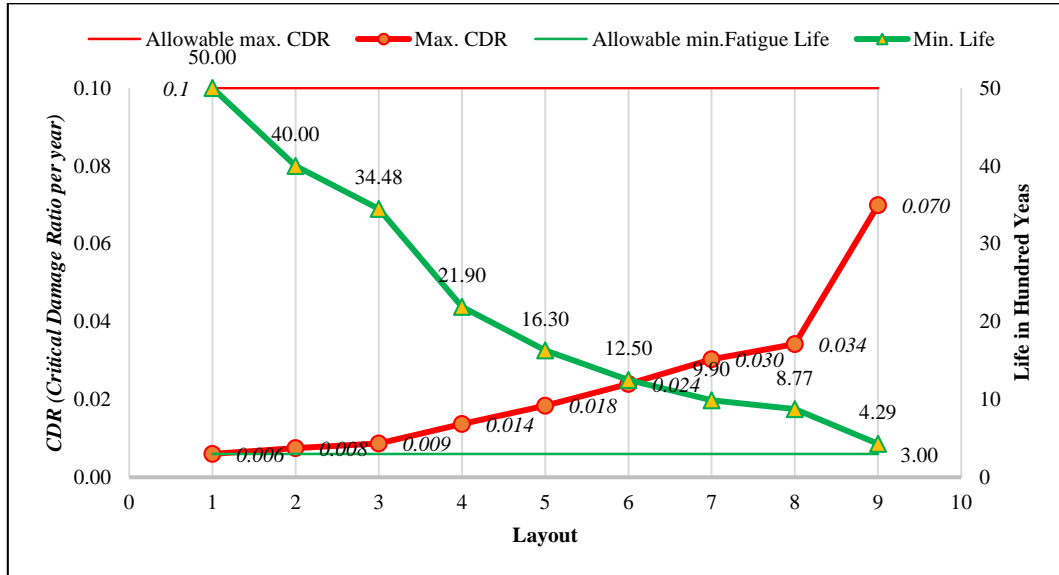


**Figure 4-29 Summary of Fatigue Analysis**

The fatigue analysis result indicated that grouping mooring pattern type have a lower fatigue life more than 50% than equally space mooring pattern type. As expected, CDR and fatigue life has reverse correlation which is the lowest CDR yield a highest fatigue life and so on.

Design of Turret mooring system is not only check the strength and fatigue performance of mooring lines, but also need to check the hull clearance, green water and slamming, and vessel offset as well. All stage has been performed for nine (9) anchor layout to get the good one. Basically mooring system design require an iteration from high number of design variable, its involved positioning of moored vessel, number and properties of lines, length and arrangements of lengths, orientation and pretension of lines, etc. This study is focused on mooring orientation based on heading analysis outcome in previous chapter. Prior to check mooring performance against the environment, the position of mooring connection is verified against hull clearance, green water and wave slamming. Thus, a 3-hour dynamic simulation has been performed, the results indicated that proposed turret location is satisfied a hull clearance, green water, and wave slamming requirements.



## 5. CONCLUSION

It can be concluded from the result that heading analysis is necessary for weathervaning turret moored unit for long-term environment operation study. The proposed methodology to solved heading analysis is compare to earlier algorithm method by in OTC21292 Paper (T. Terashima, 2011) and reported by Akashima (Laboratories, 2009). For a vessel with similar principal particular, the result has a same tendency in heading angel's probability as seen in Figure 4-10.

The proposed mooring system is designed to withstand 200yr return period cyclonic environmental condition and the system is designed to operate normally under extreme environmental condition up to 200yr return period cyclonic condition. The designed system to satisfy the specified requirements. Mooring system performance is provided in Table 4-3 and Table 4-5. As shown in this table the mooring system satisfies all the design requirements identified by Classification Society, except equally space mooring type in Layout 9.

### **Answer research question**

The research question is identified as follows:

*'How the importance of heading analysis in term of mooring system design is?'*

The answer for this question is answered in the graph shown as Figure 4-29. Heading analysis is required to do fatigue life estimation for mooring system. With heading analysis the optimum mooring layout can be determined from several mooring layout options. Since Turret moored unit don't operate in an Omni-directional wave environment. Weathervaning units predominantly sea waves between head seas and beam seas. The heading analysis result is importance for the mooring designer to determine mooring orientation and anchor location. It is also could give benefit for spread mooring type for the designer, this will help him/her to determine the optimum vessel orientation.

It is worth to mention that heading analysis is relevant for floating structure with weathervaning capabilities. Heading analysis is rather a quite complex and efficient analysis to provide the required input data for further necessary analysis.

By the design phase, one of the basic problems raised by single point mooring system is the estimation of the maximum beam waves. In one hand, the designer is happy to impose the maximum design wave all around the floater. But such assumption may lead overly design floating unit, therefore having financial and schedule consequences,

especially for unit in harsh environments. In other hand, there is the need to properly assess the wave height distribution around the floater using available tools and weather information for the specific site.

With a proper heading analysis for floating units with regard to fatigue resistance of mooring system, as relative heading between waves and vessel is believed to be critical parameter when assessing the strength and fatigue performance.

### **Recommendation**

During this thesis multiple areas are identified where additional research possibilities exists. Below these possibilities are listed:

- Hull strength and fatigue damage calculation by consider wave heading analysis. Heading analysis is based on 3 hourly hindcast metocean data and uses the results of the heading analysis directly, considering the combined effect of wind, wind-sea, current and swell. According to IACS Common Structural Rules for Double Hull Oil Tankers, an equivalent design wave is then derived based on the spectral characteristics of each response instead of the common practice for ship design which uses only the characteristics of the RAOs. Deriving equivalent design waves using only the RAO characteristics is found to give some non-conservative and unrealistic equivalent design waves in some cases.
- Long-term response for loading/offloading operability between two vessels. Evaluating offloading availability is a critical step in assessing the overall safety and efficiency of a Floating Storage Unit. Offloading availability will impact the storage required to avoid top-outs and hence production shut-ins.
- Sloshing study by considering wave heading analysis. Hydrodynamic analysis is a key point in each particular sloshing study. Directly calculated ship motions determined by such analysis are used to generate tank liquid response. For a turret moored unit vessel, the designer will ask which wave condition to be applied for any other directions, knowing that not only roll motion can induce significant sloshing, but also combined pitch and roll for quartering seas.
- Green water on deck and wave slamming probability for long-term environment. It's important to have the correct wave height distribution around the floating structure to properly asses green water and wave slamming impact and pressure not only on bow but also all along the floating structure.
- Wave heading analysis for other turret moored type, e.g. internal turret mooring.

## REFERENCES

- ABS. (2009). Guide for Building and Classing *Floating Production Installations*. Houston, TX 77060 USA: American Bureau of Shipping.
- Ardhiansyah, et al. (2016). *Heading Analysis of Weathervaning Turret Moored Units*. Paper presented at the SENTA Surabaya.
- Bhattacharyya, R. (1978). *Dynamics of Marine Vehicles*: John Wiley & Son, Inc.
- BV. (2010). Structural Analysis of Offshore Surface Units through Full Length Finite Element Models *Recommended procedure for the calculation of wave loads* (Vol. NR 551 DT R00 E). France: Marine Division.
- Chakrabarti, S.K. (1987). *Hydrodynamics of Offshore Structures*: Computational Mechanics Publications.
- CMPT. (1998). *Floating Structures: A Guide for Design and Analysis*: Oilfield Publications, Inc.
- DNV. (2010). Position Mooring *Section 2 F 100*.
- Faltinsen, O.M. (1990). *Sea Loads on Ships and Offshore Structures*: Cambridge Ocean Technology Series, Cambridge University Press.
- Francois, M., et al. (2004). Directional Metocean Criteria For Mooring and Structural Design of Floating Offshore Structure. *ISOPE, JSC147*.
- Howell, G. Boyd. , Arun S. Duggal, Caspar Heyl, Oise Ihonde. (2006). Spread Moored or Turret Moored FPSO's for Deepwater Field Developments. *Offshore West Africa*.
- Journée, J.M.J. , W.W. Massie. (2001). *OFFSHORE HYDROMECHANICS* (First Edition ed.): Delft University of Technology.
- Jun, Wong, et al. (2007). Feasibility Stage Assessment of Side-by-Side LNG Offloading Operation. *OMAE*, 29522(San Diego, USA).
- Laboratories, Akashima. (2009). Motion Prediction of Masela FLNG.
- London, T. England, Arun, S. Duggal, L. Allen Queen. (2001). A Comparison Between Turret and Spread Moored F(P)SOs for Deepwater Field Developments. *Deep Offshore Technology*.
- Morandini, Cedric., Jun Wong. (2007). Heading Analysis of Weathervaning Floating Structures: Why, How and Where to Make The Best of Them. *ISOPE*(Lisbon, Portugal).
- Munipalli, Jayanth. and Krish Thiagarajan. (2007). *Effect of Wave Steepness on Yaw Motions of a Weathervaning Floating Platform*. Paper presented at the Australasian Fluid Mechanics Conference, Crown Plaza, Gold Coast, Australia.
- Nachlinger, R. Ray. (1989). *Assessing the Integrity of a Body Subjected to a Seaway*. Paper presented at the Structural and Marine Analysis Seminar, Dr. Holmes Hotel, Geilo Norway.
- OCIMF. (1994). Prediction of Wind and Current Loads on VLCCs. In O. C. I. M. Forum (Ed.), (2nd ed.). England: British Library Cataloguing in Publication Data.
- Sarala Resmi, Hajiarab Mohammad, and Bamfrod Richard. (2011). *Equivalent Design Wave Approach for Calculating Site-Specific Environment Loads on an FPSO*. Paper presented at the ASME, The Netherlands.
- T. Terashima, K. Shimada, Y. Ichimaru, and Y. Orimo. (2011). *Methodology to Define Design Motion Criteria for Performance of Floating LNG Process Facilities*. Paper presented at the Offshore Technology Conference, USA.
- Ultramarine. (2012). Reference Manual for MOSES. In I. Ultramarine (Ed.).
- Yadav, A., S. Varghese and K. P. Thiagarajan. (2007). *Parametric Study of Yaw Instability of a Weathervaning Platform*. Paper presented at the Australasian Fluid Mechanics Conference, Crown Plaza, Gold Coast, Australia.





# CURRICULUM VITAE



## Personal Information

Name : Fahmy Ardhiansyah

Email address : [fahmyardhiansyah@gmail.com](mailto:fahmyardhiansyah@gmail.com)

Phone : +62 852 318 1039

Education : Bachelor, Ocean Engineering, ITS (2010)  
Master, Naval Architecture and Shipbuilding Engineering, ITS (2017)

Research & Course Work Projects : 1. Optimization Barge Sponsons Design for Transportation and Installation, Paper Presented in the ISOCEEN (2015)  
2. Value Improvement Practice for Floating Production Facility, PT. PERTAMINA PHE ONWJ (2015)  
3. Single Point Mooring Re-Tanker 150,000 DWT, PT. Adidaya Energy Mandiri (2015)  
4. Multi Anchor Leg Mooring Design, PT. ConocoPhillips Indonesia (2015)  
5. A Technical Investigation of KM Wihan Sejahtera Sinking in Surabaya Port, In-House Work (2015)  
6. Side-by-Side Tanker Loading/Offloading Operation Assessment, BP Tangguh (2016)  
7. Marine Current Turbine Renewable Energy Mooring System Design, P3GL *Pusat Pengkajian dan Penerapan Geologi Laut* (2016)  
8. Twin Barge-Spar Hydrodynamic Interaction on Floatover Deck Installation, paper submitted to the BPPT Wave Journal (2016)  
9. Interchange Ability SPM PERTAMINA RU VI Balongan - Fatigue Life Anchor Leg, PT. PAL (2016)  
10. Law and Regulation to Decommissioning an Offshore Oil and Gas Facility case study HCML Field, In-House Work (2016)